
**TRIBHUVAN UNIVERSITY**

**INSTITUTE OF ENGINEERING**

**PULCHOWK CAMPUS**

THESIS NO:079MSCCD005

# Assessment of Hydroclimatic Extremes Under Shifting Precipitation Patterns in The Himalayan Rain Shadow Region Mustang, Nepal.

by

Apechhya Aryal

A THESIS

SUBMITTED TO THE DEPARTMENT OF APPLIED SCIENCES AND CHEMICAL ENGINEERING IN PARTIAL FULFILLMENT OF THE REQUIREMENTS FOR THE DEGREE OF MASTER IN CLIMATE CHANGE AND DEVELOPMENT

DEPARTMENT OF APPLIED SCIENCES AND CHEMICAL ENGINEERING

LALITPUR, NEPAL

MAY, 2025

## COPYRIGHT

The author has agreed that the Library, Department of Applied Sciences and Chemical Engineering, Pulchwok Campus, Institute of Engineering, may make this thesis freely available for inspection. Moreover, the author has agreed that permission for extensive copying of this thesis for scholarly purposes may be granted by the professor(s) who supervised the work recorded herein or, in their absence, by the Head of the Department wherein the thesis was done. It is understood that the recognition will be given to the author of this thesis and to the Department of Applied Sciences and Chemical Engineering, Pulchwok Campus, Institute of Engineering, for any use of the material of this thesis. Copying or publication, or any other use of this thesis for financial gain without approval of the Department of Applied Sciences and Chemical Engineering, Pulchwok Campus, Institute of Engineering, and the author's written permission is prohibited. Request for permission to copy or to make any other use of the material in this thesis in whole or in part should be addressed to:

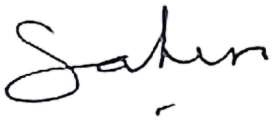

Prof. Dr. Sahira Joshi

Head

Department of Applied Sciences and Chemical Engineering

Pulchwok Campus, Institute of Engineering

Patan, Lalitpur

Nepal

TRIBHUVAN UNIVERSITY

INSTITUTE OF ENGINEERING

PULCHOWK CAMPUS

DEPARTMENT OF APPLIED SCIENCES AND CHEMICAL ENGINEERING

The thesis titled "**Assessment of hydroclimatic extremes under shifting precipitation patterns in the Himalayan rain shadow region Mustang, Nepal**" prepared and submitted by Apechhya Aryal in partial fulfilment of the requirements for the degree of Master of Science (M. Sc.) in Climate Change and Development has been examined by us and is accepted for the award of M. Sc. in Climate Change and Development by Tribhuvan University.

The undersigned certify that they have read, and recommended to the Institute of Engineering for acceptance, a thesis report entitled "**Assessment of hydroclimatic extremes under shifting precipitation patterns in the Himalayan rain shadow region Mustang, Nepal.**" submitted by Apechhya Aryal in partial fulfillment of the requirements for the degree of Master in Climate Change and Development.

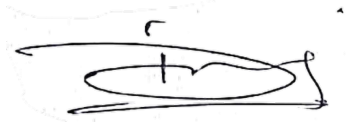

Supervisor

**Asso. Prof. Dhiraj Pradhananga**

Department of Meteorology,

Tri-Chandra Multiple Campus

Tribhuvan University

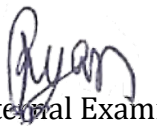

External Examiner

**Prof. Rijan Bhakta Kayastha**

Department of Environmental Science and Engineering

Kathmandu University

Program Coordinator

**Prof. Dr. Rinita Rajbhandari**

Climate Change and Development Program

Department of Applied Sciences and Chemical Engineering

Date: May, 2025

**DECLARATION**

I hereby declare that this study, "**Assessment of hydroclimatic extremes under shifting precipitation patterns in the Himalayan rain shadow region Mustang, Nepal**" is based on my original research work. Related works on the topic by other researchers have been duly acknowledged. I owe all the liabilities relating to the accuracy and authenticity of the data and any other information included here under.

Apechhya Aryal

079MSCCD005

MSc in Climate Change and Development

Date: May, 2025

**ACKNOWLEDGEMENT**

I would like to extend my sincere gratitude to Professor Rinita Rajbhandari, the program coordinator of the Applied Sciences and Chemical Engineering Department, for her continuous guidance and encouragement throughout this study. My heartfelt appreciation also goes to Professor Dr. Khem Poudyal for providing me with this valuable research opportunity.

I am deeply grateful to my Primary Supervisor, Dr. Dhiraj Pradhananga, for his invaluable support, insightful feedback, and mentorship, which played a crucial role in shaping the direction of this research.

I would also like to acknowledge the unwavering support of Mr. Aashutosh Paudel and Mr. Pramesh Karki and, whose encouragement and assistance were instrumental in completing this work.

Lastly, I express my profound gratitude to my family and friends, whose constant motivation and belief in me provided the strength and determination to complete this study. Their encouragement has been a pillar of support throughout this journey.

Apechhya Aryal

079MSCCD005

May 2025

**ABSTRACT**

The Mustang district of Nepal, a semi-arid, high-altitude region within the Himalayan rain shadow, faces exceptional vulnerability to climate change impacts on its cryosphere-dependent water resources. This study assesses historical (1980-2015) and future (2025-2100) flood and drought conditions by analyzing precipitation trends and hydrological extremes using observed and gridded (APHRODITE) datasets, alongside bias-corrected CMIP6 projections under moderate (SSP2-4.5) and high (SSP5-8.5) emission scenarios. Methodologies employed include Mann-Kendall trend analysis, drought assessment via the Standardized Precipitation Index (SPI) and Standardized Precipitation Evapotranspiration Index (SPEI), and Flood Frequency Analysis (FFA) using Generalized Extreme Value (GEV) and Gumbel distributions. Historical analysis reveals complex seasonal precipitation trends and a notable increase in drought frequency/severity since the mid-1990s. Future projections show significant divergence: SSP5-8.5 indicates a potential doubling of annual precipitation by 2100 alongside intensified drought periods and more extreme flood events (with GEV estimates consistently higher than Gumbel). The temporal analysis projects a sharp rise in flood occurrences post-2070 (SSP5-8.5). These findings highlight Mustang's transition towards a hydroclimatic regime dominated by extremes, posing severe threats and underscoring the need for scenario-specific adaptation planning.

Keywords: Mustang, Himalayan Rain Shadow, Climate Change, Precipitation Trends, Droughts, Floods, CMIP6 Projections, Flood Frequency Analysis (FFA), Generalized Extreme Value (GEV)

**TABLE OF CONTENTS**

**LIST OF FIGURES**

**LIST OF TABLES**

**ABBREVIATIONS**

| | |
|---|---|
| AD | Anderson-Darling (test) |
| AIC | Akaike Information Criterion |
| AICc | Corrected Akaike Information Criterion |
| AMS | Annual Maximum Series |
| APHRODITE | Asian Precipitation-Highly-Resolved Observational Data Integration Towards |
| ASTER | Advanced Spaceborne Thermal Emission and Reflection Radiometer |
| CMIP6 | Coupled Model Intercomparison Project Phase 6 |
| DEM | Digital Elevation Model |
| DHM | Department of Hydrology and Meteorology |
| EVT | Extreme Value Theory |
| GCM | Global Circulation Model |
| GHG | Green House Gases |
| GLOF | Glacier Lake Outburst Flood |
| GOF | Goodness-of-Fit |
| GRS | Global Ranking Score |
| IPCC | Intergovernmental Panel on Climate Change |
| KS | Kolmogorov-Smirnov (test) |
| LLOF | Landslide Lake Outburst Flood |
| LM | L-moments |
| MoM | Method of Moments (Parameter estimation method) |
| POT | Peak-Over-Threshold (FFA context) |
| PPCC | Probability Plot Correlation Coefficient |
| QM | Quantile Mapping |
| RMSE | Root Mean Square Error |
| Se | Standard Error of Estimate |
| SPI | Standard Precipitating Index |
| SPEI | Standardized Precipitation-Evapotranspiration Index |
| SSP | Shared Socioeconomic Pathways |

| | |
|---|---|
| TP | Third Pole |
| UTM | Universal Transverse Mercator |
| WMO | World Meteorological Organization |
| WRF | Weather Research & Forecasting Model |

# CHAPTER 1: INTRODUCTION

## 1.1 Background

Climate change has emerged as one of the most critical global challenges of the 21st century, significantly altering weather patterns, ecosystems, and human societies. Climate change is increasingly recognized as a defining ecological and socio-economic challenge (Wiertz & Graaf, 2022). Over the past three decades, global average surface temperatures have consistently increased, with the rate of human-induced warming exceeding 0.2°C per decade between 2013 and 2022 (Forster et al., 2023). The TP, the world's largest highland, holds a major reservoir of glacier ice and snow, serving as a vital water source for major South Asian River systems (Kuttippurath et al., 2024). Yet here temperatures are projected to rise by approximately 1–2°C, with some areas experiencing increases of up to 4–5°C by 2050 (Krishnan et al., 2019). Mountain ecosystems are increasingly at risk of extinction, as they cannot move to higher elevations to which they can migrate, extreme temperature fluctuations and shifting precipitation patterns make water availability highly fragile, with even minor climatic changes severely impacting local hydrological cycles hydrology (Seastedt & Oldfather, 2021).

Precipitation is a fundamental component of the hydrological cycle, directly influencing river flow, groundwater recharge, and agricultural productivity. Extreme rainfall events are becoming less frequent, but more violent and are likely to increase in intensity (Seneviratne et al., 2021). Climate change is altering precipitation patterns, impacting water resource sustainability, particularly in regions dependent on monsoonal rainfall and glacial meltwater (Orr et al., 2022). Mountainous and semi-arid regions are particularly vulnerable due to their reliance on seasonal precipitation and glacial melt (Sigdel et al., 2022). In the Himalayan region, long-term climatic shifts have led to increased extreme weather events (Aryal et al., 2024). Changes in precipitation and temperature patterns are altering the hydrological cycle, increasing the probability of extreme droughts and floods, particularly in arid and semi-arid regions (Abd-Elhamid et al., 2024). Floods and droughts are significant disasters with severe implications to the society (Penny et al., 2023). Prolonged dry spells have exacerbated water shortages, affected agriculture and drinking water availability, while short bursts of intense rainfall have led to flash floods and landslides, endangering local settlements and infrastructure (Khadka et al., 2021). Both dry and wet climate extremes are becoming more intense, with their impacts expected to escalate as

climate change progresses(Intergovernmental Panel On Climate Change, 2023). These trend are expected to exacerbate extreme heat events, prolonged droughts, severe storms, and intensified flooding, heightening risks to human well-being and global security (Wang et al., 2023).

Floods, one of the most destructive natural disasters, occur when excessive water overwhelms river channels, often due to extreme precipitation, ocean tides, or glacial lake outbursts (C. Sharma & Ojha, 2019). Over the past two decades, floods have accounted for 44% of all recorded natural disasters worldwide, impacting 1.65 billion people and causing $651 billion in economic losses (Maranzoni et al., 2023). Even in regions with chronic water scarcity, extreme floods can be highly destructive (Nabinejad & Schüttrumpf, 2023). Conversely, droughts, often intensified by rising global temperatures and shifting precipitation patterns, pose challenges for predicting onset, duration, and severity (Nandgude et al., 2023). Droughts can happen in all types of climate zones, including both wet and dry areas, and are typically linked to a significant decrease in rainfall over a long duration, such as a season or an entire year (Mishra & Singh, 2010). Australia's Millennium Drought (1997–2009) was a prolonged period of below-average rainfall that severely impacted the environment and economy, particularly in the Murray-Darling Basin (Aghakouchak et al., 2014). Interestingly, floods and droughts are interconnected—severe floods following prolonged droughts can lead to devastating consequences (Barendrecht et al., 2024). In early 2017, following a prolonged drought, heavy rainfall severely damaged the main and emergency spillways of California's Oroville Dam that led to evacuation of nearly 200,000 residents (Vahedifard et al., 2017). According to the United Nations Office for Disaster Risk Reduction (UNISDR), floods and droughts caused nearly USD 0.6 trillion in damages—accounting for 28% of total disaster-related losses—over the 20-year period from 1992 to 2012.

## 1.2 Problem Statement

Nepal, contributing only 0.025% of GHG emissions, experiences disproportionate impacts of climate change, particularly in its high-altitude mountain regions experiences disproportionate impacts of climate change, particularly in its high-altitude mountain regions (Shrestha & Prasain, 2016). It ranks among the most disaster-prone countries in the world (Banstola et al., 2019),with a river network of over 6,000 rivers spanning 45,000 km many originating in the high and mid-Himalayan region (Gupta et al., 2021), making Nepal’s hydrology highly sensitive

to climate variability and extreme weather events. Among these climate-induced disasters, floods are the most frequent and rank as the third most deadly natural disaster in Nepal (Banstola et al., 2019). With climate change exacerbating hydrological extremes, the frequency and severity of flood events are expected to rise, unless proactive adaptation measures are implemented (Endendijk et al., 2023). Over the past 50 years, Nepal has experienced an average of two disaster-related deaths per day, while more than 300 families have been affected daily. Specifically, floods account for 11.43% of total disaster occurrences, 9.33% of fatalities, 38.42% of missing persons, 0.75% of injuries, 61.60% of affected families, and 10.16% of property damages (A. P. Sharma et al., 2023a).

In the trans-Himalayan region of Upper Mustang, communities have endured harsher winters, prolonged droughts, and declining water availability (McChesney, 2015). Environmental degradation has disrupted agriculture, water access, livelihoods, forcing increased migration and threatening local food security (Amburgey, 2024). The unique geography of Mustang makes it particularly susceptible to flash floods, which are often triggered by the failure of natural dams, such as LLOFs, or high-intensity rainfall (Delalay et al., 2018a). The vulnerability of Mustang was highlighted on August 13, 2023, when a severe flood event struck the Muktinath area, causing extensive property and infrastructure damage estimated at USD 7.4 million in Kagbeni Village, a settlement along the Kagkhola River, a major left-bank tributary of the Kali Gandaki River. This event was particularly unusual given that the region had been experiencing prolonged drought conditions, primarily due to inconsistent and erratic rainfall. Despite its arid climate with annual rainfall below 400 mm, Mustang faces simultaneous risks of drought and flash floods, both linked to shifting precipitation patterns. Climate-induced migration is increasingly evident. Dhye village is considered Nepal's first climate refugee settlement, with three recorded mass migrations, the latest attributed directly to climate change (Mustafa & Faraz, 2023). Similarly, 17 households, comprising 86 residents, were permanently relocated from Samdzong to "Namashung" in 2016 after the collapse of irrigation systems and severe water scarcity (Mustafa & Faraz, 2023). The increasing frequency of extreme events in Mustang highlights the urgent need for integrated research addressing both flood and drought risks. While studies have extensively mapped flood hazards, the combined impact of shifting precipitation patterns on both hydrological extremes remains largely unexplored (Parajuli et al., 2023).

## 1.3 Research Objectives

**General Objective:**

This research aims to analyze historical and projected precipitation patterns in Mustang and their impact on flood and drought occurrences, using climate data and statistical models.

**Specific Objectives:**

1. To analyze historical trends in precipitation patterns in Mustang.
2. Use CMIP6 Models to project future precipitation changes in Mustang using CMIP6 models under moderate SSP2-4.5 and high SSP5-8.5 emission scenarios.
3. To assess flood and drought occurrences over time.

## 1.4 Significance of Study

Mustang, located in the Himalayan rain shadow and heavily dependent on cryosphere-fed water sources, is highly vulnerable to changing precipitation patterns, rising temperatures, and associated hydrological extremes. This study addresses critical knowledge gaps by analyzing historical precipitation and temperature trends using observed and gridded datasets (DHM, APHRODITE) with robust statistical methods such as the Mann-Kendall test and Sen's Slope estimator. It evaluates both historical and future drought and flood risks through standardized indices (SPI and SPEI) and Flood Frequency Analysis (FFA), offering a comprehensive assessment of compound climate extremes. By employing CMIP6 model projections under SSP2-4.5 and SSP5-8.5 pathways, the research highlights the future trajectory of hydroclimatic conditions under varying emission scenarios. The findings provide essential, evidence-based insights for local communities, policymakers, and disaster management agencies, supporting the development of targeted adaptation strategies such as early warning systems, water conservation, climate-resilient agriculture, and infrastructure planning.

## 1.5 Scope and Limitations

**Scope of the Study**

Study Area: The research focuses on Mustang, Nepal, located in the rain shadow of the Annapurna and Dhaulagiri ranges. The district is divided into Upper Mustang (arid) and Lower Mustang (semi-arid), both experiencing unique precipitation and hydrological dynamics.

Time Frame: The study will analyze historical climate data (1980–2015) and future projections (2025–2100) to assess precipitation variability over time.

Data Sources: The study will use observational data from APHRODITE, and DHM Nepal, along with climate model outputs from CMIP6 (SSP2-4.5 and SSP5-8.5 scenarios).

**Limitations of the Study**

The following are the limitations of my study:

- Due to Mustang's remote location, high-resolution meteorological station data are limited. Reliance on reanalysis datasets and satellite-derived information may introduce uncertainties in analysis.
- Very few temperatures Station are available for the study.
- Future precipitation projections are dependent on Global Climate Models (GCMs), which have inherent uncertainties, particularly for complex mountain regions.
- The interplay between glacial melt, monsoonal precipitation, and local topography makes flood and drought modeling challenging, requiring assumptions and simplifications in some cases.

# CHAPTER 2: LITERATURE REVIEW

## 2.1 General Trends in Climate Variability in the Himalayan Region

The Himalayan region is a climate hotspot where changes have far-reaching consequences for millions of people. Krishnan et al. (2020) analyzed climate change impacts on precipitation in Northeastern India, highlighting increased monsoonal variability, leading to unpredictable water availability and disruptions in agriculture. Similarly, Kumar et al. (2023) examined precipitation trends in Lahaul-Spiti, Himachal Pradesh, observing significant shifts in monsoonal and winter rainfall over the past four decades, pointing to a larger climate-induced transformation in seasonal precipitation regimes. These studies suggest that the historical stability of monsoonal cycles is being disrupted, which has direct consequences for rivers, agriculture, and water-dependent sectors. Historical climate patterns reconstructed by Pandey et al.(2025) through dendrochronology (tree-ring analysis) reveal that human-induced warming has intensified extreme weather events in the Pir Panjal range. Further, Ahmed et al. (2025) investigated climate variability's influence on Himalayan glacial lakes, showing that unpredictable precipitation cycles and rising temperatures have increased the risk of glacial lake outburst floods (GLOFs).Additionally, research by Haq et al.( 2025) on localized climate variability in the Hindukush-Himalayan region highlights how changing precipitation cycles, rising temperatures, and altered monsoonal patterns are affecting regional hydrology, groundwater reserves, and seasonal water availability. A study by Fujinami et al. (2025) on monsoonal shifts over the southern Himalayan slopes found that rising temperatures are causing more intense but shorter-duration rainfall events, significantly increasing flood risks due to rapid runoff and soil erosion.

Further research by Mahakur et al. (2025) examined large-scale precipitation variability across the tropics and identified that Himalayan monsoons are becoming increasingly unpredictable due to changes in atmospheric circulation patterns, shifting jet streams, and altered oceanic interactions. This unpredictability affects seasonal water availability, creating difficulties in water management, agriculture, and disaster preparedness. Additionally, Anand et al. (2025) explored rainfall variability in the Upper Kumaon region, revealing that seasonal imbalances are becoming more pronounced, with wetter summers and drier winters, leading to reduced agricultural productivity and heightened water stress. Studies have shown that climate change is intensifying these extreme

events, with rising temperatures leading to erratic precipitation patterns and increased glacial melt Kashyap et al. (2025). Additionally, Thapa et al. (2025) modeled sediment transport in Himalayan Rivers and found that climate-induced flooding is significantly altering river morphology, increasing erosion rates and affecting riverbank stability.

## 2.2 Methodologies for Climate Projection: Models, Techniques, and Bias Correction

### *2.2.1 Climate models*

Climate models are key tools for predicting future temperature, precipitation, and extreme events. This section reviews Global and Regional Climate Models, bias correction methods, and CMIP6 projections. GCMs simulate atmosphere, ocean, and land interactions based on physical laws, helping to project climate patterns under different emission scenarios. GCMs are instrumental in assessing the impact of anthropogenic emissions on future climate scenarios and are widely used for climate change projections and policy development (Li et al., 2025). However, GCMs have limitations, particularly in regional climate modeling, as their coarse spatial resolution (approximately 100–300 km grid) makes them less effective in capturing localized extreme weather events such as flash floods and severe droughts(Qiu et al., 2022). Due to these constraints, downscaling techniques either statistical or dynamic are necessary to enhance the accuracy of regional climate projections (Goodarzi et al., 2024).

Meliho et al. (2025b) analyzed GCM uncertainties for future climate change projections in the Sousse watershed, Morocco, showing that regional-scale corrections are essential for improving reliability in climate impact studies. Future research should focus on refining GCM algorithms, incorporating machine learning approaches for statistical downscaling, and developing hybrid models that combine GCMs with remote sensing data(Sithara et al., 2022). Additionally, better representation of land-atmosphere interactions and extreme precipitation events will enhance the predictive capabilities of GCMs, making them more effective for regional climate adaptation planning(Mohapatra et al., 2025) .

### *2.2.2 Coupled model intercomparison project and future emission scenarios*

The CMIP  was established to coordinate, study, and compare climate simulations produced by coupled ocean–atmosphere–cryosphere–land GCMs(Meehl et al., 2000). The World Climate Research Programme (WCRP) launched CMIP6, the

latest phase of the Coupled Model Intercomparison Project, to address emerging scientific questions in climate change(Zhou et al., 2019). Recent studies have emphasized the importance of high-resolution modeling and bias correction in improving GCM-based climate projections. For instance, Li et al. (2025) assessed bias correction methods for CMIP6 GCMs, finding that raw GCMs tend to overestimate precipitation levels and perform better in winter than in summer seasons. Similarly, Qiu et al. (2022)applied CMIP6-based RCMs (Regional Climate Models) in Central Asia, showing that downscaled models significantly improve precipitation variability predictions, particularly in high-altitude and semi-arid regions. Further research by Sangroula et al.(n.d.)integrated CMIP6 projections into flood modeling for Nepal, demonstrating enhanced seasonal flow variability predictions in glacier-fed river basins. Meliho et al. (2025a)conducted GCM selection analysis for climate change impact studies in Morocco, concluding that CMIP6 models provide more accurate long-term climate projections compared to earlier CMIP5 models. Additionally, Gulakhmadov et al. (2025) evaluated temperature, and precipitation changes in the Panj River Basin, Central Asia, using both CMIP5 and CMIP6 projections, confirming that newer GCMs exhibit improved representation of temperature extremes but still require regional calibration for precipitation predictions. For example, Ghazi et al. ( 2025) projected drought events in Poland using CMIP6 models, revealing an increased likelihood of severe dry spells due to global warming trends. Similarly, Drisya & Al-Zubari, (2025) examined future precipitation changes in the Middle East, utilizing six different GCMs from CMIP6, showing that precipitation will decline significantly across arid regions under higher emissions scenarios. Moreover, Shanmugam & Lakshmanan, (2025) developed a multi-model ensemble approach for bias correction of CMIP6 precipitation projections in semi-arid regions of India, improving forecasting accuracy for extreme weather events A major feature of CMIP6 is the integration of Shared Socioeconomic Pathways (SSPs), which explore a range of future emission and land-use scenarios to improve projections of climate impacts under varying mitigation efforts (O'Neill et al., 2016).

SSPs combine narratives of socio-economic development (such as population growth, technological advancement, and policy choices) with Representative Concentration Pathways (RCPs) that describe the level of radiative forcing by 2100. For example, SSP2-4.5 represents a "middle-of-the-road" scenario with moderate emissions, while SSP5-8.5 assumes rapid economic growth based on fossil fuels and results in very high GHG emissions (Riahi et al. 2017).

### *2.2.3 Bias correction methods for improving precipitation estimates*

Systematic biases represent a recognized challenge in climate modeling, affecting both General Circulation Models (GCMs) and Regional Climate Models (RCMs), with precipitation estimates being particularly susceptible. These discrepancies often stem from inherent simplifications within physical parameterizations, limitations imposed by model resolution, and the incomplete representation of complex local climatic processes. To mitigate these issues and enhance the usability of model outputs, various bias correction methodologies are widely employed. The primary goal of these techniques is to adjust simulated climate variables, ensuring they align more closely with historical observations and thereby improving the reliability of regional climate projections (De la Cruz et al., 2025)Prominent approaches include Quantile Mapping (QM), which modifies the probability distribution of modeled precipitation to match observed distributions, reducing biases across mean and extreme values (Wu et al., 2025), and Statistical Downscaling Methods (SDMs), which utilize established empirical relationships between large-scale atmospheric variables and local climate observations (Hoseini et al., 2025). Empirical Quantile Mapping (EQM) offers a more refined application of QM by correcting distinct parts of the precipitation distribution separately, leading to improved accuracy, especially for extreme event prediction (Vásquez et al., 2024).Alternatively, the Delta Method (DM) applies additive or multiplicative correction factors derived from the historical period, effectively adjusting for model biases while preserving the model-projected climate change trends (Li & Li, 2025). The practical utility of bias correction is highlighted in recent studies; for example, (Chae & Chung, 2024)demonstrated its effectiveness in reducing uncertainty within precipitation-driven runoff projections, bolstering the reliability of hydrological models. Furthermore, Bañares et al. (2024) applied bias correction techniques to CMIP6 GCM outputs in the Bicol River Basin, Philippines, achieving significant improvements in streamflow projections and subsequent flood risk assessments.

## 2.3 Floods and Droughts in Semi-Arid and High-Altitude Regions

High-altitude and semi-arid regions are particularly vulnerable to climate extremes due to their unique topographical and climatic conditions. Droughts in rain shadow areas like Ladakh, Tibet, and the Mongolian steppe arise from topographical barriers where moisture-laden winds lose their water content on

the windward side of mountains, leaving the leeward side arid(Schaller, 1998). Qiao et al. (2022) found that precipitation extremes in semi-arid regions of China are declining, leading to longer dry spells and reduced water availability. Similarly, Liu et al., (2023) linked land desertification in the Qilian Mountains to rising temperatures and declining precipitation. The economic impacts are significant, as agriculture and hydropower projects suffer losses due to infrastructure damage and unpredictable water flows. Recent studies highlight these growing threats; Tan et al. (2023) documented an increase in flash floods in Xinjiang, attributing them to precipitation variability. Similarly, Rahman et al. (2024)studied spatial-temporal patterns of droughts and floods in Khyber Pakhtunkhwa, Pakistan, linking the rise in flood occurrences to monsoonal shifts and deforestation. These findings emphasize the urgent need for improved climate adaptation strategies, including sustainable water management, afforestation efforts, and advanced flood forecasting systems, to mitigate the growing risks of floods and droughts in semi-arid and high-altitude regions.

### *2.3.1 Introduction to flood frequency analysis*

Flood frequency analysis is a core aspect of hydrological modeling, crucial for estimating the probability of extreme flood events and informing the design of flood control infrastructure. This analysis relies on statistical modeling, often applied to AMS or POT data, utilizing principles from EVT .Within EVT-based FFA, the Gumbel distribution Extreme Value Type I and the GEV family are particularly prominent for modeling annual maximum flood flows(Twinomuhangi et al., 2025). The GEV distribution offers significant flexibility as a three-parameter model, capable of representing the Gumbel (Type I), Fréchet (Type II, heavy-tailed), and Weibull (Type III, bounded) distributions depending on the value of its shape parameter(Papalexiou & Koutsoyiannis, 2013).

**Extreme Value Distributions: Gumbel and GEV**

The Gumbel distribution (Type I Extreme Value) has traditionally been used in FFA for its simplicity and closed-form solutions (Hamed & Rao, 2019).However, it does not account for skewness in data, which can lead to under- or over-estimation in tail extremes. This limitation is addressed by the GEV distribution, which incorporates three forms: Type I (Gumbel), Type II (Fréchet), and Type III (Weibull), offering greater flexibility in modeling flood extremes (Pandey et al., 2018). Recent studies have shown the effectiveness of GEV over Gumbel in varied climatic regions. For example, Sharma et al. (2020) found GEV to outperform

Gumbel in modeling annual maximum rainfall in the Upper Ganga Basin due to better tail fit. Similarly, Adeyeye and Abiodun (2019) highlighted GEV's ability to capture heavy-tailed flood behavior in West African basins. Notably, GEV's extra shape parameter allows it to accommodate skewed flood distributions, which can improve fitness when flood data exhibits significant positive skewness. In fact, if the sample skew is far from zero, the two-parameter Gumbel model may be statistically inadequate even if it passes goodness-of-fit tests (Khan et al., 2023)

**Parameter Estimation Methods**

Accurate parameter estimation is truly the bedrock of reliable flood predictions in FFA, as getting these parameters right is crucial for effectively fitting the extreme value models we use. Three prominent methods stand out: the Method of Moments, Maximum Likelihood Estimation, and L-moments. MoM is often straightforward to apply, essentially matching theoretical distribution moments to those calculated from the actual flood data, but it can be significantly skewed by outliers. MLE takes a different approach, finding parameter values that make the observed flood data most probable under the assumed distribution, proving statistically efficient, especially with larger datasets (Pathak & Mishra, 2021). L-moments, calculated using linear combinations of sorted data, are generally considered more robust and less influenced by extreme values, making them particularly valuable when dealing with smaller sample sizes, outliers, or the heavy-tailed distributions common in hydrology (Fawad et al., 2022). For these reasons, L-moments are frequently the preferred method for fitting distributions like the GEV (Hosking, 1990; Khanal et al., 2022). The practical advantages of L-moments have been clearly demonstrated in studies; for instance, Yadav & Singh (2022) found they consistently yielded more stable parameter estimates for Kosi River Basin flood data compared to MoM and MLE, while Rana et al. (2020) highlighted their utility in Himalayan catchments known for extreme outliers, further emphasizing their suitability for challenging datasets

**Goodness-of-Fit Tests**

After fitting candidate distributions, goodness-of-fit (GOF) tests are used to check how well each model represents the observed flood data. The Kolmogorov–Smirnov (KS) test and Anderson–Darling (AD) test are two widely used GOF tests in flood frequency.The KS test is non-parametric and based on the maximum absolute difference between empirical and theoretical CDFs, Recent applications show that no single test is conclusive. In a study across Nepalese basins, Shrestha

et al. (2021) used KS and AD together and found AD more sensitive in identifying the best distribution under extreme rainfall. The Filliben coefficient was also used by Bhattacharya & Jain (2019) to support model ranking based on graphical fitting. Another useful GOF measure is the Filliben correlation coefficient**,** also known as the probability plot correlation coefficient (PPCC) test. This method, introduced by Filliben (1975), evaluates how well flood data aligns on a theoretical probability paper plot. The correlation between observed and model quantiles is calculated – the closer it is to 1, the better the fit. Recent non-stationary FFA research has adopted Filliben's test for selecting the optimal distribution, citing its convenience and reliability(Qu et al., 2020) Overall, modern FFA studies employ a battery of GOF tests – KS for overall fit, AD for tail-sensitive assessment, and sometimes Filliben's PPCC for an intuitive gauge of fit on probability plots. Using multiple tests ensures that the selected distribution not only passes formal criteria but also captures the distributional shape of extreme floods.

**Model Selection Criteria**

Choosing the most appropriate statistical distribution is a critical step when flood frequency analysis suggests several plausible candidates fit the observed data. Researchers rely on quantitative model selection criteria to make this decision objectively. A fundamental approach involves assessing the model's prediction accuracy using metrics like the Standard Error of Estimate (Se), often calculated as a root-mean-square error (RMSE) between observed flood magnitudes and the values predicted by the fitted distribution (Fawad et al., 2022b). In practice, this often takes the form of a Root Mean Square Error (RMSE) comparing empirical data points to the fitted distribution (Fawad et al., 2022b). The most common are the Akaike Information Criterion (AIC) and the Bayesian Information Criterion (BIC), as noted by Chae & Chung (2024). These criteria effectively penalize models that use more parameters (for instance, favoring a simpler two-parameter Gumbel over a three-parameter GEV if the added complexity doesn't significantly improve the fit). The model yielding the lowest AIC or BIC value is typically preferred. For hydrological studies, which often contend with relatively short data records (perhaps only tens of years), the Corrected Akaike Information Criterion (AICc). To address this, information-theoretical criteria are widely employed because they balance goodness-of-fit with model parsimony. For hydrological applications where data records are often limited (e.g., tens of years), the Corrected Akaike Information Criterion (AICc) is particularly recommended, as it provides an

adjustment to AIC that accounts for small-sample bias (Burnham & Anderson, 2002). Using AICc helps ensure the chosen model isn't overly complex relative to the available data, a benefit highlighted in studies showing improved distribution identification for typical hydrological record lengths (e.g., Bako et al., 2024). Sometimes, results from multiple criteria are combined using a Global Ranking Score (GRS) to provide a composite assessment. Increasingly, best practice involves using several criteria together; for example, Alam & Mahmud (2022) utilized Se, AICc, and GRS in Bangladesh to determine that the GEV distribution was optimal for their study basins, illustrating the move towards comprehensive, multi-criteria model selection in recent FFA literature.

### *2.3.2 Drought*

Droughts represent complex phenomena characterized by prolonged periods of water scarcity, and they are typically classified into different types based on their underlying causes, development, and primary impacts. The main categories include meteorological, agricultural, hydrological, and socio-economic droughts, each varying significantly in their duration, intensity, and effects on both the environment and human society.

**1. Meteorological Drought**

The onset of drought typically begins with a meteorological drought, which occurs when an area experiences a significant deficit in precipitation compared to its long-term historical average over a specific period. Its severity is often influenced by related climatic factors such as rising temperatures, shifts in atmospheric circulation patterns, and increased evaporation rates (Xuehua et al., n.d.) If a meteorological drought persists, it frequently acts as a trigger, leading to the development of other forms, notably agricultural and hydrological droughts (Dirnböck et al., 2025).

A primary tool for quantifying meteorological drought is the Standardized Precipitation Index (SPI**)**(Ganguli et al., 2025a). Developed by McKee, Doesken, and Kleist (1993), the SPI is globally recognized for its ability to characterize precipitation deficits or surpluses across various time scales. Its strength lies in its standardization, allowing for meaningful drought condition comparisons between different regions and climates. The calculation requires a long-term precipitation record (typically 30+ years) and involves fitting a probability distribution (often Gamma) to aggregated precipitation totals for a chosen timescale (e.g., 1, 3, 6, 12 months). The cumulative probability of the observed precipitation is then

transformed into a standard normal distribution value –the SPI – representing how many standard deviations the observed precipitation deviates from the long-term mean for that timescale (McKee et al., 1993; World Meteorological Organization, 2012). SPI values are interpreted using standardized categories, ranging from extremely wet (SPI ≥ 2.0) to extreme drought (SPI ≤ -2.0). The chosen timescale is critical for interpretation, reflecting impacts from short-term soil moisture (3-month SPI) to long-term hydrological systems (12+ month SPI) (Hayes et al., 1999).

While the SPI's simplicity and standardization are valuable, a notable weakness is its failure to incorporate the influence of temperature and potential evapotranspiration (PET) on water availability. This is particularly relevant in a warming climate where rising temperatures increase evaporative demand, potentially intensifying drought conditions even without changes in precipitation. To address this limitation, the Standardized Precipitation Evapotranspiration Index (SPEI) was developed (Vicente-Serrano et al., 2010). The SPEI follows a similar calculation methodology to the SPI but uses the monthly difference between precipitation (P) and potential evapotranspiration (PET) as the input variable, rather than precipitation alone. PET represents the atmospheric demand for moisture and is typically estimated using temperature data along with other variables depending on the chosen method (e.g., Thornthwaite, Penman-Monteith). However, the SPEI requires additional input data (at least temperature) and its results can be influenced by the method used to estimate PET. Like the SPI, its accuracy can also be sensitive to the choice of probability distribution (Stagge et al., 2015).

**2. Agricultural Drought**

Following or overlapping with meteorological droughts, agricultural droughts occur when soil moisture levels fall below what is needed to sustain healthy crop growth and livestock production. While often triggered by prolonged lack of rain (meteorological drought), it can be exacerbated by factors like inefficient irrigation practices, increased evaporative demand (linked to temperature, as captured by indices like SPEI), and soil degradation (Eshetae et al., 2025). Indicators used to monitor this type of drought include various soil moisture indices and the Crop Moisture Index (CMI) (Leguizamón et al., 2025). With climate change increasing the frequency of extreme weather, agricultural droughts are

expected to become more severe, particularly impacting vulnerable arid and semi-arid regions (Sanusi & Dries, 2025).

### 3. Hydrological Drought

Hydrological drought occurs when water levels in rivers, lakes, reservoirs, and groundwater sources fall below their long-term averages. Unlike meteorological drought, which focuses on precipitation deficits, hydrological drought deals with water availability and storage issues (van der Sleen et al., 2025). This type of drought can take months or years to develop and is commonly assessed using the Streamflow Drought Index (SDI) and the Groundwater Drought Index (GDI) (Ganguli et al., 2025b)(. It significantly impacts domestic water supply, agriculture, and hydropower production (Alotaibi et al., 2025).

## 2.4 Similar Regions

Comparing high-altitude semi-arid regions such as Ladakh (India), Tibet (China), and Central Asia highlights common climate challenges, including droughts, extreme precipitation events, and water resource dependency on glacial melt. Recent research further underscores these regional trends. Ayugi et al. (2019) compared precipitation trends across Kenya, Central Asia, and Ladakh, finding that drought conditions in these regions are intensifying due to rising temperatures and changing monsoonal behavior. Similarly, (Bammou et al., 2024) optimized flood risk mapping in semi-arid Morocco, providing applicable methodologies for flood-prone regions like Central Asia. In addition,(Dar et al., 2024) conducted satellite-based flood monitoring in semi-arid regions, enhancing predictive flood modeling techniques for Ladakh and Tibet, thereby improving disaster preparedness and water resource management.

## 2.5 Comparative Study: Floods and Droughts in Spiti Valley (India) vs. Mustang (Nepal)

Both Spiti Valley (India) and Mustang (Nepal) are high-altitude, semi-arid regions located in the rain shadow of the Himalayas. These regions experience extreme climatic conditions, including prolonged droughts and sudden flash floods, primarily influenced by glacier melt, monsoon variability, and climate change. Despite these similarities, differences in geography, hydrology, and cultural adaptation strategies shape their distinct climate challenges and responses.

*Table 2-1 Comparison between Spiti Valley (India) and Mustang (Nepal)*

| **Feature** | Spiti Valley (India) | Mustang (Nepal) |
|---|---|---|
| **Location** | Himachal Pradesh, India | Gandaki Province, Nepal |
| **Altitude** | 3,300m – 4,600m | 2,500m – 4,200m |
| **Climate Type** | Cold Desert, Semi-Arid | Semi-Arid, Alpine Desert |
| **Annual Precipitation** | < 200 mm | 250-400 mm |
| **Monsoon Influence** | Minimal (Rain Shadow of the Himalayas) | Weak but slightly stronger than Spiti |
| **Glacier Dependency** | High (Snow-fed Rivers) | High (Glacial Melt Rivers) |
| **Major Water Sources** | Spiti River, Snowmelt | Kali Gandaki River, Glacial Melt |
| **Extreme Weather Events** | Cloudbursts, Flash Floods, GLOFs, Droughts | Flash Floods, , Droughts |

**Key Similarities**

1. **Rain Shadow Effect**: Both Spiti and Mustang lie in the rain shadow of the Himalayas, receiving very little precipitation, making them highly arid and water scarce.
2. **Glacier Dependency**: Water resources in both regions rely on glacial melt, as there is minimal rainfall to sustain rivers.
3. **Extreme Weather Events**: Both regions face frequent flash floods and GLOFs, primarily due to climate change-driven glacial melting and high-intensity rainfall events.
4. **Drought Conditions**: Due to low rainfall and increasing evapotranspiration, both regions experience long dry periods, which exacerbate water scarcity and soil degradation.

## 2.6 Gaps in Existing Research on Climate Change in Mustang

Mustang, a semi-arid, high-altitude region in Nepal, is highly vulnerable to climate change impacts, including droughts, floods, glacial retreat, and temperature extremes. However, significant gaps remain in research, particularly in long-term climate datasets, localized flood and drought modeling, and the integration of socioeconomic impacts into climate projections. One of the major gaps in climate research in Mustang is the lack of long-term climate datasets. The region has sparse weather stations, leading to incomplete climate records, and data collection has been discontinuous, making it difficult to analyze temperature and precipitation trends over time. The absence of long-term hydrological data also affects water resource management, particularly in understanding glacial meltwater fluctuations and river flow patterns. Studies such as (Shrestha & Prasain, 2016) have identified major climate data gaps, emphasizing that the lack of high-altitude climate monitoring stations creates barriers for water stress modeling and climate-induced migration assessments.

Another major challenge is the lack of localized flood and drought modeling, as existing General Circulation Models (GCMs) lack regional precision, failing to capture Mustang's complex topography. Apart from hydrological and meteorological aspects, socioeconomic factors play a crucial role in understanding climate change impacts in Mustang. Climate change affects livelihoods, agriculture, and migration patterns, yet most climate models focus only on physical changes, ignoring the human dimensions of climate adaptation. Farmers in Mustang are experiencing declining crop yields due to erratic rainfall, soil degradation, and failing traditional irrigation systems, which depend on glacier-fed rivers. Additionally, climate-induced migration is increasing, as many households abandon villages due to water shortages and unpredictable weather patterns, leading to a rise in "climate refugees" migrating to urban areas in search of economic stability. Bom et al. (2023)found that Mustang's economy is deeply tied to climate-dependent tourism and agriculture, making it particularly vulnerable to climate variability. By improving climate data collection, refining localized climate models, and incorporating socioeconomic factors into climate projections, Mustang can develop more effective adaptation strategies to withstand the growing impacts of climate change.

## CHAPTER 3: STUDY AREA

Mustang, located in the rain shadow of the Annapurna and Dhaulagiri ranges, is a semi-arid, high-altitude region in western Nepal. Its hydrological and meteorological conditions are influenced by its unique topography, dependence on glacial meltwater, and seasonal climate variations. The low precipitation levels, high evaporation rates, and strong diurnal temperature differences create extreme climatic conditions, making water availability a major challenge for local communities. The following sections explore the rain shadow effect on precipitation, seasonal and interannual climate variations

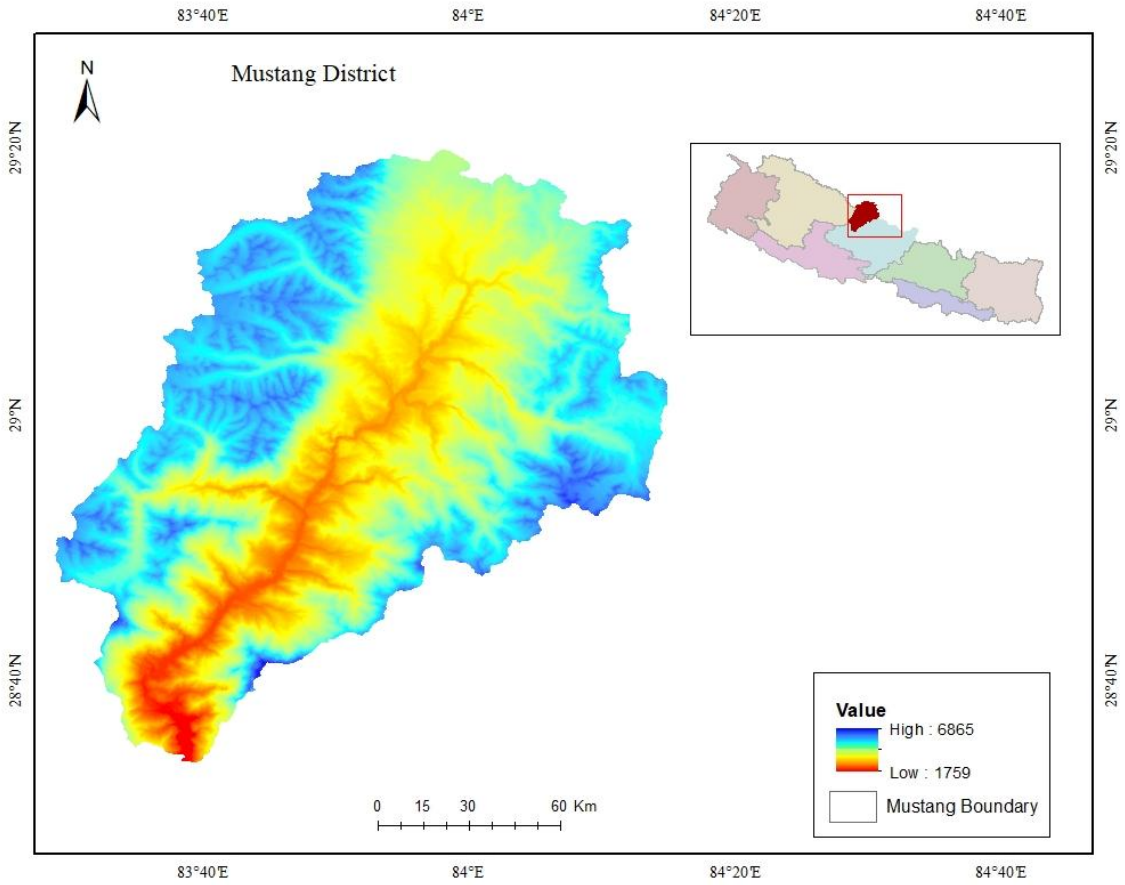


*Figure 3-1 Location and topographic variation of the study area. A map of Nepal is shown in the inset.*

### 3.1 Rain Shadow Effect and Its Impact on Precipitation Levels

The rain shadow effect plays a crucial role in shaping Mustang's climate. The Himalayan ranges, particularly Annapurna and Dhaulagiri (over 8,000 meters high), act as a natural barrier, blocking moisture-laden monsoonal winds from the south. This leaves Mustang dry and arid, receiving significantly less precipitation

than the southern slopes of the Himalayas, where rainfall can exceed 3,000 mm annually. Mustang, in contrast, receives only 250–400 mm of rainfall per year, making it one of the driest regions in Nepal. Although monsoonal storms occasionally spill over, the precipitation contribution is minimal, and winter snowfall from westerly disturbances remains a crucial moisture source for the region's glacier-fed rivers.

Due to this low precipitation, Mustang exhibits desert-like conditions, where vegetation is sparse, and agriculture depends on glacial meltwater. The strong diurnal temperature variation, caused by the absence of cloud cover, results in hot days and freezing nights, further complicating water conservation. High solar radiation and low humidity levels lead to significant water loss through evaporation, exacerbating drought risks. Recent research by (Dhakal et al., 2024) used remote sensing data to analyze groundwater and precipitation variability in Mustang, finding that declining water availability is directly linked to the rain shadow effect and increasing temperatures.

### 3.2 Seasonal and Interannual Variations in Temperature and Precipitation

The hydroclimatic regime of Mustang is distinctly characterized by its location within a Himalayan rain shadow, differentiating it significantly from the monsoon-dominated patterns prevalent in southern Nepal. Consequently, the summer monsoon (June–September) contributes a relatively modest portion (approximately 30%) of the annual precipitation budget. Instead, winter precipitation, primarily snowfall derived from western disturbances (December–February), assumes a critical role in sustaining regional water resources. However, contemporary climate change is demonstrably altering these established patterns, leading to increased frequency of droughts and hydroclimatic extremes. Corroborating this, (Dhakal et al., 2024) observed trends of declining annual precipitation alongside rising temperature extremes, which collectively exert negative pressure on agricultural productivity and water security. Complementing these precipitation dynamics, Mustang exhibits pronounced temperature variability, both seasonally – with summer averages ranging from 10°C to 25°C contrasted against winter lows potentially below -15°C – and diurnally, marked by rapid daytime warming and freezing nocturnal temperatures attributed to the thin, arid atmosphere. Significantly, this region is experiencing an accelerated warming trend, estimated at approximately 0.5°C per decade. This warming is a primary driver of accelerated glacial melt and permafrost degradation, further

impacting downstream river discharge regimes, overall water availability, and landscape stability.

### 3.3 Role of Glacial Meltwater, Permafrost, and Runoff in Mustang's Hydrology

Given its low precipitation levels, Mustang's hydrology is heavily dependent on glacial meltwater, runoff patterns, and the stability of permafrost.Mustang's hydrology is intricately linked to its high-altitude cryosphere, particularly the glaciers of the Damodar, Dhaulagiri, and Annapurna ranges which feed vital river systems like the Kali Gandaki. However, this reliance creates significant vulnerability in the face of climate change. Rising temperatures are driving accelerated glacial retreat, presenting a concerning paradox: while the rapid melting initially boosts river runoff, this is a short-term effect.

Alongside glacial changes, the thawing of high-altitude permafrost represents another major climate change impact in Mustang. This degradation of permanently frozen ground triggers several critical consequences. Firstly, it destabilizes mountain slopes, increasing the frequency and severity of landslides and rockfalls, which pose direct threats to infrastructure and settlements. Secondly, permafrost acts as a significant, often overlooked, frozen water reservoir; its thaw leads to the loss of this stored moisture, further compounding water availability issues, particularly in drier periods. Thirdly, meltwater from both thawing permafrost and shrinking glaciers carries higher sediment loads into rivers like the Kali Gandaki. These changes directly influence Mustang's highly seasonal runoff cycle. River discharge peaks during the summer months (June–September), fed by intensified glacial melt and any monsoonal rains. Conversely, the winter period sees minimal precipitation and reduced melt, leading to pronounced water shortages that impact local communities and agriculture.

## CHAPTER 4: METHODOLOGY

The methodology adopted in this study integrates both drought and flood analysis using observed and climate model data. Initially, precipitation and temperature data from the Department of Hydrology and Meteorology (DHM) were supplemented with missing values using the APHRODITE dataset. Multiple Global Climate Models (GCMs) and scenarios were selected to generate bias-corrected historical and future datasets. These datasets were then used for two separate analyses. For drought assessment, the standardized indices SPI and SPEI were computed. For flood analysis, annual maximum precipitation series were extracted and fitted to Generalized Extreme Value (GEV) and Gumbel distributions. The best-fitting models were selected based on goodness-of-fit evaluations and return levels representing different flood magnitudes were calculated.

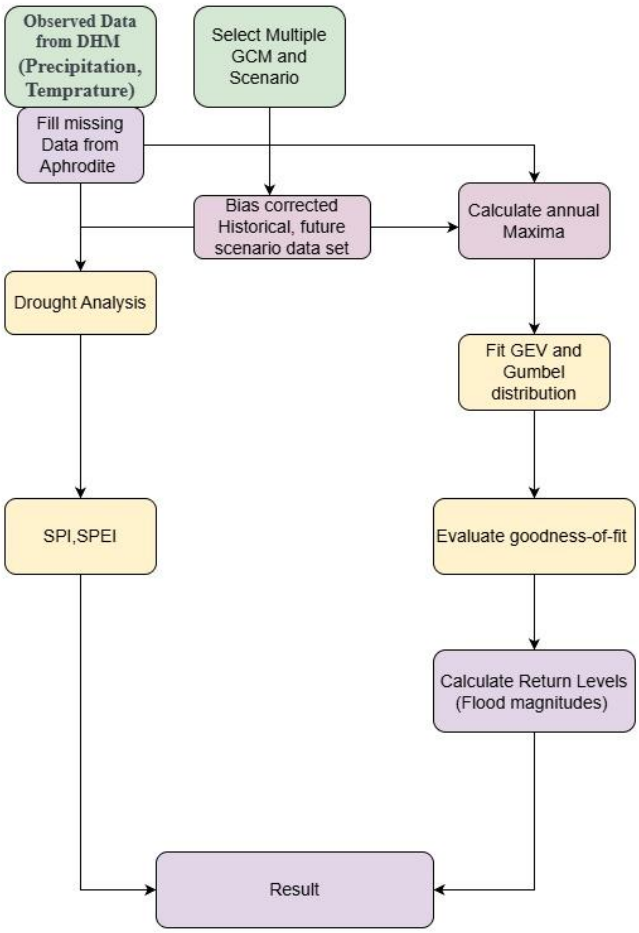


*Figure 4-1 Methodological framework*

## 4.1 Data Collection

### *4.1.1 Climate data sources for Mustang, Nepal*

Historical climate data for Mustang is primarily collected from global reanalysis datasets, regional climate archives, and Nepal's Department of Hydrology and Meteorology (DHM Nepal). APHRODITE (Asian Precipitation - Highly Resolved Observational Data Integration Towards Evaluation): A high-resolution gridded precipitation dataset for Asia, covering daily precipitation records from 1951 onward. APHRODITE's precipitation data (0.25° × 0.25° resolution) is particularly useful for understanding monsoon variability, extreme rainfall events, and seasonal trends in Mustang.

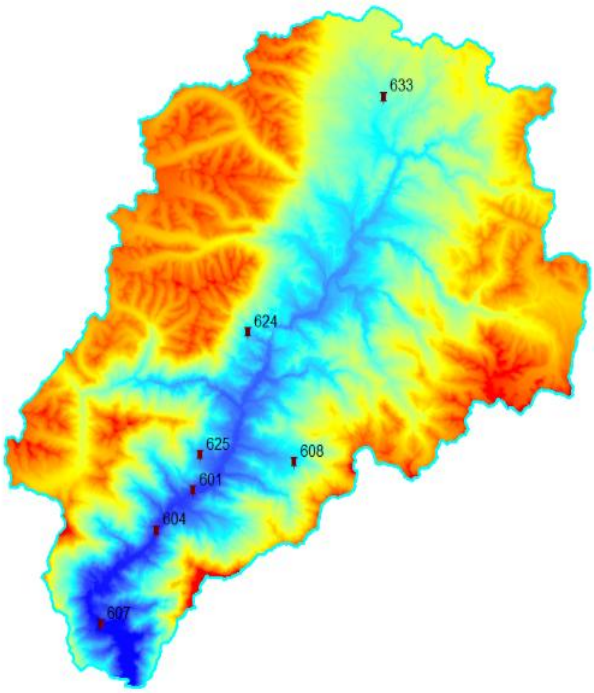


*Figure 4-2 Location of meteorological stations used in this study in Mustang.*

*Table 4-1 Meteorological Stations in Mustang District*

| Station ID | Stations | Lat | lon | Elevation(m) |
|---|---|---|---|---|
| 601 | Jomsom | 28.78 | 83.78 | 2741 |
| 604 | Thakmarpha | 28.72 | 83.67 | 2655 |
| 607 | Lete | 28.62 | 83.59 | 2490 |
| 608 | Ranipauwa | 28.4 | 84 | 3671 |
| 624 | Samar Gaun | 28.52 | 84.25 | 3610 |
| 625 | Dhakarjhong | 28.88 | 84.5 | 3200 |
| 633 | Chhoser | 28.98 | 84.34 | 3886 |

### *4.1.2 Future climate projections*

**(A) Climate Models: CMIP6 (SSP2-4.5, SSP5-8.5)**

The Coupled Model Intercomparison Project Phase 6 (CMIP6) provides multi-model climate projections that improve upon previous CMIP5 models by incorporating higher spatial resolution, refined emission scenarios, and improved cloud-aerosol interactions. Two key Shared Socioeconomic Pathways (SSPs) used for future projections are:

- **SSP2-4.5 (Intermediate Emissions Scenario)**: Represents a middle-of-the-road pathway where global efforts to mitigate climate change continue but are not aggressive enough, resulting in a moderate increase in temperature and associated climate impacts.
- **SSP5-8.5 (High Emissions Scenario)**: Represents a high-emissions, fossil-fuel-driven economy, where carbon-intensive energy use dominates, leading to a drastic rise in global temperatures and severe climate consequences.

**(B). Downscaling Techniques for Regional Accuracy**

While CMIP6 models offer robust global climate projections, their coarse resolution (~50–100 km grids) limits accuracy for regional applications. To improve precision for Mustang Statistical Downscaling is used. It uses historical climate data and statistical relationships to adjust GCM outputs to local scales, improving accuracy for precipitation and temperature variability. Gamma distribution for precipitation was used for bias correction(Gadouali et al., 2024)

*Table 4-2 Details of GCM used on this study*

| Model Name | Latitude Resolution | Longitude Resolution | Historical Period | Projection Period |
|---|---|---|---|---|
| ACCESS-ESMI-5 | 1.5 | 1.875 | 1980-2014 | 2025-2100 |
| EC-EARTH3-VEG | 0.7018 | 0.7031 | 1980-2014 | 2025-2100 |
| EC-EARTH3 | 0.7018 | 0.7031 | 1980-2014 | 2025-2100 |
| MPI-ESMI-2-HR | 0.9351 | 0.9375 | 1980-2014 | 2025-2100 |
| MPI-ESMI-2-LR | 1.8653 | 1.875 | 1980-2014 | 2025-2100 |
| MRI-ESM2-0 | 1.1215 | 1.1215 | 1980-2014 | 2025-2100 |

## 4.2 Trend Analysis of Precipitation and Temperature

To assess long-term trends in precipitation and temperature patterns in the Mustang region, statistical methods will be employed to detect monotonic trends and estimate their magnitude:

**Mann-Kendall Test:** A non-parametric test used to identify significant trends in climatic variables over time, making it suitable for non-normally distributed and missing data.

**Sen's Slope Estimator:** A robust method for determining the magnitude of trends, providing a median slope that is less sensitive to outliers compared to parametric regression methods.

### Spatial Averaging Using the Thiessen Polygon Method

The Thiessen polygon method, a widely used spatial interpolation technique in hydrology (Zhou et al., 2009), is applied to calculate basin-averaged climatic variables, particularly precipitation. The watershed is divided into polygons (also known as Voronoi diagrams), with each polygon corresponding to the nearest meteorological station. It is assumed that the measured value at a station represents the entire area of its respective polygon. The basin-wide average precipitation is then estimated using a weighted average based on the area each station influences. To estimate the region's average precipitation, a weighted mean

is calculated where each station's measurement is multiplied by the area of its corresponding polygon. The general expression for this calculation is:

$\bar{P} = (1 / A\_total) \times \Sigma (P_i \times A_i)$……(1)

Here,

**$\bar{P}$** is the average precipitation over the entire basin,
**$P_i$** is the precipitation recorded at station i,
**$A_i$** is the area of the polygon assigned to station i,
**A_total** is the total area of the watershed,
**n** is the number of observation stations.

### 4.3 Drought Analysis

Drought conditions in Mustang are assessed using two key components: spatial averaging of precipitation using the Thiessen polygon method and the computation of the Standardized Precipitation Index (SPI).

**Standardized Precipitation Index (SPI):**

Computed based on precipitation anomalies over different timescales (e.g., 3, 6, 12 months), providing a probabilistic measure of meteorological drought severity. SPI is calculated using a gamma distribution fitted to long-term monthly precipitation data.

**Equations for SPI**

Step 1: Fit Gamma Distribution

Gamma Probability Density Function:

$$g(x) = \frac{1}{\beta^{\alpha}\Gamma(\alpha)} x^{\alpha-1} e^{-x/\beta} \quad \ldots\ldots\ldots\ldots\ldots\ldots (2)$$

Where:

x = Precipitation amount

α = Shape parameter

β = Scale parameter

Γ(α) = Gamma function

Parameters α and β are estimated using:

$\alpha = \ln(\bar{x}) - \frac{1}{n}\sum_{i=1}^{n} \ln(x_i)$ …….. (3)

$\beta \approx \frac{\bar{x}}{\alpha}$ …….. (4)

Step 2: Compute Cumulative Probability

Compute the cumulative probability and adjust for zero precipitation events.

Step 3: Standardize Using Normal Distribution

$SPI = \Phi^{-1}\big(F(x)\big)$ …….. (5)

Where:

F(x) = Cumulative probability

$\Phi^{-1}$ = Inverse standard normal distribution

**Standardized Precipitation Evapotranspiration Index (SPEI):**

Extends SPI by incorporating potential evapotranspiration (PET), making it more suitable for assessing droughts influenced by temperature variations and precipitation. Both indices will be computed using historical observed from DHM and future (CMIP6 projections) climate datasets, with bias correction applied where necessary.

**Equations for SPEI**

SPEI is based on the climatic water balance and incorporates temperature via PET:

D = P – PET…….. (6)

Where:

P = Precipitation

PET = Potential evapotranspiration

Thornthwaite PET Equation

$PET = 16\left(\frac{L}{12}\right)\left(\frac{N}{30}\right)\left(\frac{10T}{I}\right)^{a}$ …….. (7)

Where:

T = mean monthly temperature (°C)

I = annual heat index = $I = \sum_{i=1}^{12} \left(\frac{T_i}{5}\right)^{1.514}$ ……(8)

$a = 6.75 \times 10^{-7} I^3 - 7.71 \times 10^{-5} I^2 + 1.79 \times 10^{-2} I + 0.49239$

L = average day length (hours)

N = number of days in month

Step 2: Fit Log-Logistic Distribution

To the series D (deficit/surplus):

F(x) = $F(D) = \left[1 + \left(\frac{\beta}{D-\gamma}\right)^{\alpha}\right]^{-1}$ …… (9)

Step 3: Standardize Using Normal Distribution

SPEI is calculated by applying the inverse standard normal distribution to F(x).

### 4.4 Procedure for Probability-Based Flood Frequency Estimation

This methodology involves several steps to analyze extreme rainfall events and determine suitable probability distribution models. Daily rainfall data were collected and used as the primary input for flood frequency analysis. To model the extremes, both the Gumbel distribution (Type I Extreme Value) and the Generalized Extreme Value (GEV) distribution were applied. The GEV distribution, which is a flexible family of distributions for modeling maxima, includes three types: Type I (Gumbel), Type II (Fréchet), and Type III (Weibull). For estimating the parameters of these distributions, three statistical methods were employed: the Method of Moments (MoM), Maximum Likelihood Estimation (MLE), and the L-Moments (LM) method. These methods provide different approaches to derive the parameters based on sample data characteristics. To assess the suitability and accuracy of the fitted models, various goodness-of-fit tests—also known as adhesion tests—were conducted. These included the Kolmogorov–Smirnov (KS) test, the Anderson–Darling (AD) test, and the Filliben Correlation Coefficient (RT), each offering different sensitivity to deviations between observed and modeled data. Finally, model selection was based on performance metrics such as the Standard Error of Estimate (Se), the Corrected Akaike Information Criterion (AICc), and the Global Ranking Score (GRS), ensuring a robust comparison to identify the most appropriate model for representing extreme rainfall behavior.

# CHAPTER 5: RESULT AND DISCUSSIONS

## 5.1 Trend Analysis of Seasonal Precipitation Across Seven Stations in Mustang

The precipitation trend analysis across multiple stations, including Chhoser, Dhakarjhong, Jomsom, Lete, Ranipauwa, Samargaun, and Thakmarpha, reveals distinct seasonal variations over time. Most stations show an increasing trend in monsoon precipitation, with Ranipauwa (3.77 mm per year) and Thakmarpha (1.93 mm per year) experiencing the highest rise, suggesting intensified monsoon rainfall and potential flood risks. In contrast, post-monsoon precipitation is either slightly declining or showing minimal change, as seen in Chhoser (-0.0648 mm per year), Jomsom (-0.07 mm per year), and Thakmarpha (-0.0302 mm per year), which may reduce water availability during the dry season. Pre-monsoon precipitation is generally increasing across most stations, including Chhoser (0.53 mm per year), Jomsom (0.53 mm per year), and Ranipauwa (1.55 mm per year), indicating possible shifts in early-season rainfall that could impact snowmelt timing and agricultural cycles. Additionally, winter precipitation is on the rise in multiple locations, with Chhoser (1.45 mm per year), Jomsom (1.43 mm per year), and Thakmarpha (1.49 mm per year) showing significant increases, which could contribute to higher snowfall in high-altitude regions and influence glacial melt patterns.

## 5.2 Trend Analysis of Seasonal Temperature Trends in Mustang:

The analysis of seasonal temperature trends in Chhoser, Jomsom, and Lete reveals distinct patterns of warming and cooling over time. Chhoser exhibits an overall cooling trend across all seasons, with the most significant decline in winter (-0.14°C per year) and pre-monsoon (-0.14°C per year), suggesting a shift toward colder conditions that could impact agriculture and water availability. In contrast, Jomsom shows mixed trends, with warming in winter (0.02°C per year) and post-monsoon (0.06°C per year), but a slight cooling during the monsoon (-0.013°C per year) and pre-monsoon (-0.019°C per year) seasons, indicating changing seasonal dynamics. Meanwhile, Lete experience an overall warming trend, particularly in winter (0.038°C per year), monsoon (0.05°C per year), and post-monsoon (0.056°C per year), with only a slight pre-monsoon cooling (-0.019°C per year). These findings suggest that Chhoser is becoming colder, Jomsom is experiencing seasonal temperature shifts, and Lete is generally warming.

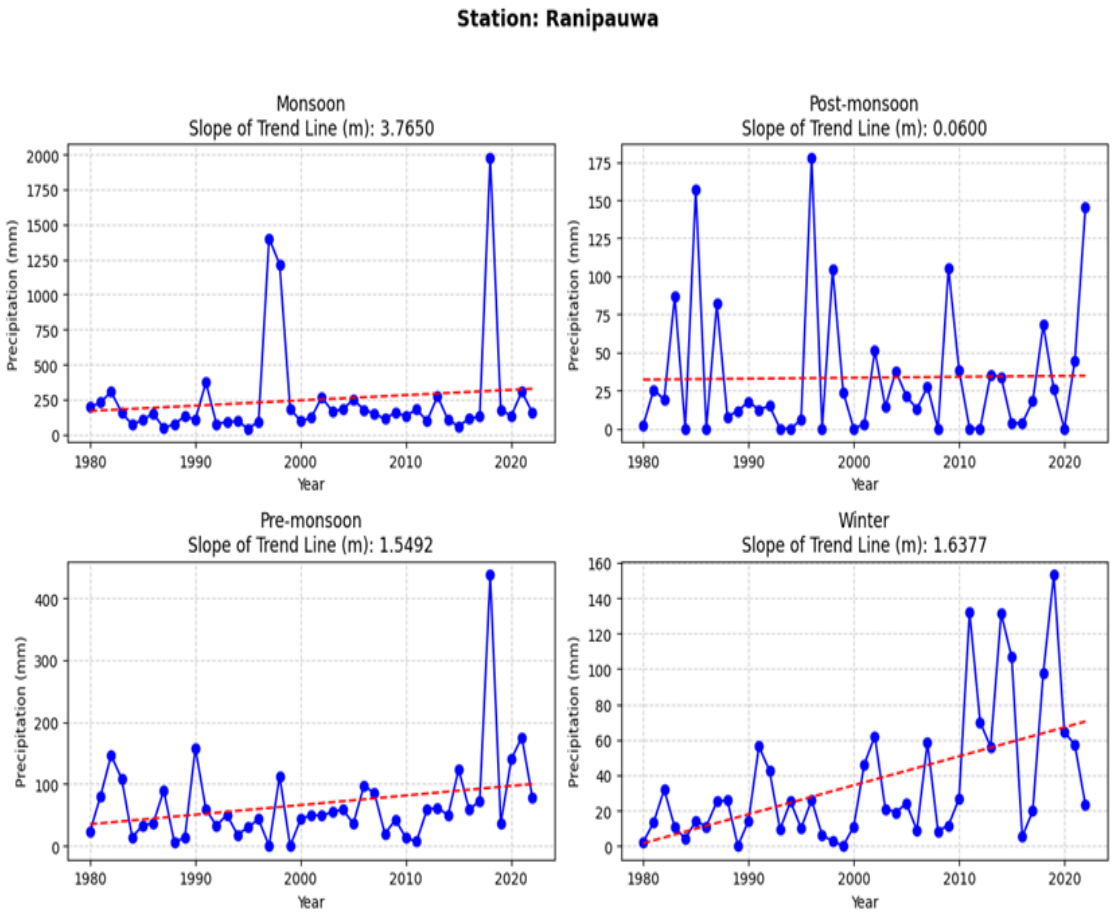


*Figure 5-1 Precipitation trend in monsoon, pre-monsoon, post-monsoon and winter across Ranipauwa*

**Station: Samargaun**

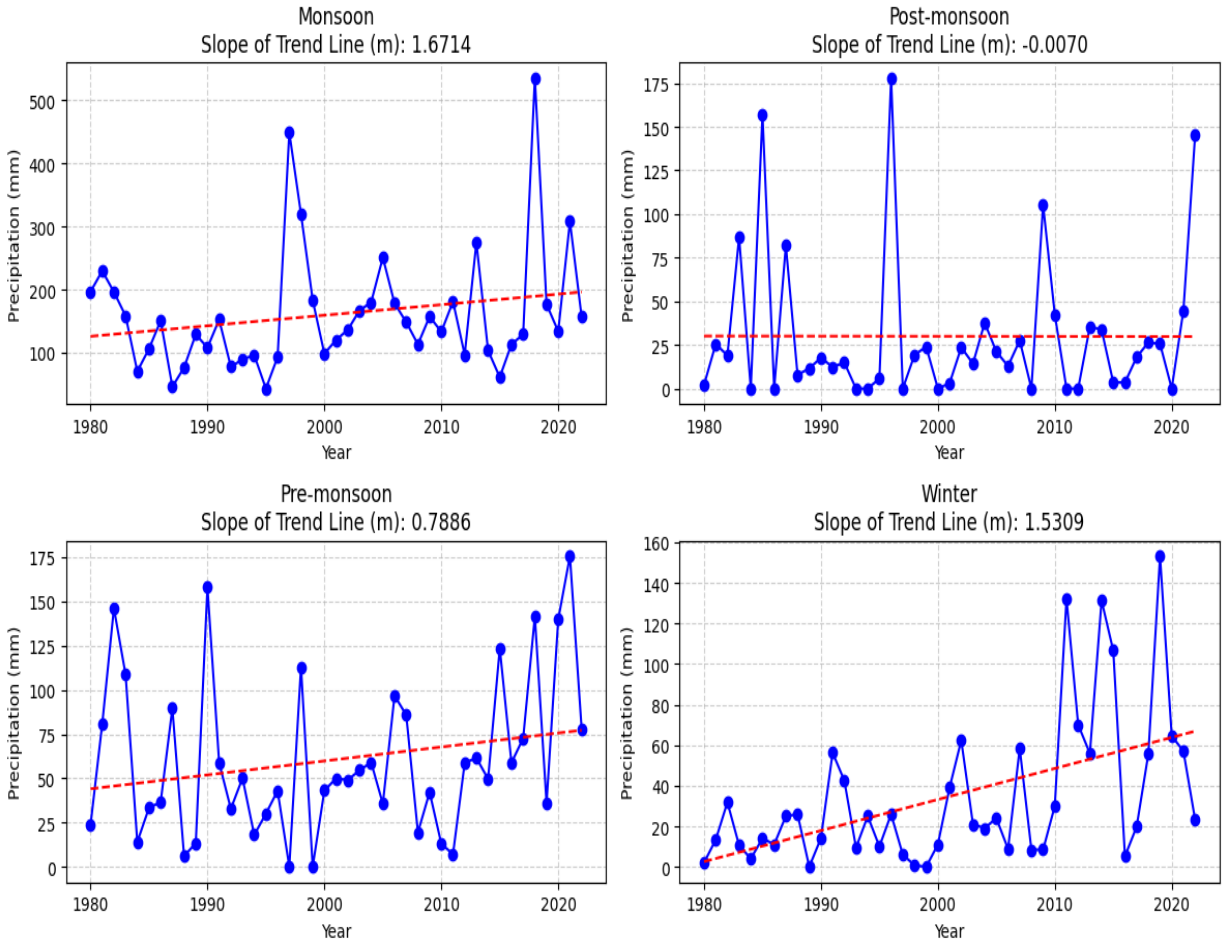

*Figure 5-2 Precipitation trend in monsoon, pre-monsoon, post-monsoon and winter across SamarGaun*

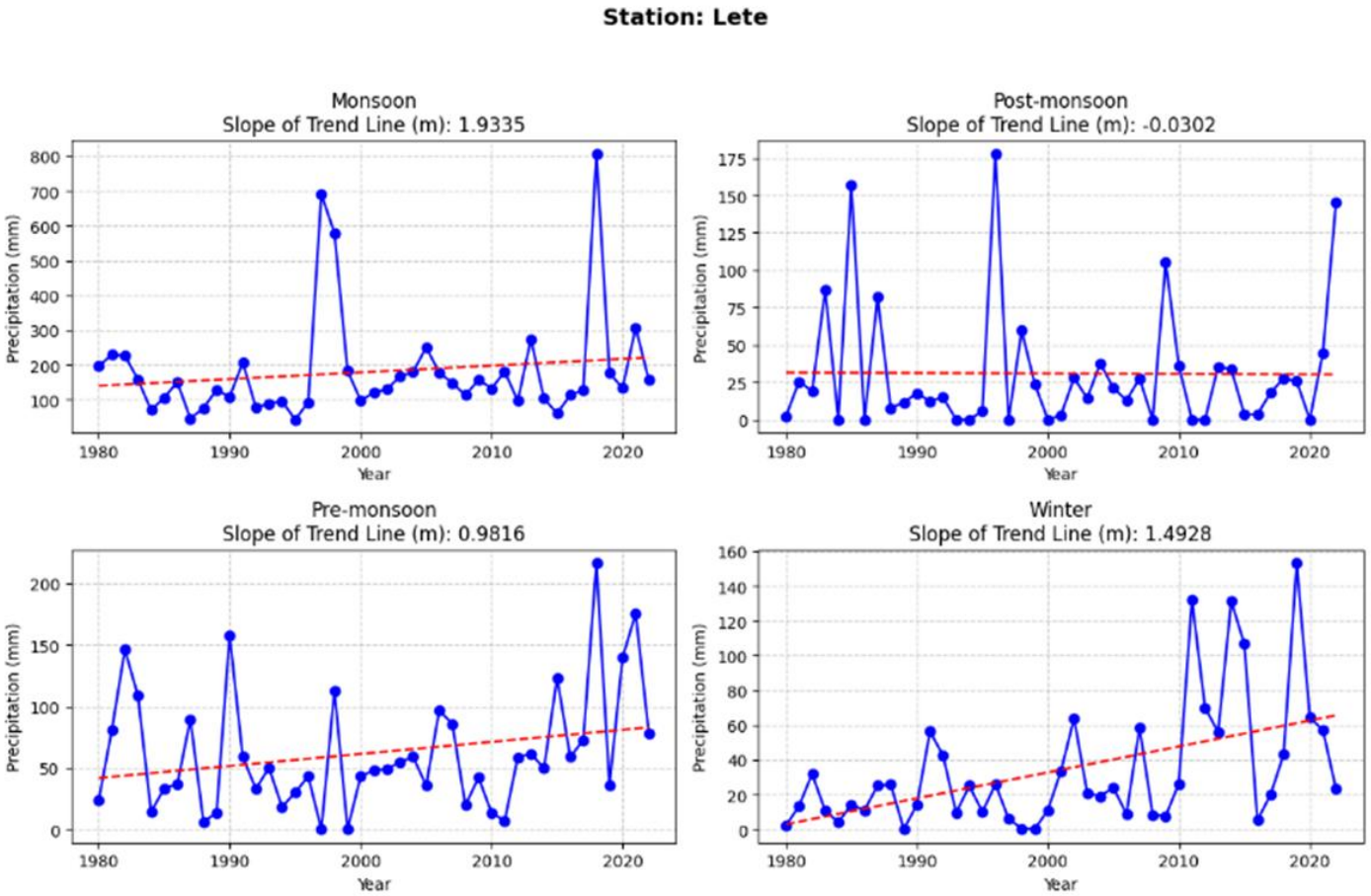


*Figure 5-3 Precipitation trend in monsoon, pre-monsoon, post-monsoon and winter across Lete*

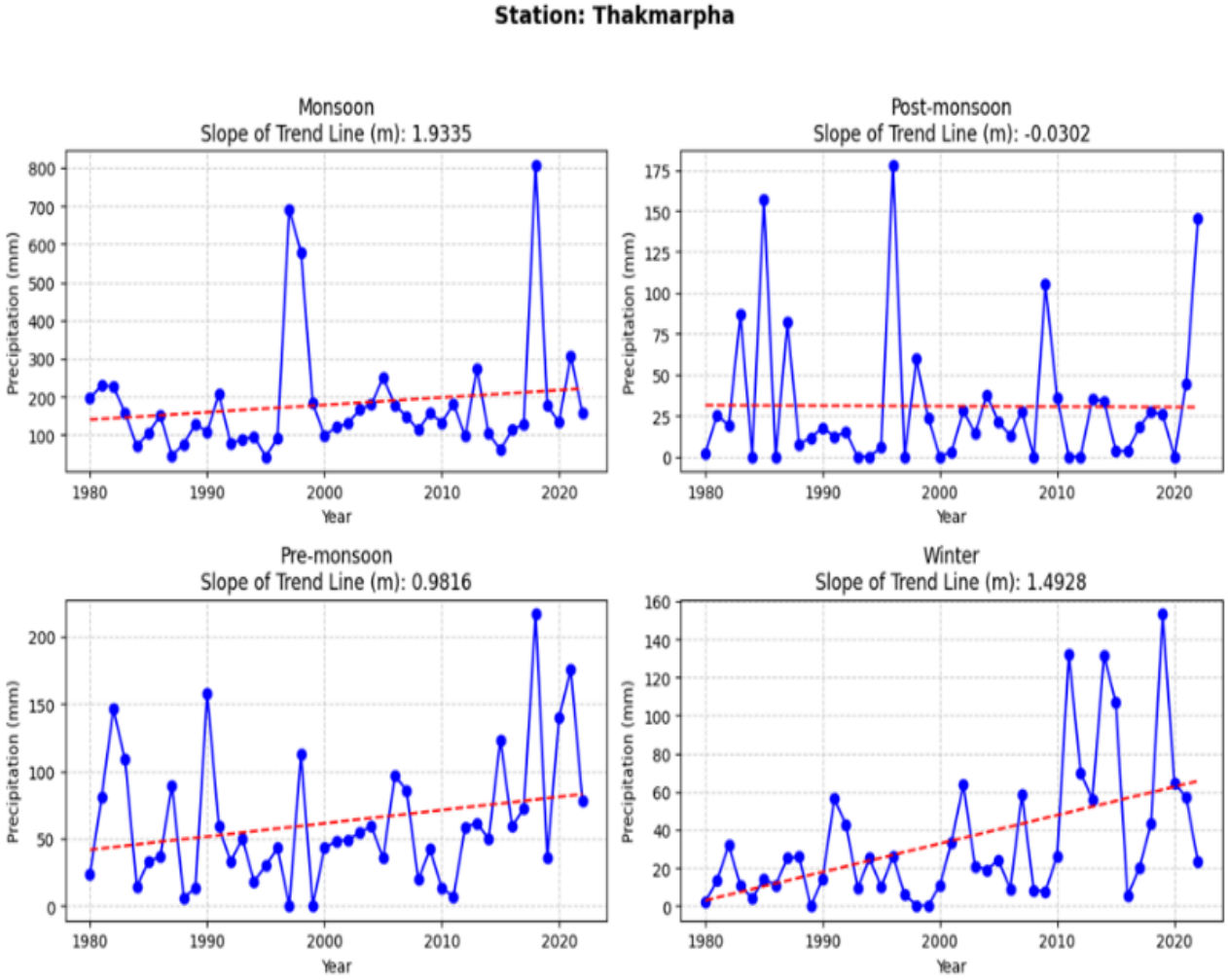


*Figure 5-4 Precipitation trend in monsoon, pre-monsoon, post-monsoon and winter season across Thakmarpha*

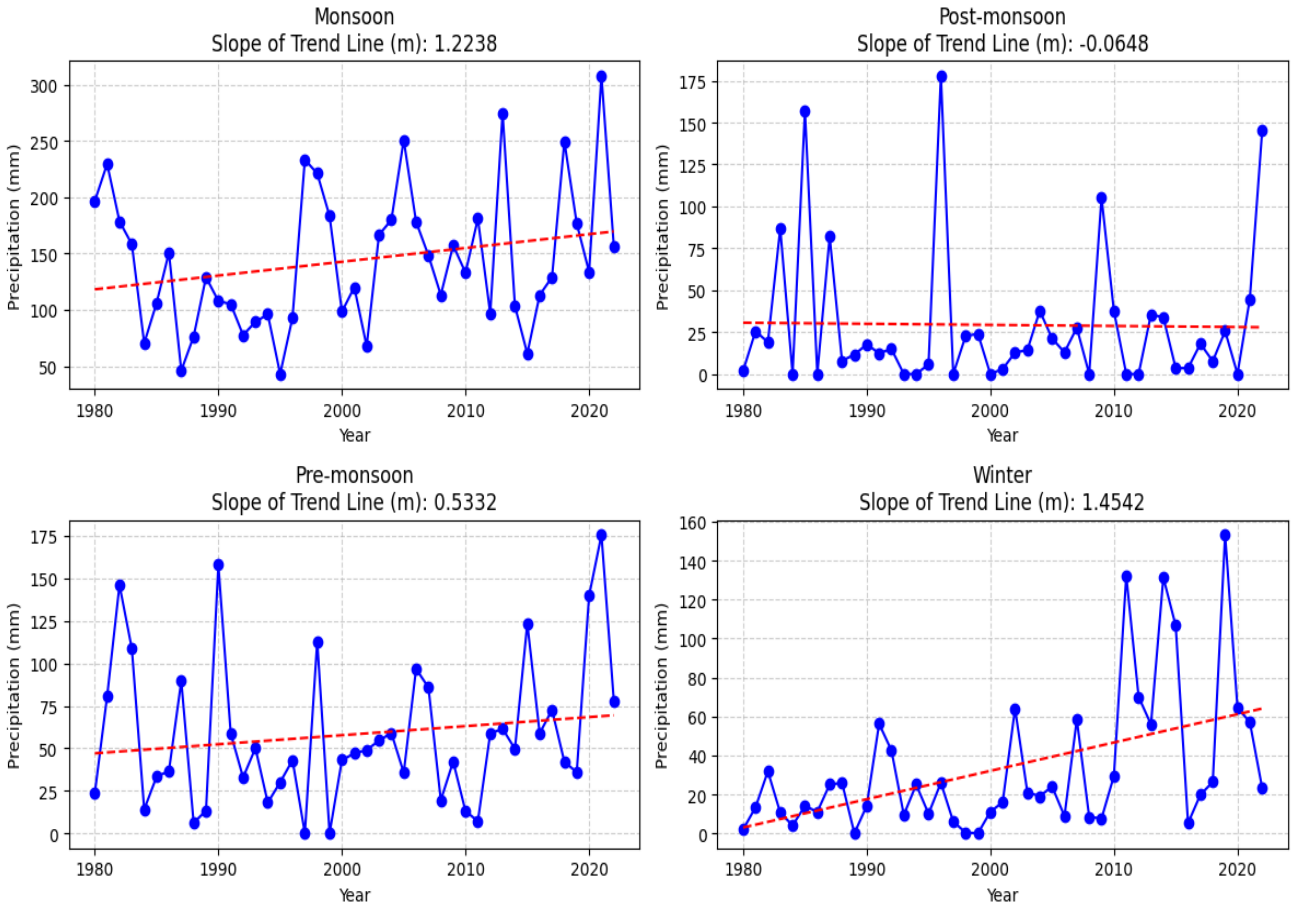


*Figure 5-5 Precipitation trend in monsoon, pre-monsoon, post-monsoon and winter season across Dhakarjhong*

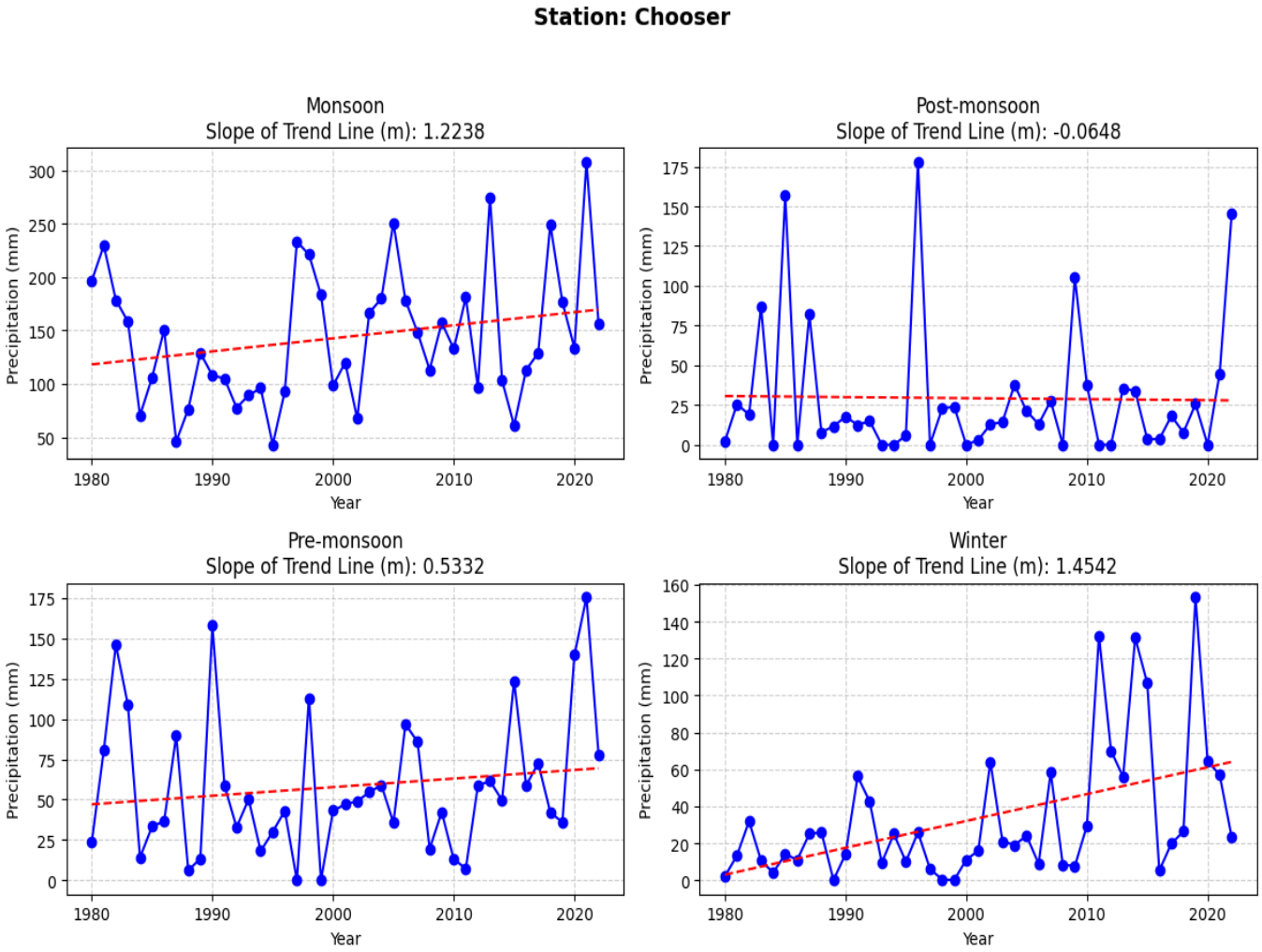


*Figure 5-6 Precipitation trend in monsoon, pre-monsoon, post-monsoon and winter across Chooser*

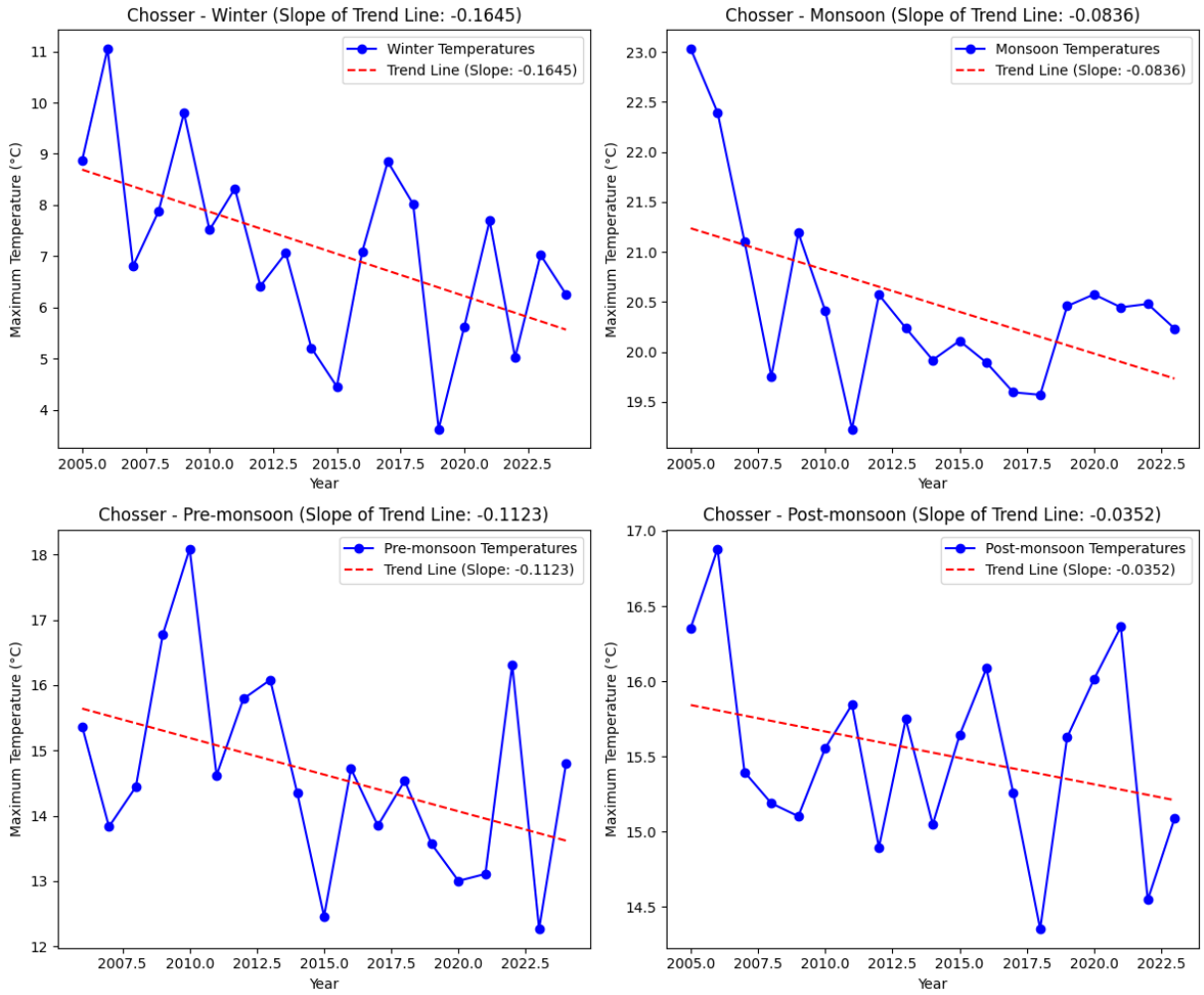


*Figure 5-7 Temperature trend across Chhoser in monsoon, pre-monsoon, post-monsoon and winter season*

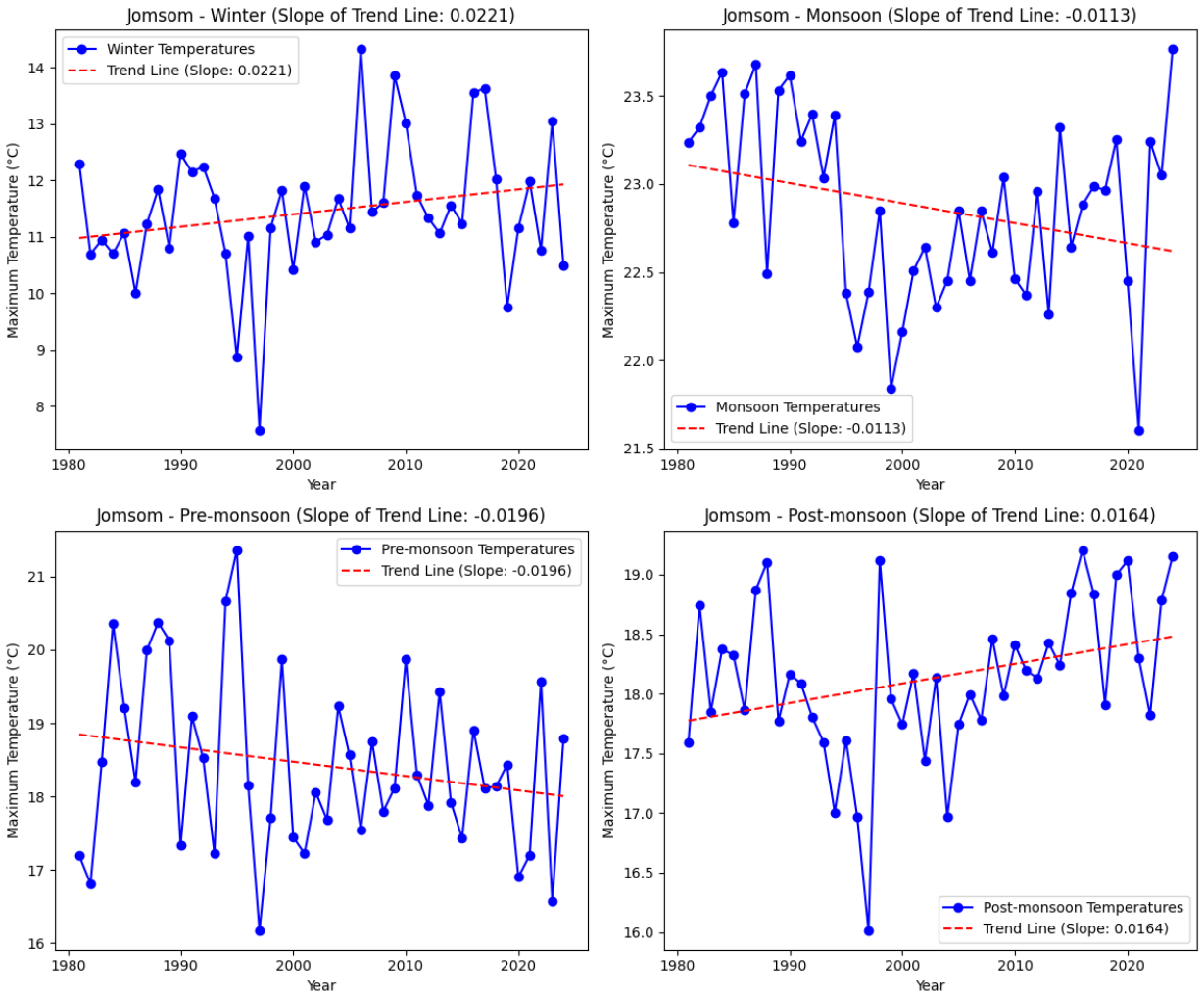


*Figure 5-8 Temperature trend across Jomsom in monsoon, pre-monsoon, post-monsoon and winter season*

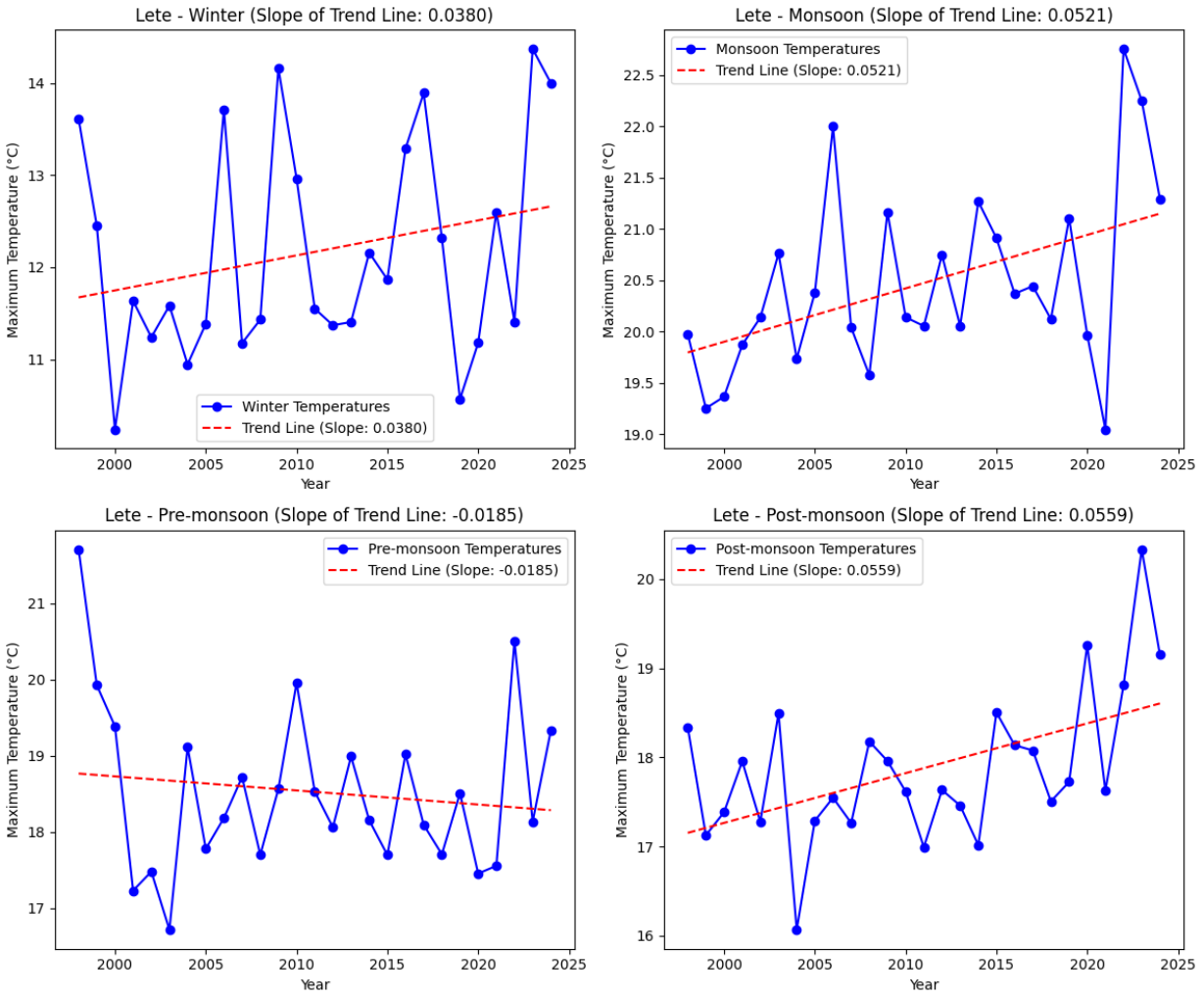


*Figure 5-9 Temperature trend across Lete in monsoon, pre-monsoon, post-monsoon and winter season*

## 5.3 Projected Shifts in Annual Precipitation in Mustang Under CMIP6 Scenario

The annual precipitation trend in the Mustang region, as illustrated by the CMIP6 historical and future scenario projections (SSP245 and SSP585), shows a significant shift over time. Historical simulations and observed data (1980–2015) indicate considerable year-to-year variability, with no clear long-term increasing or decreasing trend. However, future projections suggest a marked divergence based on emission scenarios. Under the SSP245 pathway, which assumes moderate global mitigation efforts, annual precipitation increases slightly with considerable interannual variability. In contrast, the SSP585 scenario, reflecting a high-emissions futures shows a substantial rise in precipitation, especially after 2060, with values reaching nearly double those of the historical average by the end of the 21st century.

When compared to global precipitation trends, the Mustang region reflects a localized intensification pattern that aligns with broader climate model findings. Globally, climate models project an overall increase in precipitation, particularly in high latitudes and the tropics, while some mid-latitude and subtropical regions are expected to become drier. The Intergovernmental Panel on Climate Change (IPCC AR6) reports that with rising global temperatures, the water cycle is expected to intensify, leading to more frequent heavy rainfall events in wet regions and prolonged dry periods in already dry areas. Mustang's projected increase in precipitation under SSP585, particularly after mid-century, is consistent with this intensification of the hydrological cycle, although its high interannual variability suggests continued exposure to climate extremes such as droughts and flood.

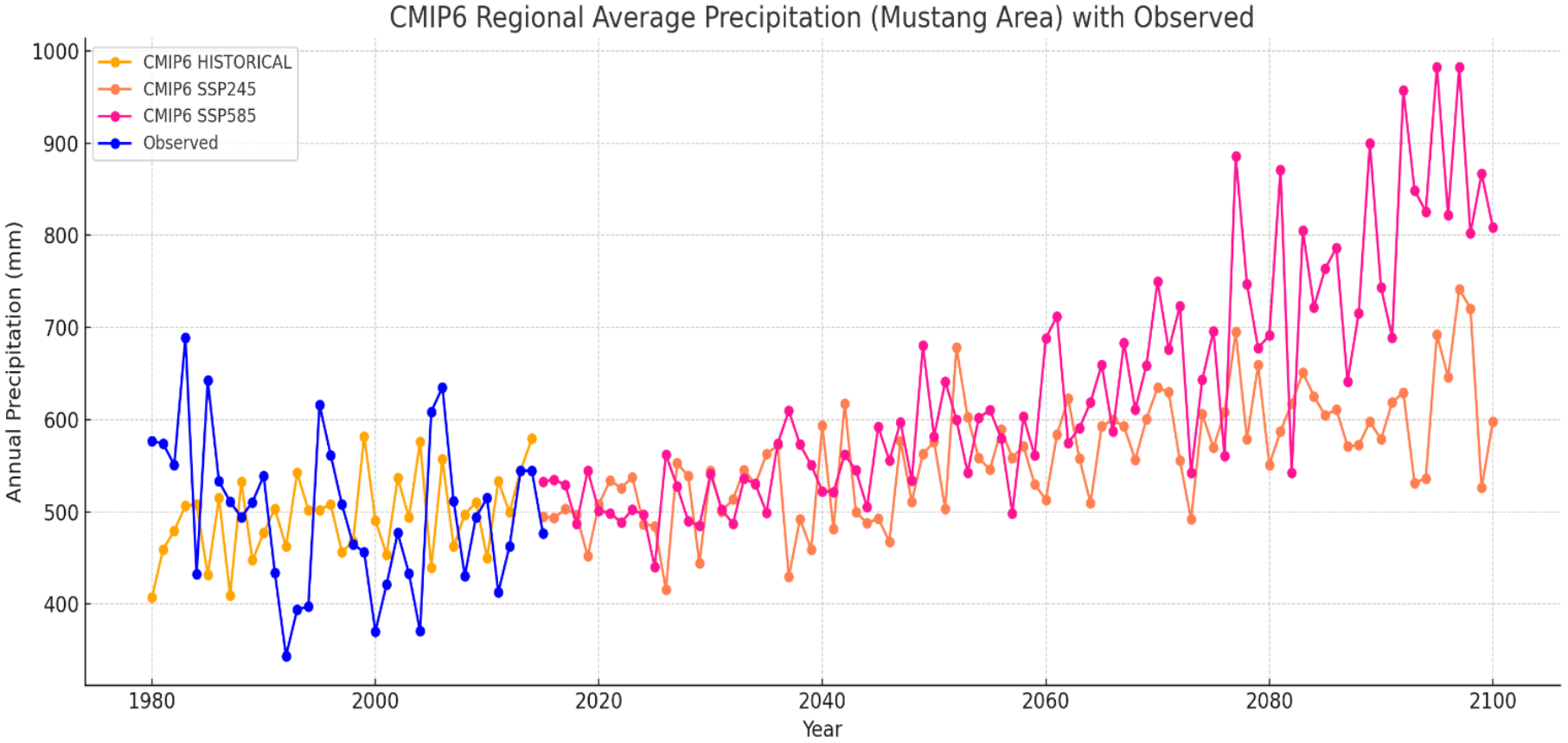


*Figure 5-10 Projected shifts in annual precipitation in Mustang under SSP245 and SSP585 scenario*

## 5.4 Increasing Drought Frequency and Severity in Mustang

Analysis of SPI-12 values from seven meteorological stations in Mustang (Thakmarpha, Samargaun, Ranipauwa, Lete, Jomsom, Dhakarjhong, and Chhoser) clearly reflects changes in precipitation patterns when comparing historical and future climate conditions. Historical data from 1980 to 2015, along with observed records up to 2015, show that the region has already experienced notable variability in precipitation, with alternating dry and wet periods. Notably, observed records highlight a significant rise in both the frequency and duration of droughts after the mid-1990s. This trend indicates that climate-induced stress is already affecting the region, likely driven by rising temperatures and shifts in precipitation patterns.

According to projections under both SSP245 and SSP585 scenarios, these trends are expected to persist and become more severe in the coming decades. Under the moderate emission pathway (SSP245), drought conditions are likely to worsen until mid-century, after which wetter conditions may become more dominant by century's end. The high-emissions SSP585 scenario presents a more concerning future, with Mustang potentially facing prolonged and severe drought throughout much of the 21st century, followed by a rapid transition to wetter conditions in the latter half. This increase in variability signals a heightened risk of both water scarcity and flooding.

Overall, Mustang appears to be transitioning from a historically balanced precipitation regime to one marked by more extreme fluctuations. The severity of this shift heavily depends on future global greenhouse gas emissions. Increasingly frequent and prolonged droughts pose serious risks to agriculture, water supply, and local ecosystems, while the potential for intense rainfall, flooding, and landslides later in the century adds to the growing concerns

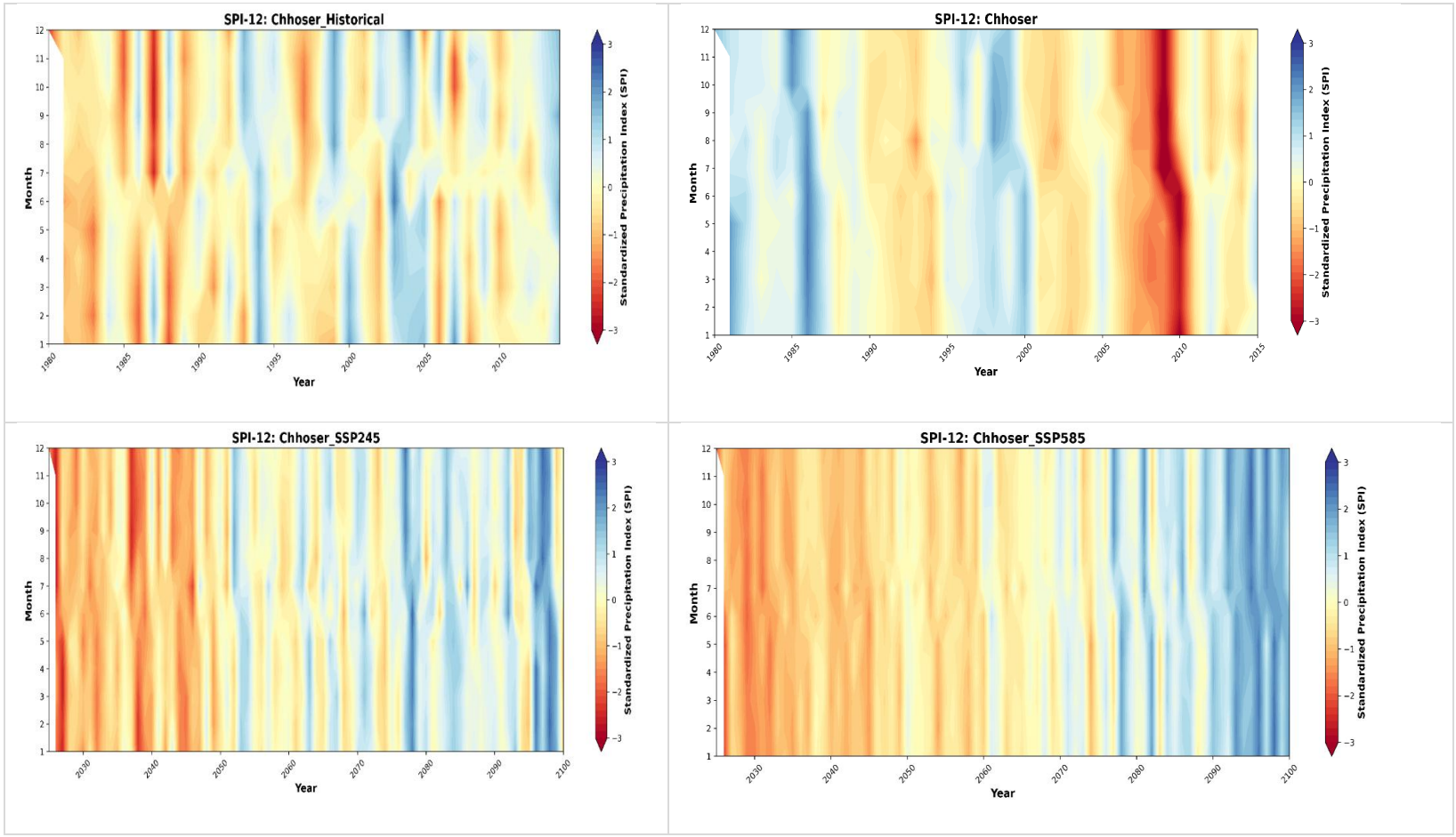


*Figure 5-11 SPI-12 analysis in Chhoser station on observed and historical period and SSP245 and SSP585 scenario*

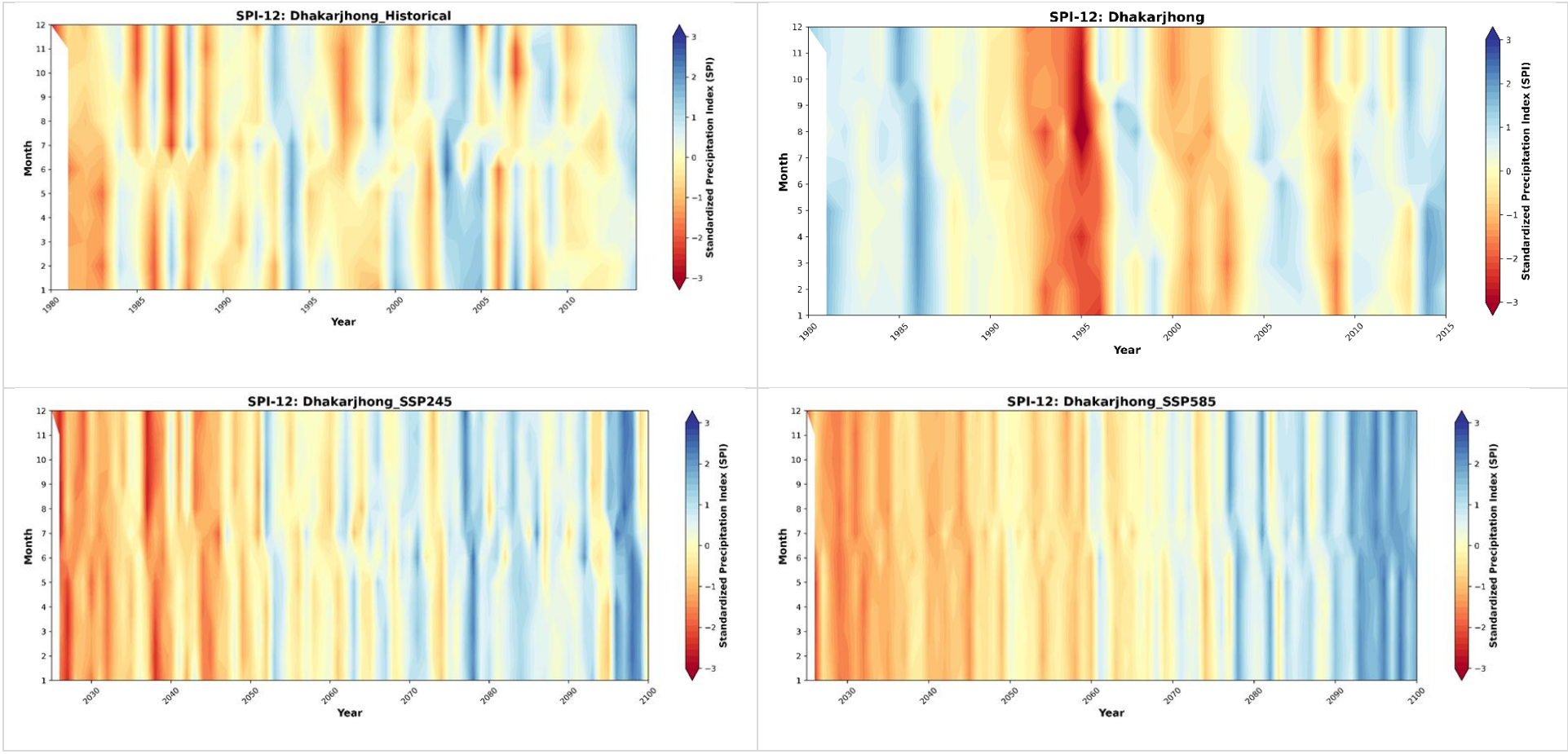


*Figure 5-12 SPI-12 analysis in Dhakarjhong station on observed and historical period and SSP245 and SSP585 scenario*

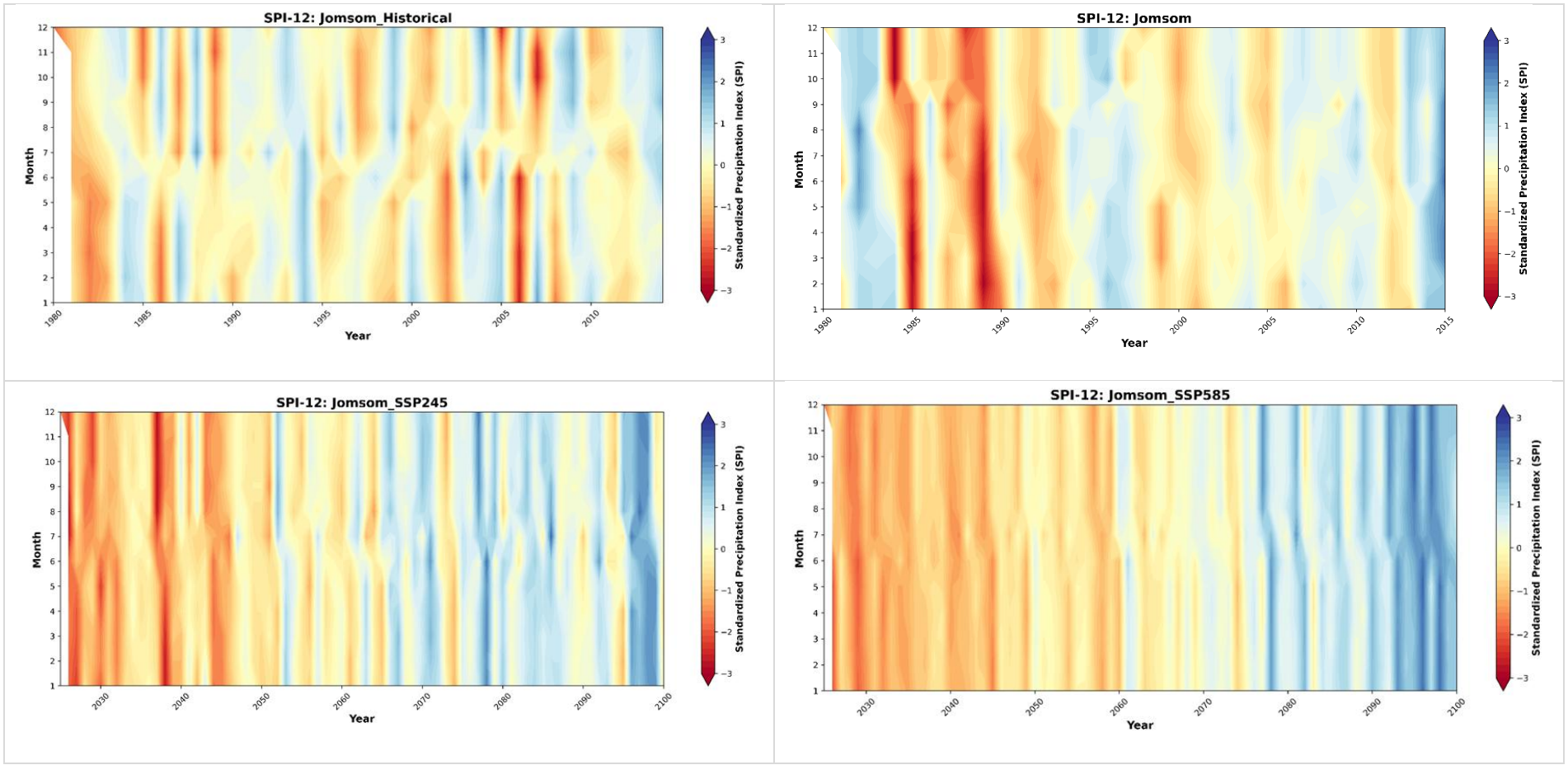


*Figure 5-13 SPI-12 analysis in Jomsom station on observed and historical period and SSP245 and SSP585 scenario*

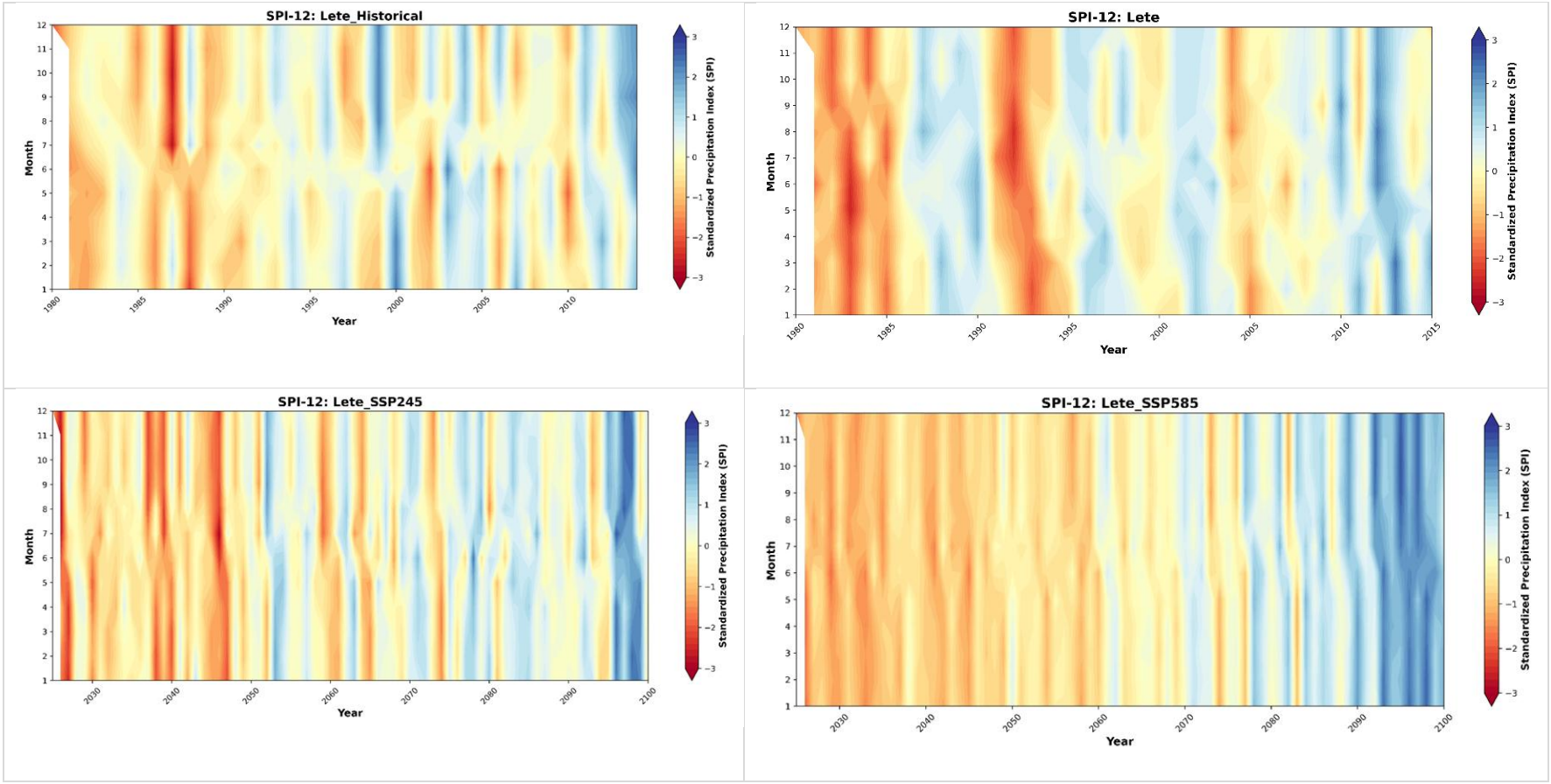


*Figure 5-14 SPI-12 analysis in Lete station on observed and historical period and SSP245 and SSP585 scenario*

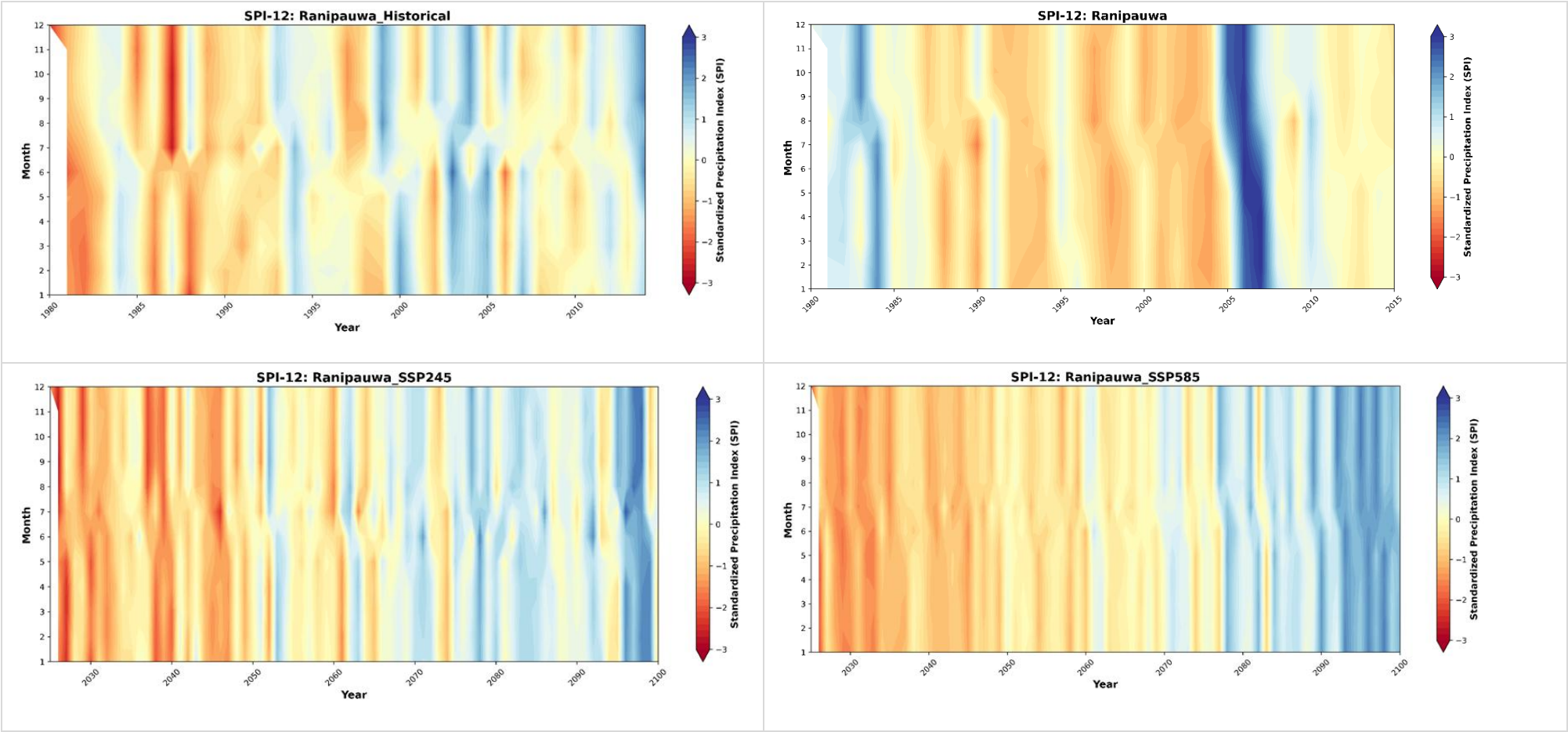


*Figure 5-15 SPI-12 analysis in Ranipauwa station on observed and historical period and SSP245 and SSP585 scenario*

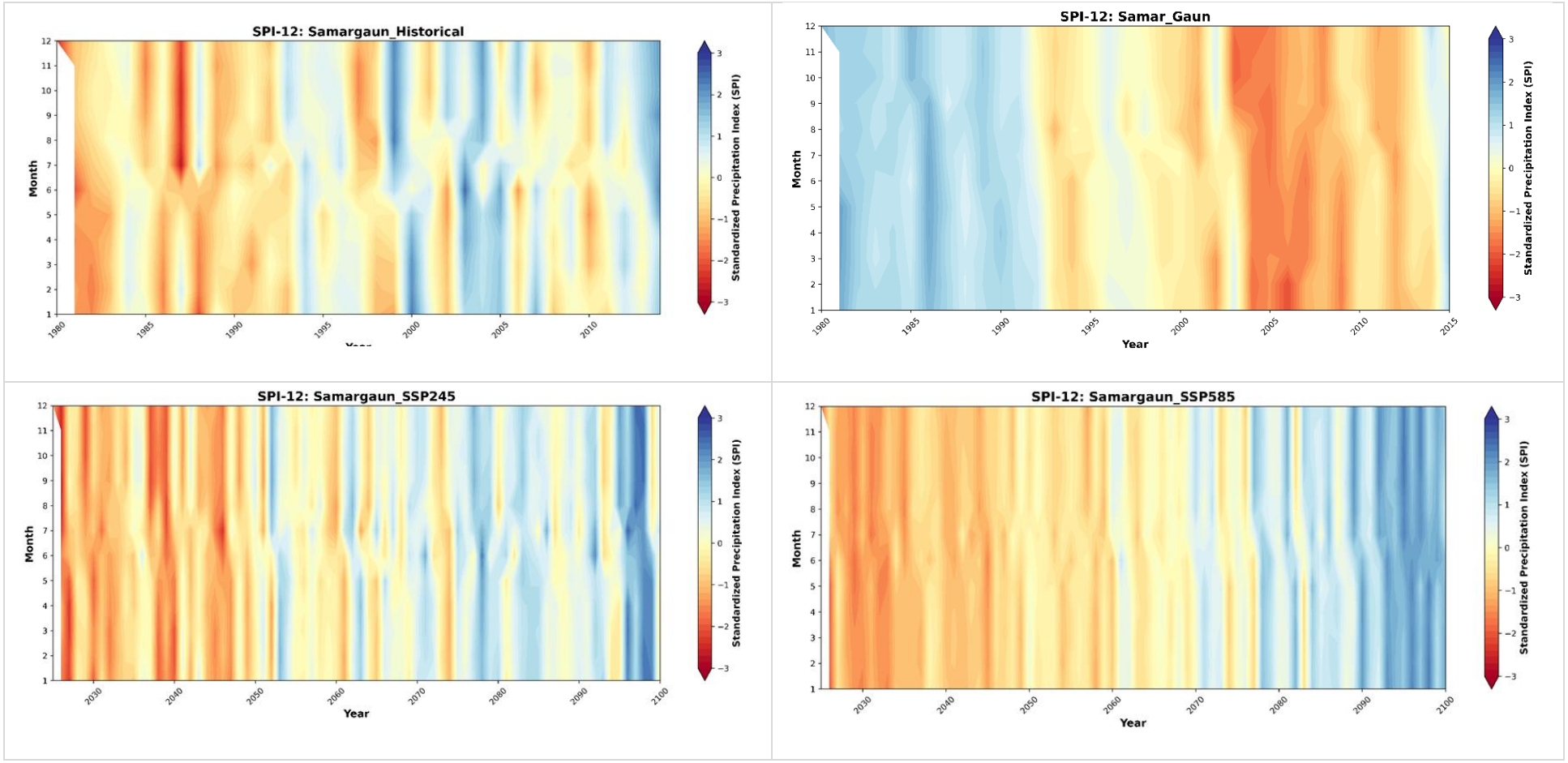


*Figure 5-16 SPI-12 analysis in Samar Gaun station on observed and historical period and SSP245 and SSP585 scenario*

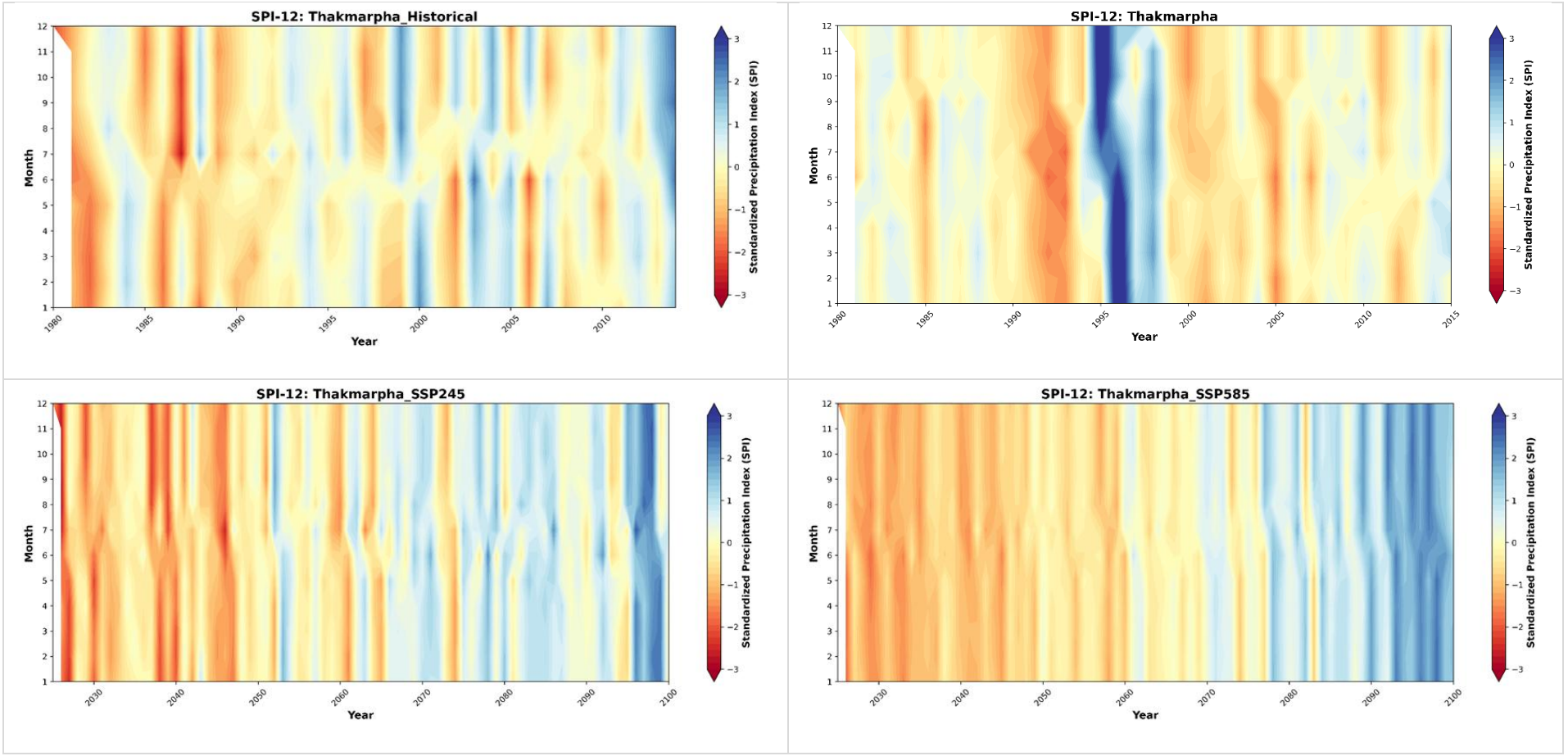


*Figure 5-17 SPI-12 analysis in Thakmarpha station on observed and historical period and SSP245 and SSP585 scenario*

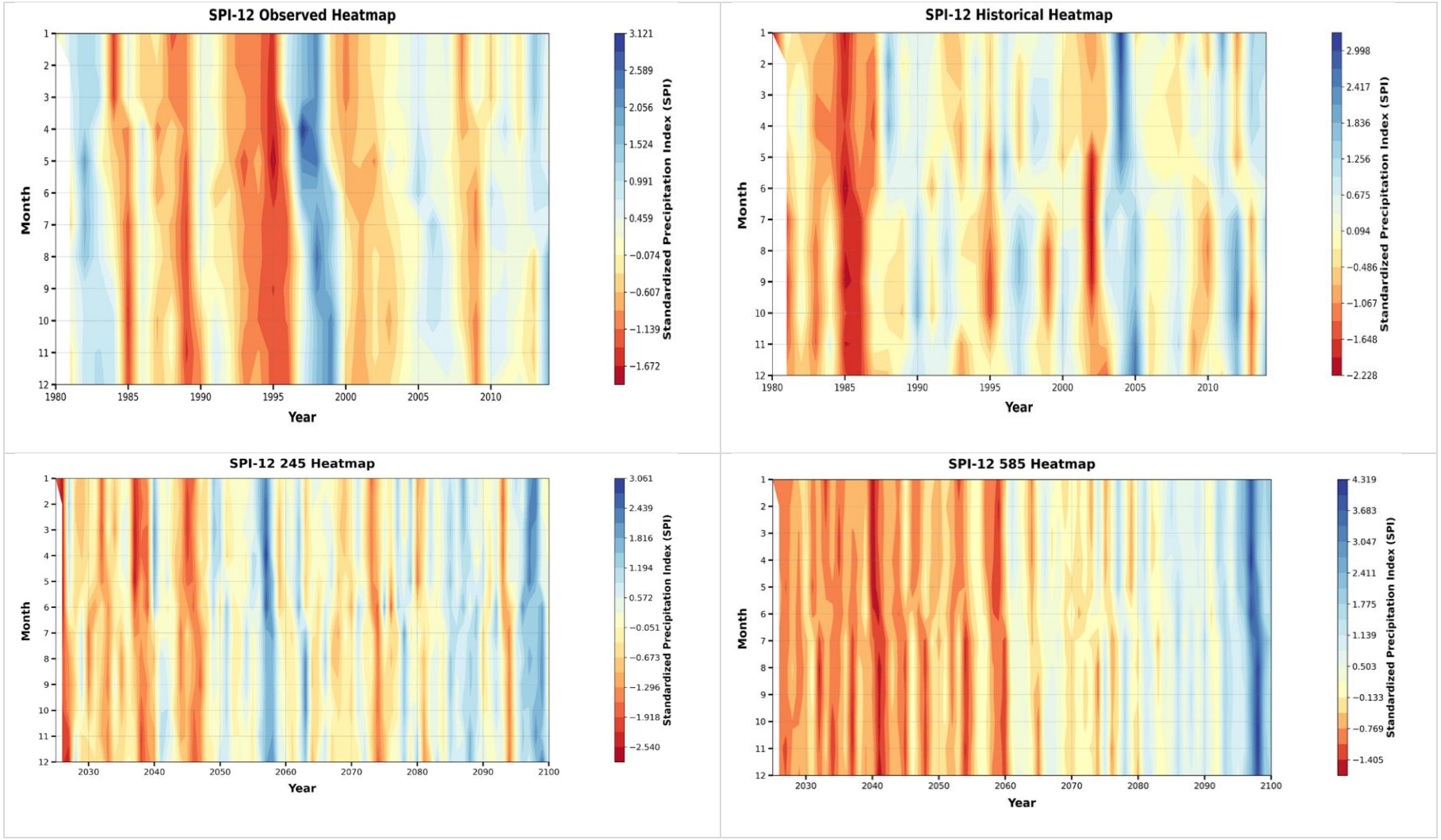


*Figure 5-18 SPI-12 analysis across Mustang on observed and historical period and SSP245 and SSP585 scenario*

## 5.5 Hydroclimatic Extremes in Mustang: SPEI12-Based Assessment of Past and Future Drought Patterns

Analysis of the Standardized Precipitation Evapotranspiration Index over a 12-month timescale (SPEI-12) for the Jomsom and Lete stations provides critical insights into the evolving hydroclimatic conditions of Mustang. As an indicator integrating precipitation and potential evapotranspiration, SPEI-12 effectively captures long-term moisture deficits or surpluses. Historical data (1980–2015) reveal inherent natural variability, characterized by alternating dry and wet periods at both stations. However, superimposed on this variability is a clear trend towards more persistent and severe drought conditions, particularly evident since the late 1990s. During this observed period, Jomsom experienced notably extensive dry phases, while Lete displayed a progressive drying trend beginning around 2005, reflecting regional impacts of climate change such as increased evapotranspiration and decreased moisture availability.

Future projections under the SSP245 and SSP585 emission scenarios suggest an intensification of this hydroclimatic stress. Under the moderate SSP245 scenario, both Jomsom and Lete are projected to face increased drought frequency and intensity by mid-century, followed by a potential shift towards more frequent and intense wet periods after approximately 2070. In stark contrast, the high-emission SSP585 scenario indicates widespread and prolonged drought conditions extending throughout the latter half of the century. This scenario is also associated with significantly amplified hydroclimatic variability, featuring more extreme droughts and intense wet events, especially late in the century. Notably under SSP585, Lete exhibits increasing wet anomalies, potentially indicating an intensified hydrological cycle, whereas Jomsom shows more abrupt transitions between extreme dry and wet states.

Overall, the SPEI-12 results signal a definitive shift from Mustang's historically variable hydroclimate towards a future dominated by pronounced extremes. The alignment of currently observed drying trends with the initial stages of these projections enhances confidence in the scenarios. The divergence between SSP245 and SSP585 outcomes critically underscores the sensitivity of Mustang's future hydroclimate to global emission pathways, with the high-emission scenario portending persistent stress, and an elevated long-term risk of severe droughts, flash floods, and substantial water insecurity.

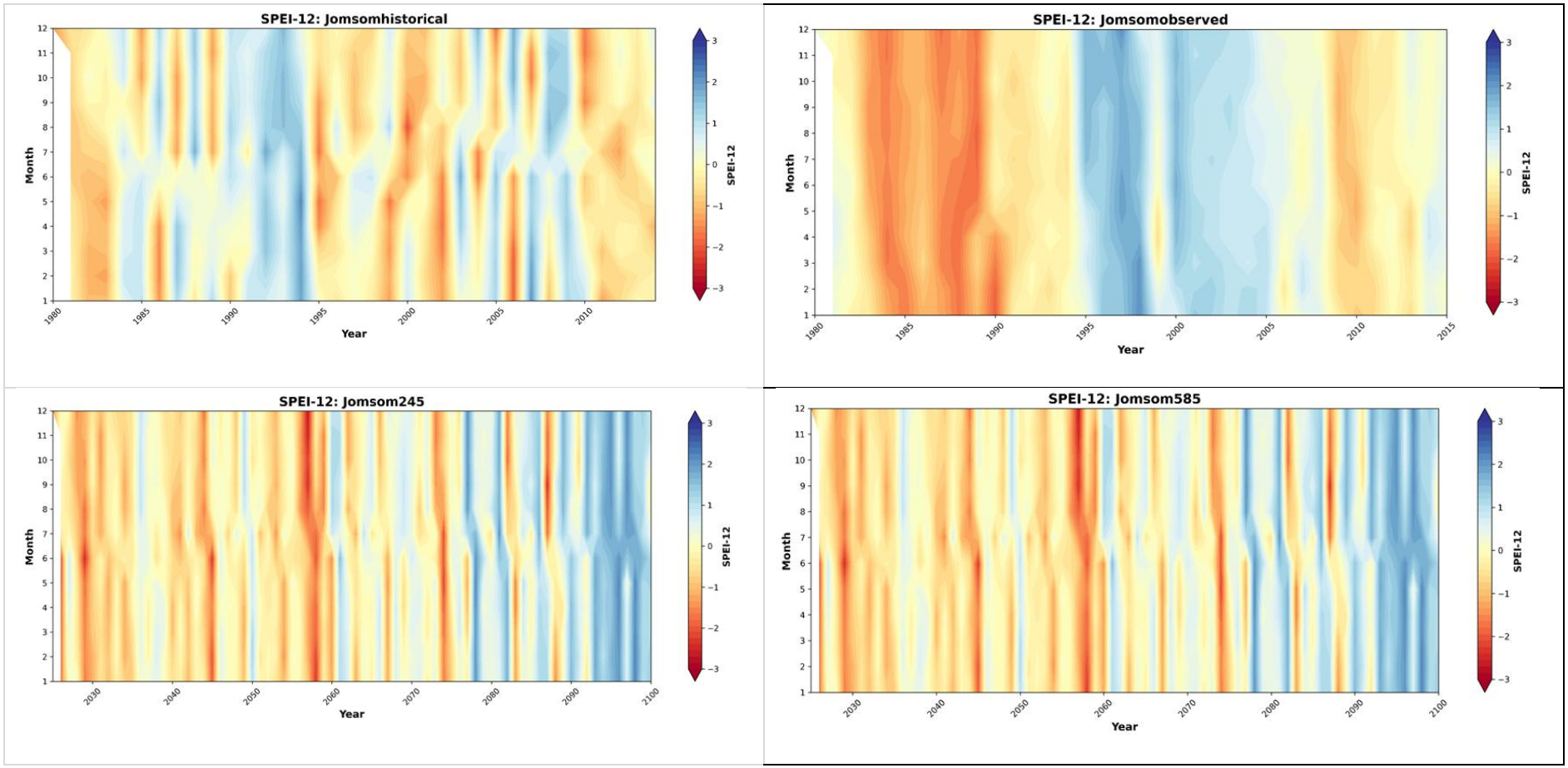


*Figure 5-19SPEI-12 analysis in Jomsom station on observed and historical period and SSP245 and SSP585 scenario*

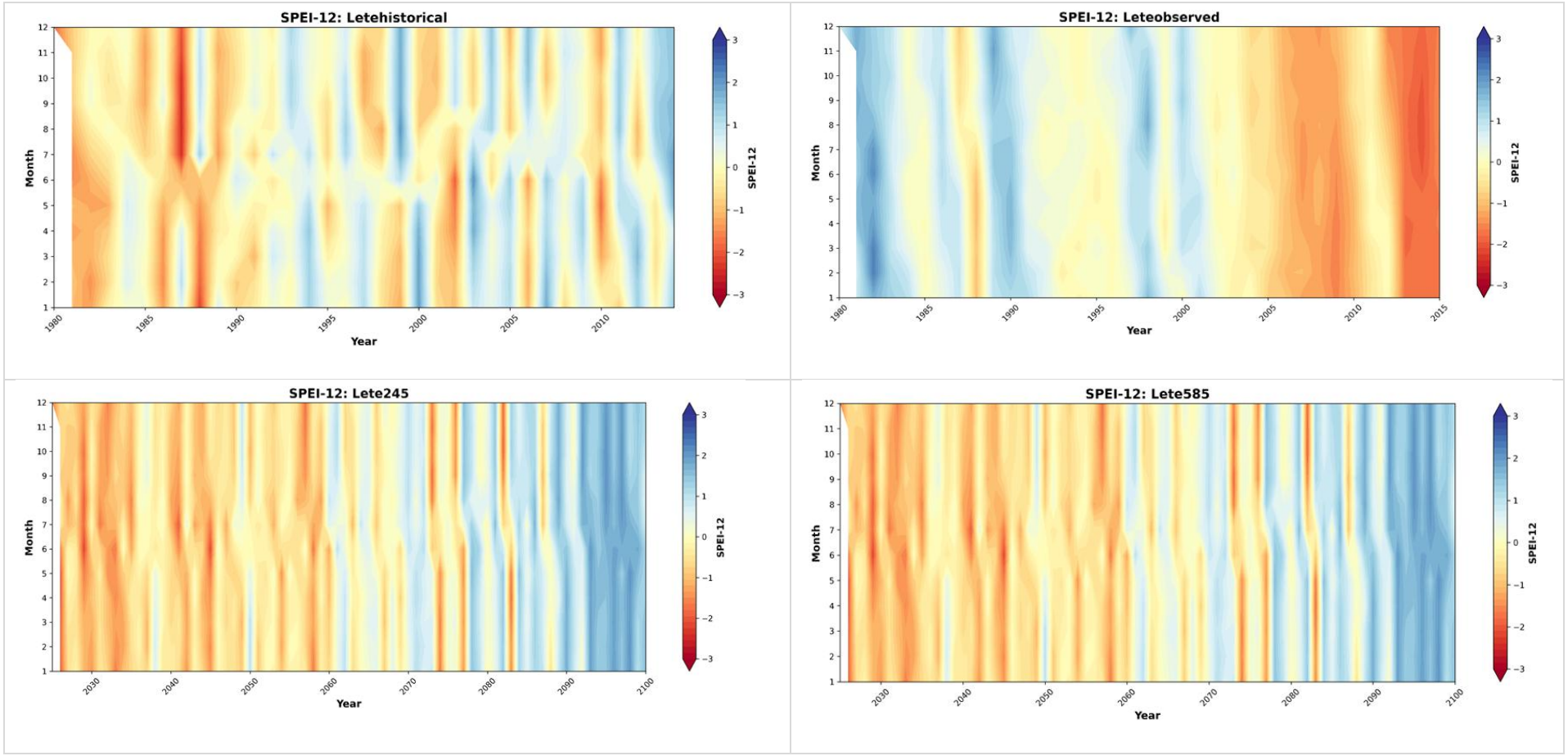


*Figure 5-20 SPEI-12 analysis in Lete station on observed and historical period and SSP245 and SSP585 scenario*

## 5.6 Sensitivity of Flood Magnitudes to Climate Scenarios: Insights from GEV and Gumbel Modeling

### *5.6.1 Return Level Estimation (GEV vs Gumbel)*

The return level plots for all scenarios—Observed, Historical, SSP245, and SSP585, demonstrate that the Generalized Extreme Value (GEV) distribution generally predicts higher flood magnitudes than the Gumbel distribution, particularly for extreme return periods (50-year and 100-year).Under the observed scenario, GEV return levels exceed Gumbel estimates across all stations, with stations like Samar Gaun and Thakmarpha showing the highest projected magnitudes (~230 mm for 100-year return).In historical simulations, both GEV and Gumbel distributions result in lower return levels compared to the observed data, with magnitudes typically below 40 mm even at the 100-year level. This suggests that the historical reanalysis data underrepresents extreme precipitation.For SSP245 (moderate emissions), there is a noticeable increase in return levels across most stations. GEV models show more pronounced curvature, indicating increased tail behavior in projected extremes.The SSP585 (high emissions) scenario yields the highest return levels, particularly at Lete, where GEV return values reach above 70 mm for 100-year floods. The divergence between GEV and Gumbel also increases under SSP585, indicating that future extremes may not be well captured by simpler distributions like Gumbel.

### *5.6.2 Flood Year Frequency Analysis*

The temporal flood frequency analysis across all stations and scenarios highlights distinct trends in the occurrence of extreme events.1980–2010: Observed and historical data show moderate flood frequencies, with 10-year and 25-year return floods being most common. High return period floods (e.g., 50-year) were sparse during this baseline period.2010–2040: A transitional phase where flood frequency declines slightly. This period corresponds to projected near-term stabilization under SSP245, though high-emission scenarios still predict sporadic events.2040–2100: A sharp increase in flood frequency is evident, particularly for the 10-year and 25-year floods, with some years experiencing floods at more than 10 stations. This surge is particularly strong post-2070 under the SSP585 scenario, signaling escalating flood risks due to climate change. Notably, 50-year flood events become more frequent after 2080 under both SSP scenarios, highlighting increasing extreme event intensity and recurrence.

The GEV model is consistently more sensitive to extreme values and is better suited for predicting rare but impactful flood events. Flood risks intensify significantly under SSP585, with an increase in both the magnitude and frequency of extreme rainfall events. Spatially, stations like Lete, Ranipauwa, and Thakmarpha emerge as high-risk zones, with both high return levels and frequent exceedance events.

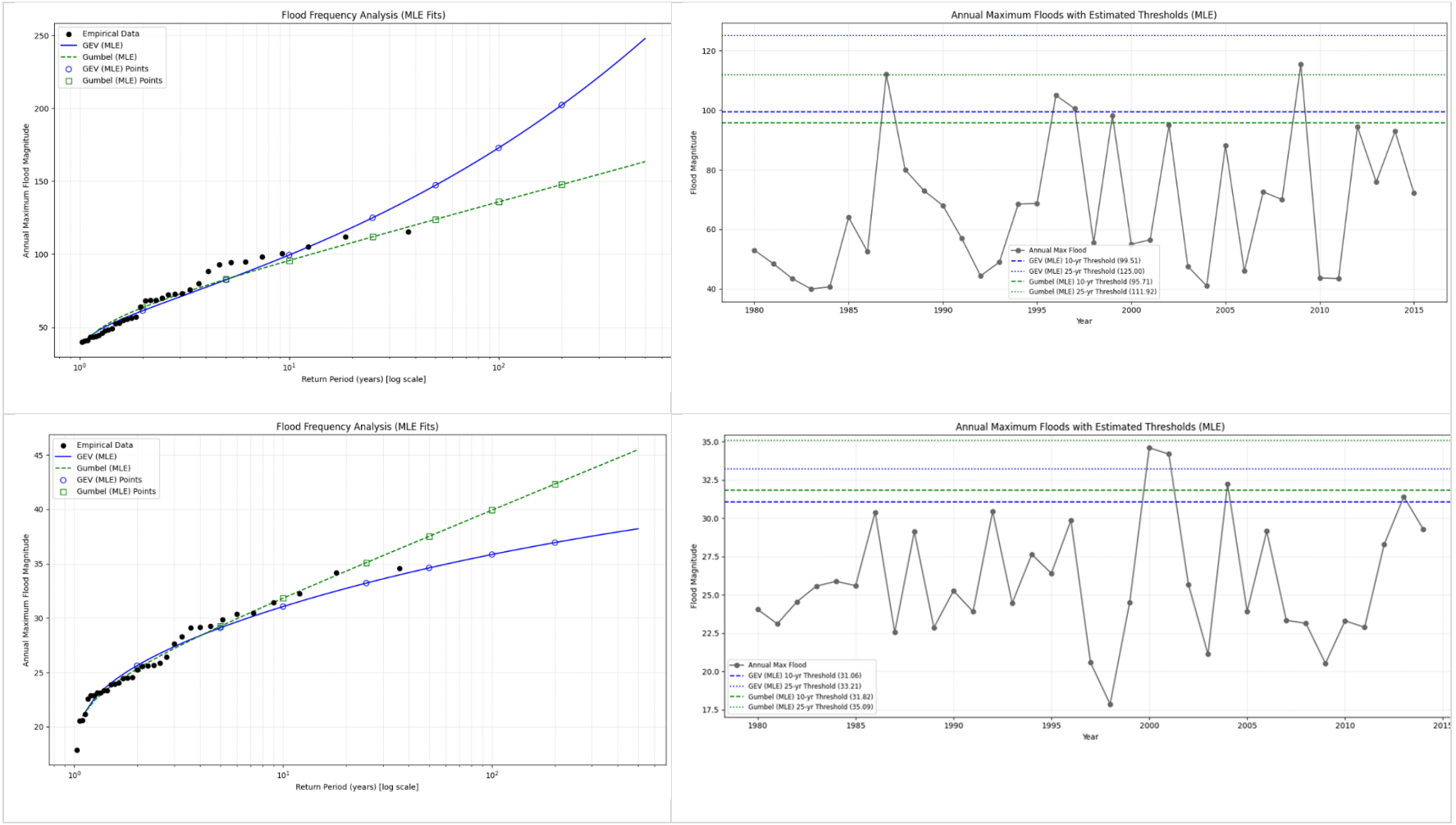


*Figure 5-21 Lete observed and historical flood frequency analysis and annual max flood estimation*

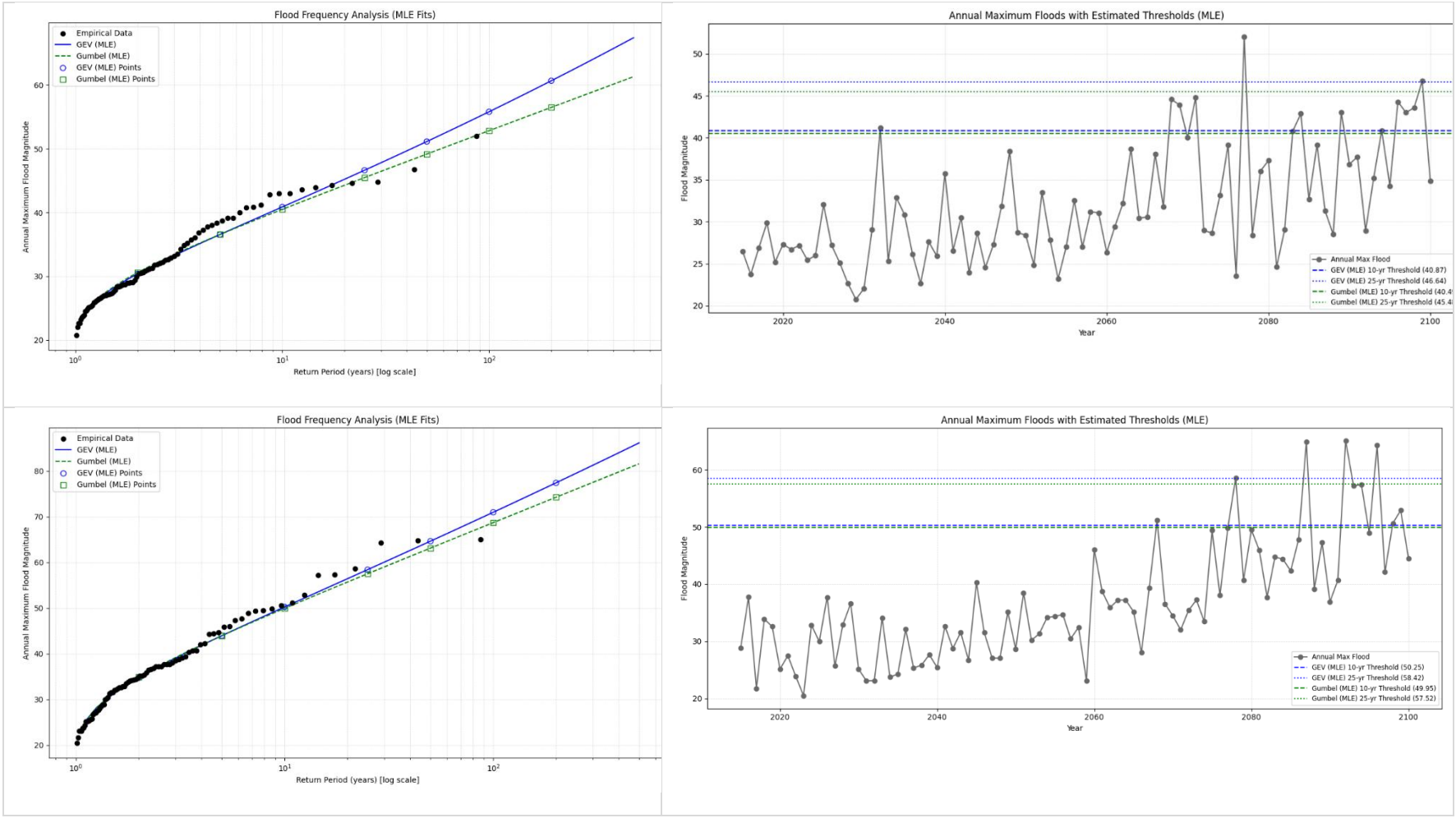


*Figure 5-22 Flood frequency analysis and annual max flood estimation for Lete (SSP245 and SSP585)*

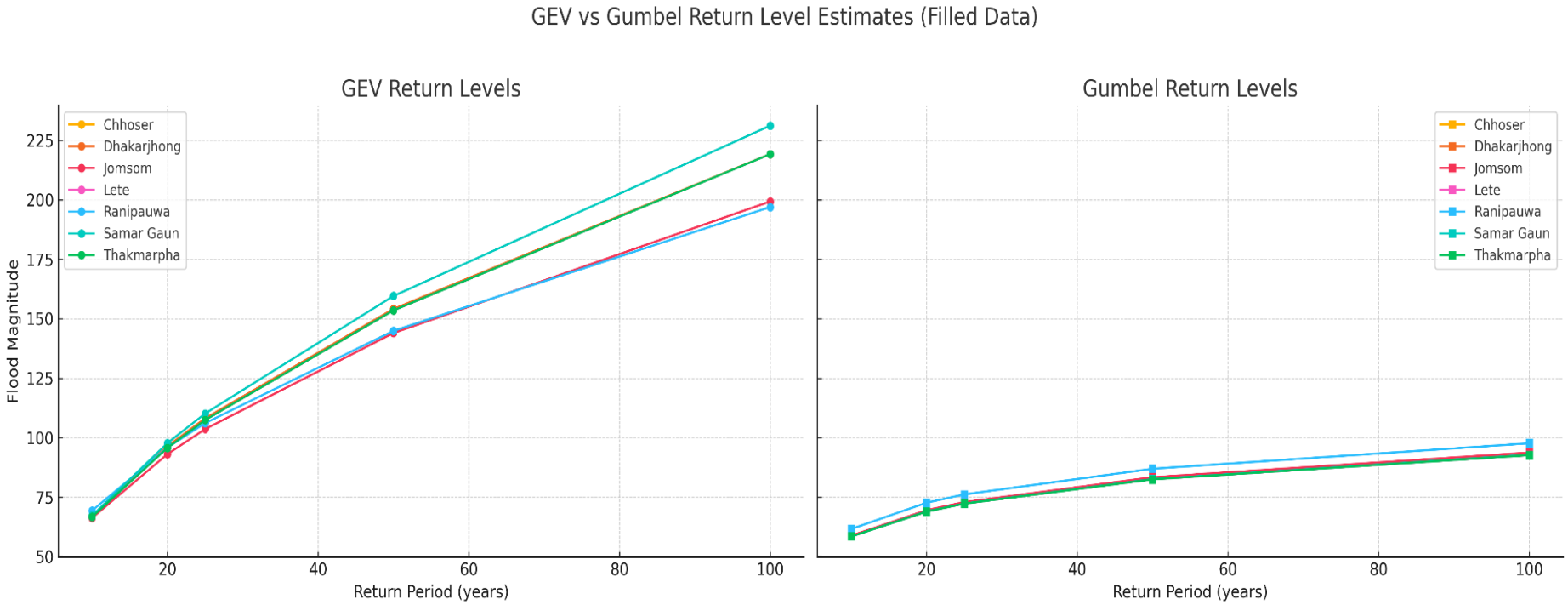


*Figure 5-23 GEV vs Gumbel return level estimates in all stations under observed period*

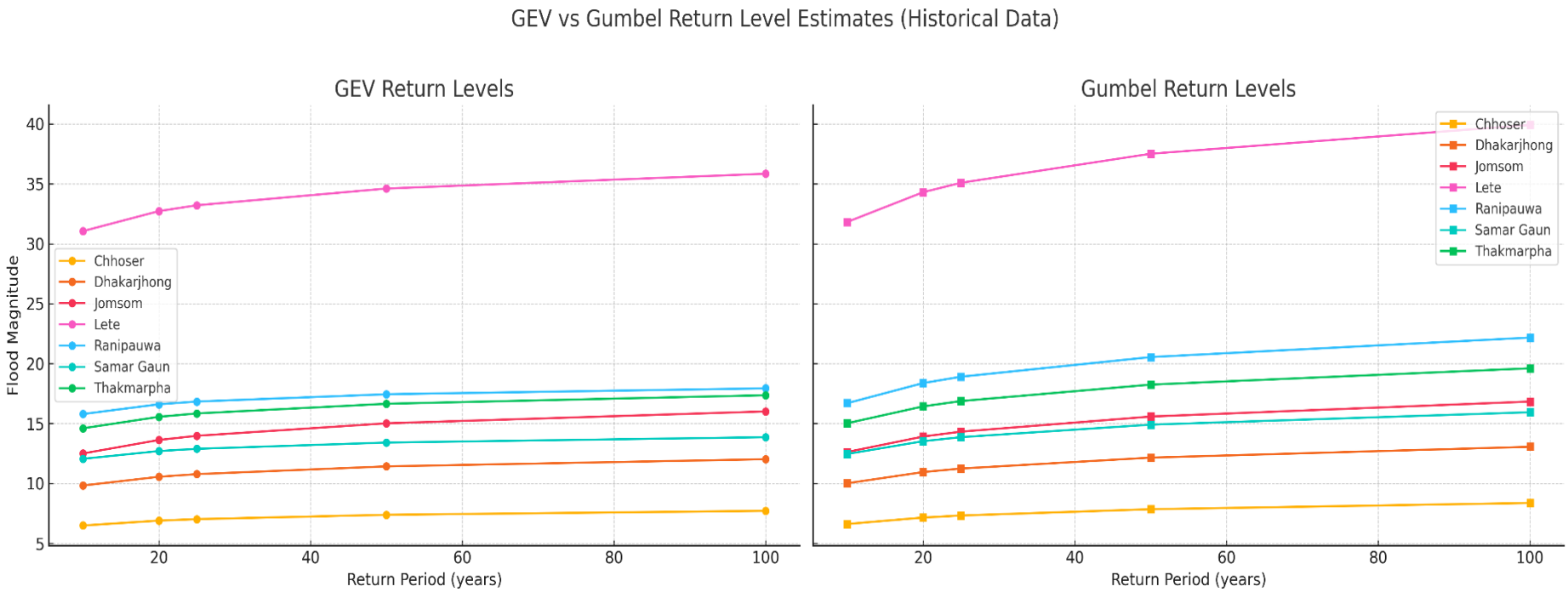


*Figure 5-24 GEV vs Gumbel return level estimates in all stations under historical period*

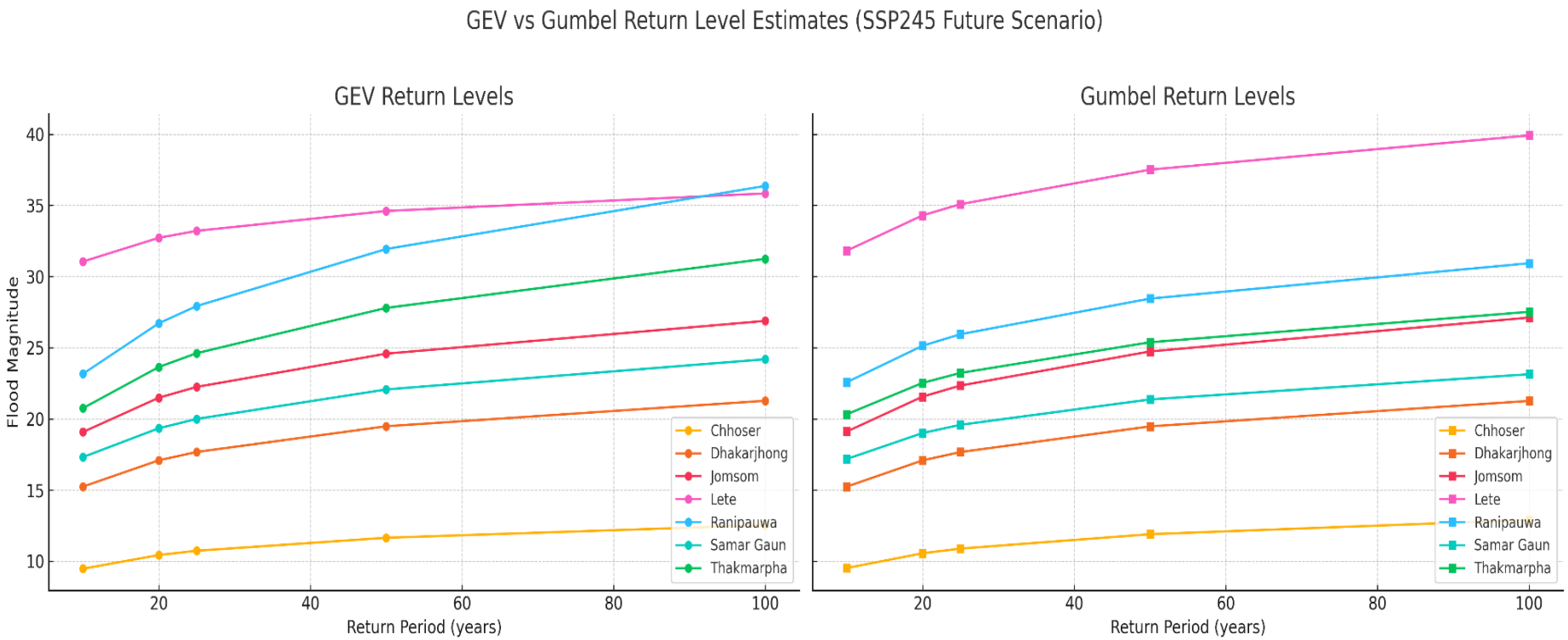


*Figure 5-25 GEV vs Gumbel Return level estimates in all station under SSP245 scenari*

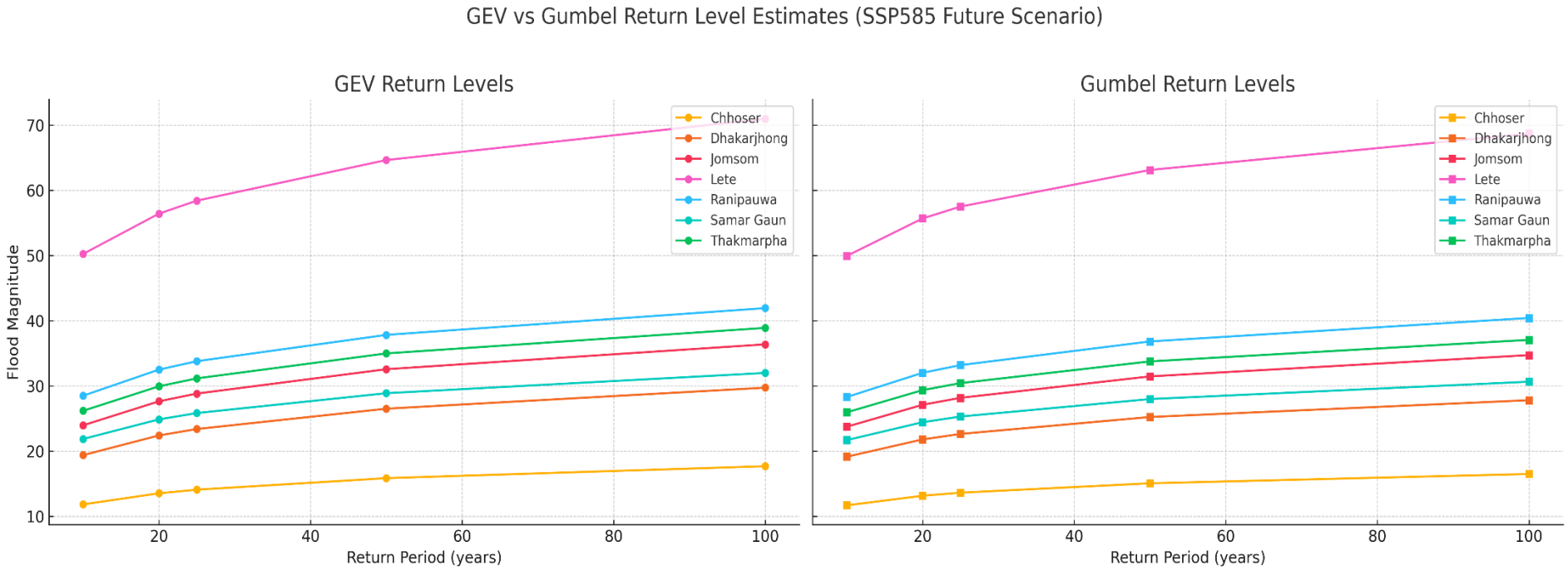


*Figure 5-26 GEV vs Gumbel Return level estimates in all stations under SSP585 scenario*

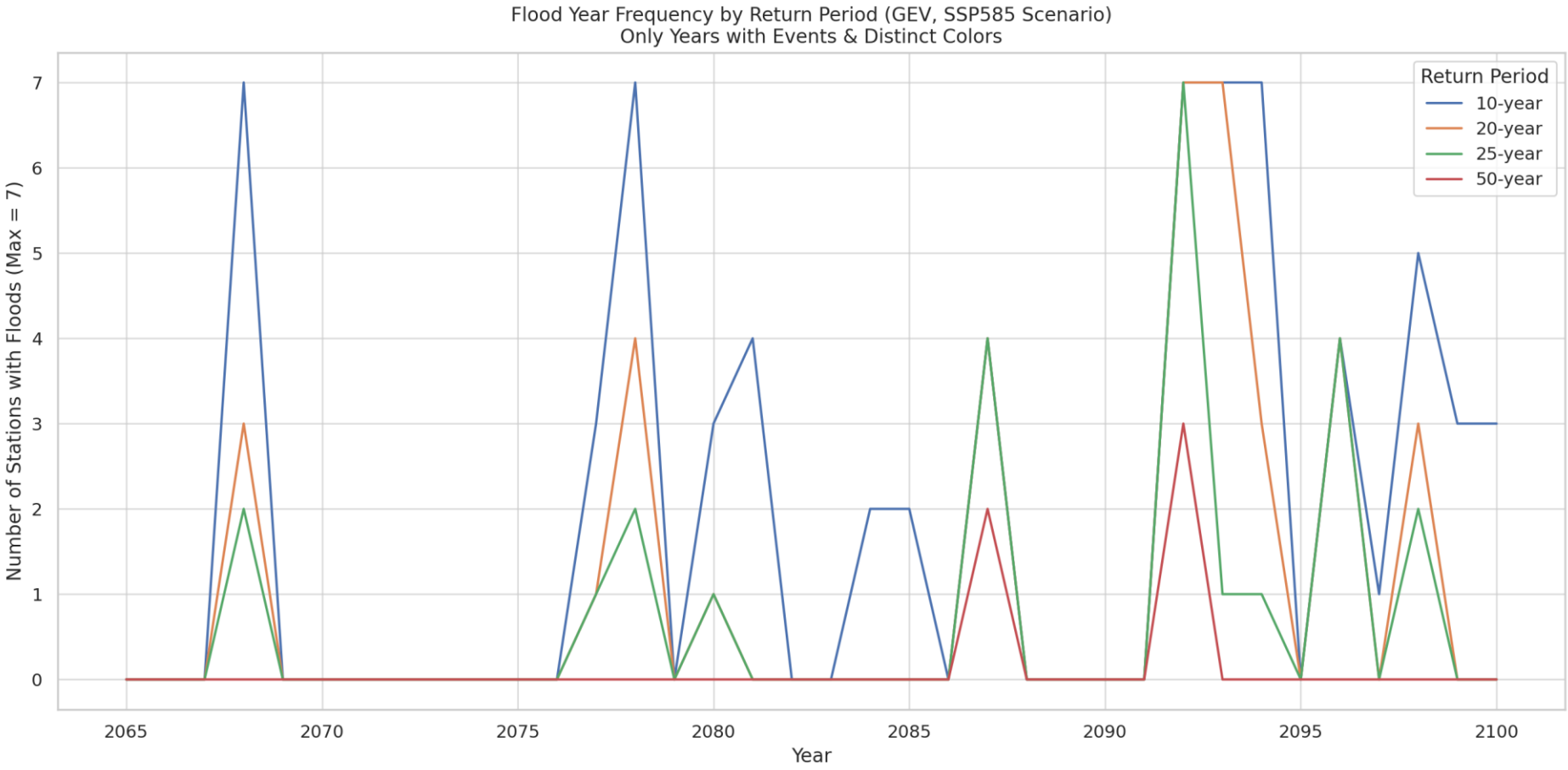


*Figure 5-27 Flood year frequency by return period by GEV under SSP585 scenario*

## 5.7 Flood Frequency Analysis Using Log-Pearson Type III Distribution of Downstream Discharge Records

In the context of Mustang's upstream hydrology, it is approximated using downstream data due to the absence of local hydrological stations. The analysis estimates the 2-year flood at around 530 $m^3/s$ and the 100-year flood at approximately 672 $m^3/s$. This indicates that extreme floods may be 25–30% larger than more frequently occurring floods. Such findings are vital for informing the design of resilient infrastructure, including bridges, culverts, and flood protection systems in the region. Due to the lack of operational gauging stations within Mustang, this study uses data from a downstream location as a proxy. This downstream station, situated along the Kali Gandaki River, receives upstream flow contributions from Mustang and is thus hydrologically relevant for understanding the flood-generating potential of the basin. While this approach may not capture localized flood characteristics within Mustang itself, it provides valuable insight into the overall hydrological behavior of the river system. Future research should prioritize the installation of hydrological monitoring stations within Mustang to enable more accurate and site-specific flood risk assessments.

The plot presents the relationship between return periods and estimated flood magnitudes based on statistical analysis of annual maximum discharge data. The x-axis, shown on a logarithmic scale, represents the return period in years, which indicates the frequency at which a particular flood magnitude is expected to occur. The y-axis displays the estimated flood discharge (Q), likely in cubic meters per second ($m^3/s$), corresponding to each return period. The curve demonstrates a sharp increase in flood magnitude between the 2-year and 10-year return periods, signifying that more frequent flood events exhibit notable increases in discharge. Beyond the 10-year return period, the curve gradually flattens, suggesting that flood magnitudes increase more slowly for rare, extreme events such as the 50-year and 100-year floods. This pattern reflects the typical behavior of skewed flood distributions, where high-magnitude floods are less common but still poss

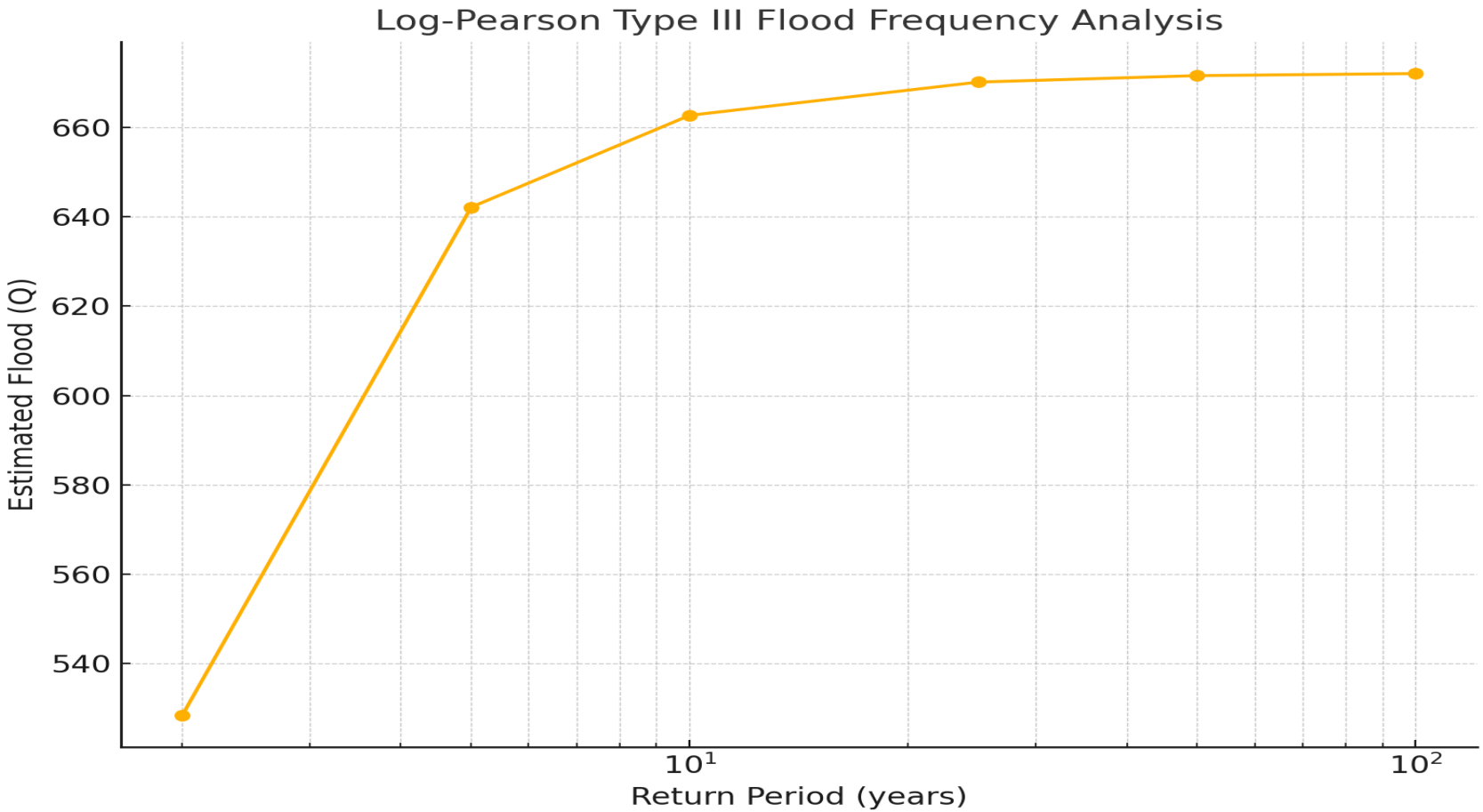


*Figure 5-28 Log Pearson III flood frequency analysis at hydrological station 404.7*

## 5.8 Observed Patterns of Drought and Flood Risks in Nepal: Insights from Previous Studies

- Trend analysis of drought index shows that most stations are characterized by increases in both severity and frequency of drought and trend is stronger for longer drought time scales (Dahal et al., 2016).
- More than 44 percent of the locations in the country were occupied under drought conditions during these extreme drought events (Bagale et al., 2021).
- More frequent drought incidents have been observed after 2010 at all the precipitation stations considered (A. Aryal et al., 2022).
- Recent flood events in Nepal have largely resulted from the rapidly increasing vulnerability of local communities, compounded by fluctuating and potentially shifting climatic patterns. Unless significant efforts are made to reduce this vulnerability, similar disasters are likely to persist. However, the current mechanisms for managing flood risks in Nepal, particularly in terms of risk assessment and disaster governance, remain limited and underdeveloped (Delalay et al., 2018b).
- Floods, among the most frequent and impactful natural hazards, have been increasingly intensified by human-induced climate change, particularly in mountainous regions, disrupting socio-economic systems throughout the 21st century (A. P. Sharma et al., 2023b).

# CHAPTER 6: CONCLUSION AND RECOMMENDATIONS

## 6.1 Conclusion

This thesis evaluated changing flood and drought conditions in the unique semi-arid, high-altitude environment of Mustang, Nepal, analyzing historical (1980-2023) hydroclimatic trends and projecting future changes using CMIP6 scenarios (SSP2-4.5, SSP5-8.5). Historical data revealed complex seasonal precipitation trends and mixed temperature signals across stations, but critically, drought analyses (SPI/SPEI) indicated significant interannual variability with a marked increase in drought frequency and severity since the mid-1990s, confirming the region's sensitivity to climate shifts.

Future projections highlighted a strong divergence based on emission pathways; while SSP2-4.5 showed moderate future changes, the high-emission SSP5-8.5 scenario projected a substantial, potentially near-doubling, increase in annual precipitation by 2100. Paradoxically, this intensification of the hydrological cycle under SSP5-8.5 is coupled with projections of more persistent and severe droughts and significantly increased flood risk. Flood Frequency Analysis consistently showed higher future flood magnitudes compared to historical levels (especially under SSP5-8.5), with GEV distributions providing more conservative (higher) estimates than Gumbel, particularly for rarer events. Temporal analysis indicated a sharp increase in the frequency and spatial extent of floods post-2070 under SSP5-8.5. Collectively, the findings demonstrate Mustang's transition from a relatively stable, albeit arid, climate towards a future increasingly marked by hydroclimatic extremes, posing significant challenges for water security, agriculture, and local livelihoods.

**Key Takeaways:**

- The region is shifting from a relatively stable climate, with natural ups and downs, to a future marked by more intense and unpredictable weather.
- Longer droughts could reduce water supply, harm farming, and increase migration. Second, heavier rainfall and faster glacier melt could lead to dangerous floods, including flash floods, and LLOFs (Landslide Lake Outburst Floods).
- The evidence points towards an era of increased extremes, more intense droughts and more severe floods.

- Addressing this challenge requires urgent, informed, and integrated action, combining robust scientific analysis with proactive adaptation planning and global climate change mitigation efforts.

### 6.2 Recommendations:

The findings underscore the profound vulnerability of the Mustang region to intensifying hydroclimatic extremes under future climate change, necessitating proactive and integrated adaptation strategies. Based on this research, key recommendations include the adoption of

- **Scenario-based adaptation planning**, ensuring flexibility to address the wide range of potential future conditions depicted by different SSPs, particularly the severe risks associated with SSP5-8.5.
- **Integrated water resource management** is crucial, requiring plans that simultaneously address water scarcity (drought) through enhanced conservation and storage, and excess water (floods) via improved infrastructure, robust early warning systems, and informed land-use planning. Given the limitations posed by data scarcity, enhanced
- **Meteorological and hydrological monitoring**, especially long-term, high-altitude networks, is vital for improving model calibration, validating projections, and supporting operational forecasting. Furthermore, effective adaptation necessitates strong
- **Community engagement**, integrating local and traditional knowledge with scientific insights to co-develop locally appropriate and sustainable solutions. Future research should prioritize refining regional climate projections through advanced downscaling or tailored modeling that better incorporates Mustang's complex topography and cryosphere processes (glacial melt, permafrost), alongside integrating socio-economic vulnerability assessments to fully capture the human dimension of climate change impacts in this unique Himalayan rain shadow environment

**REFERENCES**

Abd-Elhamid, H. F., Zeleňáková, M., Soľáková, T., Saleh, O. K., & El-Dakak, A. M. (2024). Monitoring flood and drought risks in arid and semi-arid regions using remote sensing data and standardized precipitation index: A case study of Syria. *Journal of Flood Risk Management*, *17*(1), e12961. https://doi.org/10.1111/jfr3.12961

Aghakouchak, A., Feldman, D., Stewardson, M. J., Saphores, J.-D., Grant, S., & Sanders, B. (2014). Australia's Drought: Lessons for California. *Science*, *343*(6178), 1430–1431. https://doi.org/10.1126/science.343.6178.1430

Ahmed, R., Rather, A. F., Banerjee, P., Wani, G. F., Saleem, S., Shamim, T., Wani, T. A., Ahmed, P., Almazroui, M., & Mir, R. A. (2025). Impact of Climate Variability on the Feeding Glaciers of Potentially Dangerous Glacial Lakes in the Jhelum Basin of Kashmir Himalaya, India. *Natural Hazards Review*, *26*(2), 04025001. https://doi.org/10.1061/NHREFO.NHENG-2140

Alotaibi, B. A., Abbas, A., Azeem, M. I., Shahbaz, P., ul Haq, S., & Nayak, R. K. (2025). Role of risk perception and climate change beliefs in adoption of climate-resilient agricultural practices in Saudi Arabia. *Climate Services*, *38*, 100552. https://doi.org/10.1016/j.cliser.2025.100552

Amburgey, E. (2024). *Migration and translocal livelihoods: Transformation amidst climate change in Mustang, Nepal* [University of British Columbia]. https://doi.org/10.14288/1.0437957

Anand, S., Aarti, & Singh, A. (2025). Investigation of the trends and variability in rainfall pattern in the Upper Kumaon Himalayan region. *Frontiers in Climate*, *7*. https://doi.org/10.3389/fclim.2025.1492260

Aryal, A., Maharjan, M., Talchabhadel, R., & Thapa, B. R. (2022). Characterizing Meteorological Droughts in Nepal: A Comparative Analysis of Standardized Precipitation Index and Rainfall Anomaly Index. *Earth*, *3*(1), Article 1. https://doi.org/10.3390/earth3010025

Aryal, S., Grießinger, J., Gaire, N. P., Bhattarai, T., & Bräuning, A. (2024). Drought, temperature, and moisture availability: Understanding the drivers of isotopic decoupling in native pine species of the Nepalese Himalaya. *International Journal*

*of Biometeorology*, *68*(6), 1093–1108. https://doi.org/10.1007/s00484-024-02647-z

Bagale, D., Sigdel, M., & Aryal, D. (2021). Drought Monitoring over Nepal for the Last Four Decades and Its Connection with Southern Oscillation Index. *Water*, *13*(23), Article 23. https://doi.org/10.3390/w13233411

Bammou, Y., Benzougagh, B., Bensaid, A., Igmoullan, B., & Al-Quraishi, A. M. F. (2024). Mapping of current and future soil erosion risk in a semi-arid context (haouz plain—Marrakech) based on CMIP6 climate models, the analytical hierarchy process (AHP) and RUSLE. *Modeling Earth Systems and Environment*, *10*(1), 1501–1514. https://doi.org/10.1007/s40808-023-01845-9

Bañares, E. N., Mehboob, M. S., Khan, A. R., & Cacal, J. C. (2024). Projecting hydrological response to climate change and urbanization using WEAP model: A case study for the main watersheds of Bicol River Basin, Philippines. *Journal of Hydrology: Regional Studies*, *54*, 101846. https://doi.org/10.1016/j.ejrh.2024.101846

Banstola, P., Krishna, P., & Sapkota, B. (2019). Flood Risk Mapping and Analysis Using Hydrodynamic Model HEC-RAS: A Case Study of Daraudi River, Chhepatar, Gorkha, Nepal. *Grassroots Journal of Natural Resources*, *2*(3), 25–44. https://doi.org/10.33002/nr2581.6853.02033

Barendrecht, M. H., Matanó, A., Mendoza, H., Weesie, R., Rohse, M., Koehler, J., De Ruiter, M., Garcia, M., Mazzoleni, M., Aerts, J. C. J. H., Ward, P. J., Di Baldassarre, G., Day, R., & Van Loon, A. F. (2024). Exploring drought-to-flood interactions and dynamics: A global case review. *WIREs Water*, e1726. https://doi.org/10.1002/wat2.1726

Bom, U., Tiefenbacher, J., & Belbase, S. (2023). Individual and community perceptions of climate change in Lower Mustang, Nepal. *Environment, Development and Sustainability*, *25*(7), 5997–6031. https://doi.org/10.1007/s10668-022-02291-w

Chae, S. T., & Chung, E.-S. (2024). Significant contribution of bias correction methods to uncertainty in future runoff projections under CMIP6 climate change. *Journal of Hydrology: Regional Studies*, *56*, 101973. https://doi.org/10.1016/j.ejrh.2024.101973

Dahal, P., Shrestha, N. S., Shrestha, M. L., Krakauer, N. Y., Panthi, J., Pradhanang, S. M., Jha, A., & Lakhankar, T. (2016). Drought risk assessment in central Nepal: Temporal and spatial analysis. *Natural Hazards*, *80*(3), 1913–1932. https://doi.org/10.1007/s11069-015-2055-5

Dar, F. A., Ramanathan, A., Mir, R. A., & Pir, R. A. (2024). Groundwater scenario under climate change and anthropogenic stress in Ladakh Himalaya, India. *Journal of Water and Climate Change*, *15*(4), 1459–1489. https://doi.org/10.2166/wcc.2024.307

De la Cruz, G., Huerta, A., Franco-León, P., Pino-Vargas, E., Ramos-Fernández, L., & Lavado-Casimiro, W. (2025). Future Climate Projections for Tacna, Peru: Assessing Changes in Temperature and Precipitation. *Atmosphere*, *16*(2), Article 2. https://doi.org/10.3390/atmos16020144

Delalay, M., Ziegler, A. D., Shrestha, M. S., Wasson, R. J., Sudmeier-Rieux, K., McAdoo, B. G., & Kochhar, I. (2018a). Towards improved flood disaster governance in Nepal: A case study in Sindhupalchok District. *International Journal of Disaster Risk Reduction*, *31*, 354–366.

Delalay, M., Ziegler, A. D., Shrestha, M. S., Wasson, R. J., Sudmeier-Rieux, K., McAdoo, B. G., & Kochhar, I. (2018b). Towards improved flood disaster governance in Nepal: A case study in Sindhupalchok District. *International Journal of Disaster Risk Reduction*, *31*, 354–366. https://doi.org/10.1016/j.ijdrr.2018.05.025

Dhakal, S., Subedi, R., Kandel, S., & Shrestha, S. (2024). Remote sensing and geospatial approach: Optimizing groundwater exploration in semi-arid region, Nepal. *Heliyon*, *10*(10), e31281. https://doi.org/10.1016/j.heliyon.2024.e31281

Dirnböck, T., Bahn, M., Diaz-Pines, E., Djukic, I., Englisch, M., Gartner, K., Gollobich, G., Ingrisch, J., Kitzler, B., Knaebel, K., Kobler, J., Maier, A., Malli, A., Offenthaler, I., Peterseil, J., Pröll, G., Venier, S., Wohner, C., Zechmeister-Boltenstern, S., … Glatzel, S. (2025). High-resolution carbon cycling data from 2019 to 2021 measured at six Austrian long-term ecosystem research sites. *Earth System Science Data*, *17*(2), 685–702. https://doi.org/10.5194/essd-17-685-2025

Drisya, J., & Al-Zubari, W. K. (2025). Investigating the Future Precipitation Changes Over the Kingdom of Bahrain Using CMIP6 Projections. *Earth Systems and Environment*. https://doi.org/10.1007/s41748-025-00578-2

Endendijk, T., Botzen, W. J. W., de Moel, H., Aerts, J. C. J. H., Slager, K., & Kok, M. (2023). Flood Vulnerability Models and Household Flood Damage Mitigation Measures: An Econometric Analysis of Survey Data. *Water Resources Research*, *59*(8), e2022WR034192. https://doi.org/10.1029/2022WR034192

Eshetae, M. A., Balcha, Y., Yeboah, S., Admassu, Z., & Abera, W. (2025). Targeted farm typology-based strategy for climate-smart agriculture interventions: A case study in the Guinea Savannah agro-ecological zone of Ghana. *Climate Smart Agriculture*, 100050. https://doi.org/10.1016/j.csag.2025.100050

Forster, P. M., Smith, C. J., Walsh, T., Lamb, W. F., Lamboll, R., Hauser, M., Ribes, A., Rosen, D., Gillett, N., Palmer, M. D., Rogelj, J., von Schuckmann, K., Seneviratne, S. I., Trewin, B., Zhang, X., Allen, M., Andrew, R., Birt, A., Borger, A., … Zhai, P. (2023). Indicators of Global Climate Change 2022: Annual update of large-scale indicators of the state of the climate system and human influence. *Earth System Science Data*, *15*(6), 2295–2327. https://doi.org/10.5194/essd-15-2295-2023

Fujinami, H., Sugimoto, S., & Ueno, K. (2025). Dynamics of Rainstorms Over Southern Himalayan Slopes and Foothills and Their Simulation by Numerical Models. In S. Das & W.-K. Tao (Eds.), *Severe Storms: Anatomy, Early Warning Systems and Aftermath in Changing Climate Scenarios* (pp. 333–359). Springer Nature. https://doi.org/10.1007/978-981-97-7075-5_13

Gadouali, F., Benabdelouahab, T., Boudhar, A., Hadria, R., Semane, N., Fadil, A., & Elrhaz, K. (2024). Bias correction of regional climate model simulation for hydrological climate change over Bouregrag watershed in Morocco. *International Journal of Hydrology Science and Technology*, *18*(2), 125–139. https://doi.org/10.1504/IJHST.2024.140312

Ganguli, P., Han, S., Muñoz, D. F., & Pal, S. (2025a). Editorial: Spatiotemporal Modelling and Assessment of Water-Related Multihazards. *Frontiers in Water*, *7*. https://doi.org/10.3389/frwa.2025.1579106

Ganguli, P., Han, S., Muñoz, D. F., & Pal, S. (2025b). Editorial: Spatiotemporal Modelling and Assessment of Water-Related Multihazards. *Frontiers in Water*, *7*. https://doi.org/10.3389/frwa.2025.1579106

Ghazi, B., Salehi, H., Przybylak, R., & Pospieszyńska, A. (2025). Projection of climate change impact on the occurrence of drought events in Poland. *Scientific Reports*, *15*(1), 5609. https://doi.org/10.1038/s41598-025-90488-0

Goodarzi, M. R., Hashemipour, Z., Saremi, A., & Niazkar, M. (2024). Intercomparison of machine learning methods for statistical downscaling of daily temperature under CMIP6 scenarios: A case study from Iran. *Journal of Hydroinformatics*, *26*(12), 3207–3223. https://doi.org/10.2166/hydro.2024.227

Gulakhmadov, A., Chen, X., Gulahmadov, N., Rizwan, M., Gulakhmadov, M., Nadeem, M. U., Rakhimova, M., & Liu, T. (2025). Modeling of historical and future changes in temperature and precipitation in the Panj River Basin in Central Asia under the CMIP5 RCP and CMIP6 SSP scenarios. *Scientific Reports*, *15*(1), 3037. https://doi.org/10.1038/s41598-025-86366-4

Gupta, N., Dahal, S., Kumar, A., Kumar, C., Kumar, M., Maharjan, A., Mishra, D., Mohanty, A., Navaraj, A., Pandey, S., Prakash, A., Prasad, E., Shrestha, K., Shrestha, M. S., Subedi, R., Subedi, T., Tiwary, R., Tuladhar, R., & Unni, A. (2021). Rich water, poor people: Potential for transboundary flood management between Nepal and India. *Current Research in Environmental Sustainability*, *3*, 100031. https://doi.org/10.1016/j.crsust.2021.100031

Hamed, K., & Rao, A. R. (Eds.). (2019). *Flood Frequency Analysis*. CRC Press. https://doi.org/10.1201/9780429128813

Haq, F., Afreen, M., Mark, B. G., Rahman, G., Shum, C. K., Shutkin, T. Y., & Tjoelker, A. R. (2025). Localized environmental variability within the Hindukush-Himalayan region of Pakistan. *Environmental Earth Sciences*, *84*(4), 105. https://doi.org/10.1007/s12665-025-12112-8

Hoseini, S. M., Soltanpour, M., & Zolfaghari, M. R. (2025). Climate change impacts on temperature and precipitation over the Caspian Sea. *International Journal of Water Resources Development*, *41*(1), 31–56. https://doi.org/10.1080/07900627.2024.2313050

Intergovernmental Panel On Climate Change (Ipcc). (2023). *Climate Change 2021 – The Physical Science Basis: Working Group I Contribution to the Sixth Assessment Report of the Intergovernmental Panel on Climate Change* (1st ed.). Cambridge University Press. https://doi.org/10.1017/9781009157896

Kashyap, A., Cook, K. L., & Behera, M. D. (2025). Geomorphic imprint of high-mountain floods: Insights from the 2022 hydrological extreme across the upper Indus River catchment in the northwestern Himalayas. *Earth Surface Dynamics*, *13*(1), 147–166. https://doi.org/10.5194/esurf-13-147-2025

Khan, Z., Rahman, A., & Karim, F. (2023). An Assessment of Uncertainties in Flood Frequency Estimation Using Bootstrapping and Monte Carlo Simulation. *Hydrology*, *10*(1), Article 1. https://doi.org/10.3390/hydrology10010018

Krishnan, R., Sanjay, J., Gnanaseelan, C., Mujumdar, M., Kulkarni, A., & Chakraborty, S. (2020). *Assessment of Climate Change over the Indian Region: A Report of the Ministry of Earth Sciences (MoES), Government of India*. Springer Nature.

Kumar, V., Sharma, K. V., Caloiero, T., Mehta, D. J., & Singh, K. (2023). Comprehensive Overview of Flood Modeling Approaches: A Review of Recent Advances. *Hydrology*, *10*(7), Article 7. https://doi.org/10.3390/hydrology10070141

Kuttippurath, J., Patel, V. K., & Sharma, B. R. (2024). Observed changes in the climate and snow dynamics of the Third Pole. *Npj Climate and Atmospheric Science*, *7*(1), 1–14. https://doi.org/10.1038/s41612-024-00710-5

Leguizamón, Y., Goldenberg, M. G., Jobbágy, E., Whitworth-Hulse, J. I., Satorre, E., Paolini, M., Martini, G., Micheloud, J. R., & Garibaldi, L. A. (2025). Crop diversity enhances drought tolerance and reduces environmental impact in commodity crops. *Agriculture, Ecosystems & Environment*, *385*, 109585. https://doi.org/10.1016/j.agee.2025.109585

Li, X., & Li, Z. (2025). Assessment of bias correction methods for high resolution daily precipitation projections with CMIP6 models: A Canadian case study. *Journal of Hydrology: Regional Studies*, *58*, 102223. https://doi.org/10.1016/j.ejrh.2025.102223

Liu, Z., Si, J., Deng, Y., Jia, B., Li, X., He, X., Zhou, D., Wang, C., Zhu, X., Qin, J., Ndayambaza, B., & Wang, B. (2023). Assessment of Land Desertification and Its Drivers in Semi-Arid Alpine Mountains: A Case Study of the Qilian Mountains Region, Northwest China. *Remote Sensing*, *15*(15), Article 15. https://doi.org/10.3390/rs15153836

Mahakur, M., Shige, S., & Hirose, M. (2025). Chapter 1—Multi-scale manifestation of tropical precipitation as evidenced from recent satellite observations. In P. Mukhopadhyay, B. Khouider, & S. Shige (Eds.), *Multi-Scale Precipitation Variability Over the Tropics* (pp. 1–33). Elsevier. https://doi.org/10.1016/B978-0-443-14030-3.00001-2

Maranzoni, A., D'Oria, M., & Rizzo, C. (2023). Quantitative flood hazard assessment methods: A review. *Journal of Flood Risk Management*, *16*(1), e12855. https://doi.org/10.1111/jfr3.12855

McChesney, K. (2015). *Existential avalanche the lived experience of climate change in Dolpo and Mustang, Nepal*. https://digitalcollections.sit.edu/isp_collection/2091/

Meehl, G. A., Boer, G. J., Covey, C., Latif, M., & Stouffer, R. J. (2000). The Coupled Model Intercomparison Project (CMIP). *Bulletin of the American Meteorological Society*, *81*(2), 313–318.

Meliho, M., Braun, M., Khattabi, A., & Orlando, C. A. (2025a). Selection of climate simulations for climate change impact studies: Case study of the Souss watershed, Morocco. *Theoretical and Applied Climatology*, *156*(2), 115. https://doi.org/10.1007/s00704-025-05353-x

Meliho, M., Braun, M., Khattabi, A., & Orlando, C. A. (2025b). Selection of climate simulations for climate change impact studies: Case study of the Souss watershed, Morocco. *Theoretical and Applied Climatology*, *156*(2), 115. https://doi.org/10.1007/s00704-025-05353-x

Mishra, A. K., & Singh, V. P. (2010). A review of drought concepts. *Journal of Hydrology*, *391*(1), 202–216. https://doi.org/10.1016/j.jhydrol.2010.07.012

Mohapatra, M., Srivastava, A., Nadimpalli, R., & Kumar, N. (2025). Evolution of Heat Wave Monitoring and Forecasting in India. *MAUSAM*, *76*(1), Article 1. https://doi.org/10.54302/mausam.v76i1.6457

Mustafa, A., & Faraz, A. (2023). *Camel Systems and Pastoralists' Lifestyle in Semi-Deserts and Mountains: Constraints and Challenges* (pp. 305–326). https://doi.org/10.33002/mount.a/17

Nabinejad, S., & Schüttrumpf, H. (2023). Flood Risk Management in Arid and Semi-Arid Areas: A Comprehensive Review of Challenges, Needs, and Opportunities. *Water*, *15*(17), Article 17. https://doi.org/10.3390/w15173113

Nandgude, N., Singh, T. P., Nandgude, S., & Tiwari, M. (2023). Drought Prediction: A Comprehensive Review of Different Drought Prediction Models and Adopted Technologies. *Sustainability*, *15*(15), Article 15. https://doi.org/10.3390/su151511684

O'Neill, B. C., Tebaldi, C., van Vuuren, D. P., Eyring, V., Friedlingstein, P., Hurtt, G., Knutti, R., Kriegler, E., Lamarque, J.-F., Lowe, J., Meehl, G. A., Moss, R., Riahi, K., & Sanderson, B. M. (2016). The Scenario Model Intercomparison Project (ScenarioMIP) for CMIP6. *Geoscientific Model Development*, *9*(9), 3461–3482. https://doi.org/10.5194/gmd-9-3461-2016

Orr, A., Ahmad, B., Alam, U., Appadurai, A., Bharucha, Z. P., Biemans, H., Bolch, T., Chaulagain, N. P., Dhaubanjar, S., Dimri, A. P., Dixon, H., Fowler, H. J., Gioli, G., Halvorson, S. J., Hussain, A., Jeelani, G., Kamal, S., Khalid, I. S., Liu, S., … Wescoat Jr., J. L. (2022). Knowledge Priorities on Climate Change and Water in the Upper Indus Basin: A Horizon Scanning Exercise to Identify the Top 100 Research Questions in Social and Natural Sciences. *Earth's Future*, *10*(4), e2021EF002619. https://doi.org/10.1029/2021EF002619

Pandey, U., Wanwey, S. R., Gandhi, N., Ram, S., Borgaonkar, H. P., & Sangode, S. (2025). Tree growth responses to the climate variability within the Pir Panjal Range evidenced by tree-rings of Abies pindrow (Royle ex D. Don) Royle. *Theoretical and Applied Climatology*, *156*(2), 91. https://doi.org/10.1007/s00704-024-05302-0

Papalexiou, S. M., & Koutsoyiannis, D. (2013). Battle of extreme value distributions: A global survey on extreme daily rainfall. *Water Resources Research*, *49*(1), 187–201. https://doi.org/10.1029/2012WR012557

Parajuli, G., Neupane, S., Kunwar, S., Adhikari, R., & Acharya, T. D. (2023). A GIS-Based Evacuation Route Planning in Flood-Susceptible Area of Siraha Municipality, Nepal. *ISPRS International Journal of Geo-Information*, *12*(7), Article 7. https://doi.org/10.3390/ijgi12070286

Penny, J., Khadka, D., Babel, M., Alves, P., Djordjević, S., Chen, A. S., & Loc, H. H. (2023). Integrated assessment of flood and drought hazards for current and future climate in a tributary of the Mekong river basin. *Journal of Water and Climate Change*, *14*(12), 4424–4443. https://doi.org/10.2166/wcc.2023.252

Qiao, Y., Xu, W., Meng, C., Liao, X., & Qin, L. (2022). Increasingly dry/wet abrupt alternation events in a warmer world: Observed evidence from China during 1980–2019. *International Journal of Climatology*, *42*(12), 6429–6440. https://doi.org/10.1002/joc.7598

Qiu, Y., Feng, J., Yan, Z., Wang, J., & Li, Z. (2022). High-resolution dynamical downscaling for regional climate projection in Central Asia based on bias-corrected multiple GCMs. *Climate Dynamics*, *58*(3), 777–791. https://doi.org/10.1007/s00382-021-05934-2

Qu, C., Li, J., Yan, L., Yan, P., Cheng, F., & Lu, D. (2020). Non-Stationary Flood Frequency Analysis Using Cubic B-Spline-Based GAMLSS Model. *Water*, *12*(7), Article 7. https://doi.org/10.3390/w12071867

Rahman, H.-U., Khan, A., Rahman, A.-U., & Shaw, R. (2024). Spatio-Temporal Dynamics of Land Use Land Cover and Its Impact on Flood-Prone Drainage Basin of River Swat, Eastern Hindukush. In R. Mazumder & R. Shaw (Eds.), *Surface Environments and Human Interactions: Reflections from Asia* (pp. 29–40). Springer Nature. https://doi.org/10.1007/978-981-97-0112-4_3

Riahi, K., van Vuuren, D. P., Kriegler, E., Edmonds, J., O'Neill, B. C., Fujimori, S., Bauer, N., Calvin, K., Dellink, R., Fricko, O., Lutz, W., Popp, A., Cuaresma, J. C., Kc, S., Leimbach, M., Jiang, L., Kram, T., Rao, S., Emmerling, J., … Tavoni, M. (2017). The Shared Socioeconomic Pathways and their energy, land use, and greenhouse gas emissions implications: An overview. *Global Environmental Change*, *42*, 153–168. https://doi.org/10.1016/j.gloenvcha.2016.05.009

Sangroula, S., Adhikari, T. R., Parajuli, A., & Poudyal, K. (n.d.). *Impact of Climate Change on Future Flow Response in Marshyangdi River Basin, Nepal*.

Sanusi, M. M., & Dries, L. (2025). Smallholder rice farmers' resilience to water insecurity in Ogun State Nigeria. *Regional Environmental Change*, *25*(1), 30. https://doi.org/10.1007/s10113-025-02364-2

Schaller, G. B. (1998). *Wildlife of the Tibetan steppe*. University of Chicago Press.

Seneviratne, S. I., Zhang, X., Adnan, M., Badi, W., Dereczynski, C., Luca, A. D., Ghosh, S., Iskandar, I., Kossin, J., Lewis, S., Otto, F., Pinto, I., Satoh, M., Vicente-Serrano, S. M., Wehner, M., Zhou, B., & Allan, R. (2021). *Weather and climate extreme events in a changing climate* (V. P. Masson-Delmotte, A. Zhai, S. L. Pirani, & C. Connors, Eds.; pp. 1513–1766). Cambridge University Press. https://centaur.reading.ac.uk/101846/

Shanmugam, H., & Lakshmanan, V. R. (2025). Development of stacking algorithm for bias-correcting the precipitation projections using a multi-model ensemble

of CMIP6 GCMs in a semi-arid basin, India. *Theoretical and Applied Climatology*, *156*(2), 129. https://doi.org/10.1007/s00704-024-05321-x

Sharma, A. P., Fu, X., & Kattel, G. R. (2023a). Is there a progressive flood risk management in Nepal? A synthesis based on the perspective of a half-century (1971–2020) flood outlook. *Natural Hazards*, *118*(2), 903–923. https://doi.org/10.1007/s11069-023-06035-5

Sharma, A. P., Fu, X., & Kattel, G. R. (2023b). Is there a progressive flood risk management in Nepal? A synthesis based on the perspective of a half-century (1971–2020) flood outlook. *Natural Hazards*, *118*(2), 903–923. https://doi.org/10.1007/s11069-023-06035-5

Sharma, C., & Ojha, C. (2019). Changes of Annual Precipitation and Probability Distributions for Different Climate Types of the World. *Water*, *11*, 2092. https://doi.org/10.3390/w11102092

Shrestha, H. K., & Prasain, S. (2016). Climate change impact and adaptation measures needed in upper Mustang to prevent more climate refugees. *Research Briefs*, *125*, 1–6.

Sigdel, K. P., Ghimire, N. P., Pandeya, B., & Dawadi, B. (2022). Historical and Projected Variations of Precipitation and Temperature and Their Extremes in Relation to Climatic Indices over the Gandaki River Basin, Central Himalaya. *Atmosphere*, *13*(11), Article 11. https://doi.org/10.3390/atmos13111866

Sithara, S., Pramada, S. K., & Thampi, S. G. (2022). Statistical downscaling of sea levels: Application of multi-criteria analysis for selection of global climate models. *Environmental Monitoring and Assessment*, *194*(10), 764. https://doi.org/10.1007/s10661-022-10449-2

Stagge, J. H., Tallaksen, L. M., Gudmundsson, L., Loon, A. F. V., & Stahl, K. (2015). Candidate Distributions for Climatological Drought Indices (SPI and SPEI). *International Journal of Climatology*, *35*(13), Article 13. https://doi.org/10.1002/joc.4267

Tan, Y., Dong, N., Hou, A., & Yan, W. (2023). An Improved Xin'anjiang Hydrological Model for Flood Simulation Coupling Snowmelt Runoff Module in Northwestern China. *Water*, *15*(19), Article 19. https://doi.org/10.3390/w15193401

Twinomuhangi, M. B., Bamutaze, Y., Kabenge, I., Wanyama, J., Kizza, M., Gabiri, G., & Egli, P. E. (2025). Analysis of stationary and non-stationary hydrological extremes

under a changing environment: A systematic review. *HydroResearch*, *8*, 332–350. https://doi.org/10.1016/j.hydres.2024.12.007

Vahedifard, F., AghaKouchak, A., Ragno, E., Shahrokhabadi, S., & Mallakpour, I. (2017). Lessons from the Oroville dam. *Science*, *355*(6330), 1139–1140. https://doi.org/10.1126/science.aan0171

van der Sleen, P., Decuyper, M., Flores, B. M., Householder, J. E., & Holmgren, M. (2025). ENSO Wildfires Impact Amazonian Floodplains in Complex Ways. *Ecosystems*, *28*(2), 20. https://doi.org/10.1007/s10021-025-00966-9

Wang, F., Harindintwali, J. D., Wei, K., Shan, Y., Mi, Z., Costello, M. J., Grunwald, S., Feng, Z., Wang, F., Guo, Y., Wu, X., Kumar, P., Kästner, M., Feng, X., Kang, S., Liu, Z., Fu, Y., Zhao, W., Ouyang, C., … Tiedje, J. M. (2023). Climate change: Strategies for mitigation and adaptation. *The Innovation Geoscience*, *1*(1), 100015–100095. https://doi.org/10.59717/j.xinn-geo.2023.100015

Wiertz, D., & Graaf, N. D. de. (2022). *Chapter 24: The climate crisis: what sociology can contribute*. https://www.elgaronline.com/edcollchap-oa/book/9781789909432/book-part-9781789909432-35.xml

Wu, X., Liu, Z., & Duan, Q. (2025). A combined wavelet analysis-quantile mapping (WA-QM) method for bias correction: Capturing the intra-annual temporal patterns in climate model precipitation simulations and projections. *Environmental Research Letters*, *20*(2), 024049. https://doi.org/10.1088/1748-9326/adae23

Xuehua, A., Shanlei, S., Qianrong, M., Hao, W., Daiyuan, L., & Wei, W. (n.d.). Elucidating the Varied Characteristics of Compound Hot–Drought From Two Distinctive Extreme Events in the Yangtze River Valley. *International Journal of Climatology*, *n/a*(n/a), e8809. https://doi.org/10.1002/joc.8809

Zhou, T.-J., Zou, L.-W., & Chen, X.-L. (2019). Commentary on the Coupled Model Intercomparison Project Phase 6 (CMIP6). *Advances in Climate Change Research*, *15*(5), 445. https://doi.org/10.12006/j.issn.1673-1719.2019.193

## ANNEX

*Table A: Observed flood frequency analysis*

| Scenario | Station | Model | Return Period | Threshold | Flood Years | Fit_AICc | Preferred_Model |
|---|---|---|---|---|---|---|---|
| Observed | Chhoser | GEV | 10 | 67.15 | 1985, 1987, 1997, 1998, 2005 | 370.78 | TRUE |
| Observed | Chhoser | GEV | 20 | 96.37 | 2005 | 370.78 | TRUE |
| Observed | Chhoser | GEV | 25 | 108.10 | None | 370.78 | TRUE |
| Observed | Chhoser | GEV | 50 | 154.09 | None | 370.78 | TRUE |
| Observed | Chhoser | GEV | 100 | 219.22 | None | 370.78 | TRUE |
| Observed | Chhoser | Gumbel | 10 | 58.68 | 1980, 1985, 1987, 1996, 1997, 1998, 2005 | 378.77 | FALSE |
| Observed | Chhoser | Gumbel | 20 | 69.33 | 1985, 1987, 1997, 1998, 2005 | 378.77 | FALSE |
| Observed | Chhoser | Gumbel | 25 | 72.70 | 1985, 1987, 1997, 1998, 2005 | 378.77 | FALSE |
| Observed | Chhoser | Gumbel | 50 | 83.11 | 1985, 1997, 2005 | 378.77 | FALSE |
| Observed | Chhoser | Gumbel | 100 | 93.44 | 2005 | 378.77 | FALSE |
| Observed | Dhakarjhong | GEV | 10 | 67.15 | 1985, 1987, 1997, 1998, 2005 | 370.78 | TRUE |
| Observed | Dhakarjhong | GEV | 20 | 96.37 | 2005 | 370.78 | TRUE |
| Observed | Dhakarjhong | GEV | 25 | 108.10 | None | 370.78 | TRUE |
| Observed | Dhakarjhong | GEV | 50 | 154.09 | None | 370.78 | TRUE |
| Observed | Dhakarjhong | GEV | 100 | 219.22 | None | 370.78 | TRUE |
| Observed | Dhakarjhong | Gumbel | 10 | 58.68 | 1980, 1985, 1987, 1996, 1997, 1998, 2005 | 378.77 | FALSE |
| Observed | Dhakarjhong | Gumbel | 20 | 69.33 | 1985, 1987, 1997, 1998, 2005 | 378.77 | FALSE |
| Observed | Dhakarjhong | Gumbel | 25 | 72.70 | 1985, 1987, 1997, 1998, 2005 | 378.77 | FALSE |
| Observed | Dhakarjhong | Gumbel | 50 | 83.11 | 1985, 1997, 2005 | 378.77 | FALSE |

| Scenario | Station | Model | Return Period | Threshold | Flood Years | Fit_AICc | Preferred_Model |
|---|---|---|---|---|---|---|---|
| Observed | Dhakarjhong | Gumbel | 100 | 93.44 | 2005 | 378.77 | FALSE |
| Observed | Jomsom | GEV | 10 | 66.26 | 1985, 1987, 1997, 1998, 2005 | 372.04 | TRUE |
| Observed | Jomsom | GEV | 20 | 93.08 | 2005 | 372.04 | TRUE |
| Observed | Jomsom | GEV | 25 | 103.61 | None | 372.04 | TRUE |
| Observed | Jomsom | GEV | 50 | 143.98 | None | 372.04 | TRUE |
| Observed | Jomsom | GEV | 100 | 199.29 | None | 372.04 | TRUE |
| Observed | Jomsom | Gumbel | 10 | 58.79 | 1980, 1985, 1987, 1996, 1997, 1998, 2005 | 379.06 | FALSE |
| Observed | Jomsom | Gumbel | 20 | 69.49 | 1985, 1987, 1997, 1998, 2005 | 379.06 | FALSE |
| Observed | Jomsom | Gumbel | 25 | 72.89 | 1985, 1987, 1997, 1998, 2005 | 379.06 | FALSE |
| Observed | Jomsom | Gumbel | 50 | 83.35 | 1985, 1997, 2005 | 379.06 | FALSE |
| Observed | Jomsom | Gumbel | 100 | 93.73 | 2005 | 379.06 | FALSE |
| Observed | Lete | GEV | 10 | 66.68 | 1985, 1987, 1997, 1998, 2005 | 368.68 | TRUE |
| Observed | Lete | GEV | 20 | 95.71 | 2005 | 368.68 | TRUE |
| Observed | Lete | GEV | 25 | 107.41 | None | 368.68 | TRUE |
| Observed | Lete | GEV | 50 | 153.50 | None | 368.68 | TRUE |
| Observed | Lete | GEV | 100 | 219.19 | None | 368.68 | TRUE |
| Observed | Lete | Gumbel | 10 | 58.44 | 1980, 1985, 1987, 1996, 1997, 1998, 2005 | 377.62 | FALSE |
| Observed | Lete | Gumbel | 20 | 68.91 | 1985, 1987, 1997, 1998, 2005 | 377.62 | FALSE |
| Observed | Lete | Gumbel | 25 | 72.23 | 1985, 1987, 1997, 1998, 2005 | 377.62 | FALSE |
| Observed | Lete | Gumbel | 50 | 82.46 | 1985, 1997, 2005 | 377.62 | FALSE |
| Observed | Lete | Gumbel | 100 | 92.61 | 2005 | 377.62 | FALSE |
| Observed | Ranipauwa | GEV | 10 | 69.33 | 1985, 1987, 1997, 1998, 2005 | 376.18 | TRUE |
| Observed | Ranipauwa | GEV | 20 | 95.84 | 2005 | 376.18 | TRUE |
| Observed | Ranipauwa | GEV | 25 | 106.11 | None | 376.18 | TRUE |

| Scenario | Station | Model | Return Period | Threshold | Flood Years | Fit_AICc | Preferred_Model |
|---|---|---|---|---|---|---|---|
| Observed | Ranipauwa | GEV | 50 | 144.90 | None | 376.18 | TRUE |
| Observed | Ranipauwa | GEV | 100 | 196.94 | None | 376.18 | TRUE |
| Observed | Ranipauwa | Gumbel | 10 | 61.61 | 1985, 1987, 1996, 1997, 1998, 2005 | 380.29 | FALSE |
| Observed | Ranipauwa | Gumbel | 20 | 72.65 | 1985, 1987, 1997, 1998, 2005 | 380.29 | FALSE |
| Observed | Ranipauwa | Gumbel | 25 | 76.14 | 1985, 1987, 1997, 2005 | 380.29 | FALSE |
| Observed | Ranipauwa | Gumbel | 50 | 86.93 | 1985, 1997, 2005 | 380.29 | FALSE |
| Observed | Ranipauwa | Gumbel | 100 | 97.63 | 2005 | 380.29 | FALSE |
| Observed | Samar Gaun | GEV | 10 | 67.26 | 1985, 1987, 1997, 1998, 2005 | 368.67 | TRUE |
| Observed | Samar Gaun | GEV | 20 | 97.73 | 2005 | 368.67 | TRUE |
| Observed | Samar Gaun | GEV | 25 | 110.15 | None | 368.67 | TRUE |
| Observed | Samar Gaun | GEV | 50 | 159.57 | None | 368.67 | TRUE |
| Observed | Samar Gaun | GEV | 100 | 231.16 | None | 368.67 | TRUE |
| Observed | Samar Gaun | Gumbel | 10 | 58.44 | 1980, 1985, 1987, 1996, 1997, 1998, 2005 | 377.98 | FALSE |
| Observed | Samar Gaun | Gumbel | 20 | 68.96 | 1985, 1987, 1997, 1998, 2005 | 377.98 | FALSE |
| Observed | Samar Gaun | Gumbel | 25 | 72.29 | 1985, 1987, 1997, 1998, 2005 | 377.98 | FALSE |
| Observed | Samar Gaun | Gumbel | 50 | 82.57 | 1985, 1997, 2005 | 377.98 | FALSE |
| Observed | Samar Gaun | Gumbel | 100 | 92.77 | 2005 | 377.98 | FALSE |
| Observed | Thakmarpha | GEV | 10 | 66.68 | 1985, 1987, 1997, 1998, 2005 | 368.68 | TRUE |
| Observed | Thakmarpha | GEV | 20 | 95.71 | 2005 | 368.68 | TRUE |
| Observed | Thakmarpha | GEV | 25 | 107.41 | None | 368.68 | TRUE |
| Observed | Thakmarpha | GEV | 50 | 153.50 | None | 368.68 | TRUE |
| Observed | Thakmarpha | GEV | 100 | 219.19 | None | 368.68 | TRUE |
| Observed | Thakmarpha | Gumbel | 10 | 58.44 | 1980, 1985, 1987, 1996, 1997, 1998, 2005 | 377.62 | FALSE |
| Observed | Thakmarpha | Gumbel | 20 | 68.91 | 1985, 1987, 1997, 1998, 2005 | 377.62 | FALSE |

| Scenario | Station | Model | Return Period | Threshold | Flood Years | Fit_AICc | Preferred_Model |
|---|---|---|---|---|---|---|---|
| Observed | Thakmarpha | Gumbel | 25 | 72.23 | 1985, 1987, 1997, 1998, 2005 | 377.62 | FALSE |
| Observed | Thakmarpha | Gumbel | 50 | 82.46 | 1985, 1997, 2005 | 377.62 | FALSE |
| Observed | Thakmarpha | Gumbel | 100 | 92.61 | 2005 | 377.62 | FALSE |

Table B: Historical flood frequency analysis

| Scenario | Station | Model | Return Period | Threshold | Flood Years | Fit_AICc | Preferred_Model |
|---|---|---|---|---|---|---|---|
| Historical | Chhoser | GEV | 10 | 6.48 | 2000, 2001, 2006 | 92.77 | FALSE |
| Historical | Chhoser | GEV | 20 | 6.89 | 2000, 2001, 2006 | 92.77 | FALSE |
| Historical | Chhoser | GEV | 25 | 7.02 | 2000, 2001, 2006 | 92.77 | FALSE |
| Historical | Chhoser | GEV | 50 | 7.38 | 2001, 2006 | 92.77 | FALSE |
| Historical | Chhoser | GEV | 100 | 7.71 | None | 92.77 | FALSE |
| Historical | Chhoser | Gumbel | 10 | 6.61 | 2000, 2001, 2006 | 91.45 | TRUE |
| Historical | Chhoser | Gumbel | 20 | 7.15 | 2001, 2006 | 91.45 | TRUE |
| Historical | Chhoser | Gumbel | 25 | 7.32 | 2001, 2006 | 91.45 | TRUE |
| Historical | Chhoser | Gumbel | 50 | 7.84 | None | 91.45 | TRUE |
| Historical | Chhoser | Gumbel | 100 | 8.36 | None | 91.45 | TRUE |
| Historical | Dhakarjhong | GEV | 10 | 9.82 | 2000, 2001, 2006 | 132.35 | FALSE |
| Historical | Dhakarjhong | GEV | 20 | 10.55 | 2000, 2001, 2006 | 132.35 | FALSE |
| Historical | Dhakarjhong | GEV | 25 | 10.77 | 2001, 2006 | 132.35 | FALSE |
| Historical | Dhakarjhong | GEV | 50 | 11.42 | 2006 | 132.35 | FALSE |
| Historical | Dhakarjhong | GEV | 100 | 12.02 | None | 132.35 | FALSE |
| Historical | Dhakarjhong | Gumbel | 10 | 10.01 | 2000, 2001, 2006 | 130.74 | TRUE |
| Historical | Dhakarjhong | Gumbel | 20 | 10.94 | 2001, 2006 | 130.74 | TRUE |
| Historical | Dhakarjhong | Gumbel | 25 | 11.24 | 2001, 2006 | 130.74 | TRUE |
| Historical | Dhakarjhong | Gumbel | 50 | 12.15 | None | 130.74 | TRUE |
| Historical | Dhakarjhong | Gumbel | 100 | 13.05 | None | 130.74 | TRUE |
| Historical | Jomsom | GEV | 10 | 12.50 | 1986, 2000, 2001, 2006 | 157.36 | FALSE |
| Historical | Jomsom | GEV | 20 | 13.62 | 2000, 2001, 2006 | 157.36 | FALSE |
| Historical | Jomsom | GEV | 25 | 13.97 | 2001, 2006 | 157.36 | FALSE |
| Historical | Jomsom | GEV | 50 | 15.01 | 2001 | 157.36 | FALSE |
| Historical | Jomsom | GEV | 100 | 16.01 | None | 157.36 | FALSE |

| Scenario | Station | Model | Return Period | Threshold | Flood Years | Fit_AICc | Preferred_Model |
|---|---|---|---|---|---|---|---|
| Historical | Jomsom | Gumbel | 10 | 12.62 | 2000, 2001, 2006 | 155.12 | TRUE |
| Historical | Jomsom | Gumbel | 20 | 13.91 | 2001, 2006 | 155.12 | TRUE |
| Historical | Jomsom | Gumbel | 25 | 14.32 | 2001 | 155.12 | TRUE |
| Historical | Jomsom | Gumbel | 50 | 15.58 | None | 155.12 | TRUE |
| Historical | Jomsom | Gumbel | 100 | 16.83 | None | 155.12 | TRUE |
| Historical | Lete | GEV | 10 | 31.06 | 2000, 2001, 2004, 2013 | 199.87 | FALSE |
| Historical | Lete | GEV | 20 | 32.72 | 2000, 2001 | 199.87 | FALSE |
| Historical | Lete | GEV | 25 | 33.21 | 2000, 2001 | 199.87 | FALSE |
| Historical | Lete | GEV | 50 | 34.61 | None | 199.87 | FALSE |
| Historical | Lete | GEV | 100 | 35.84 | None | 199.87 | FALSE |
| Historical | Lete | Gumbel | 10 | 31.82 | 2000, 2001, 2004 | 198.98 | TRUE |
| Historical | Lete | Gumbel | 20 | 34.30 | 2000 | 198.98 | TRUE |
| Historical | Lete | Gumbel | 25 | 35.09 | None | 198.98 | TRUE |
| Historical | Lete | Gumbel | 50 | 37.51 | None | 198.98 | TRUE |
| Historical | Lete | Gumbel | 100 | 39.92 | None | 198.98 | TRUE |
| Historical | Ranipauwa | GEV | 10 | 15.79 | 2000, 2001, 2004, 2013 | 167.40 | TRUE |
| Historical | Ranipauwa | GEV | 20 | 16.61 | 2000, 2001, 2004 | 167.40 | TRUE |
| Historical | Ranipauwa | GEV | 25 | 16.83 | 2000, 2001, 2004 | 167.40 | TRUE |
| Historical | Ranipauwa | GEV | 50 | 17.44 | 2004 | 167.40 | TRUE |
| Historical | Ranipauwa | GEV | 100 | 17.93 | None | 167.40 | TRUE |
| Historical | Ranipauwa | Gumbel | 10 | 16.69 | 2000, 2001, 2004 | 169.60 | FALSE |
| Historical | Ranipauwa | Gumbel | 20 | 18.37 | None | 169.60 | FALSE |
| Historical | Ranipauwa | Gumbel | 25 | 18.90 | None | 169.60 | FALSE |
| Historical | Ranipauwa | Gumbel | 50 | 20.54 | None | 169.60 | FALSE |
| Historical | Ranipauwa | Gumbel | 100 | 22.17 | None | 169.60 | FALSE |
| Historical | Samar Gaun | GEV | 10 | 12.05 | 2000, 2001 | 139.02 | TRUE |

| Scenario | Station | Model | Return Period | Threshold | Flood Years | Fit_AICc | Preferred_Model |
|---|---|---|---|---|---|---|---|
| Historical | Samar Gaun | GEV | 20 | 12.70 | 2000, 2001 | 139.02 | TRUE |
| Historical | Samar Gaun | GEV | 25 | 12.88 | 2000, 2001 | 139.02 | TRUE |
| Historical | Samar Gaun | GEV | 50 | 13.41 | 2000, 2001 | 139.02 | TRUE |
| Historical | Samar Gaun | GEV | 100 | 13.86 | None | 139.02 | TRUE |
| Historical | Samar Gaun | Gumbel | 10 | 12.45 | 2000, 2001 | 139.19 | FALSE |
| Historical | Samar Gaun | Gumbel | 20 | 13.52 | 2001 | 139.19 | FALSE |
| Historical | Samar Gaun | Gumbel | 25 | 13.86 | None | 139.19 | FALSE |
| Historical | Samar Gaun | Gumbel | 50 | 14.90 | None | 139.19 | FALSE |
| Historical | Samar Gaun | Gumbel | 100 | 15.94 | None | 139.19 | FALSE |
| Historical | Thakmarpha | GEV | 10 | 14.60 | 2000, 2001, 2004, 2013 | 160.07 | FALSE |
| Historical | Thakmarpha | GEV | 20 | 15.56 | 2000, 2001 | 160.07 | FALSE |
| Historical | Thakmarpha | GEV | 25 | 15.84 | 2000, 2001 | 160.07 | FALSE |
| Historical | Thakmarpha | GEV | 50 | 16.64 | None | 160.07 | FALSE |
| Historical | Thakmarpha | GEV | 100 | 17.36 | None | 160.07 | FALSE |
| Historical | Thakmarpha | Gumbel | 10 | 15.02 | 2000, 2001 | 159.11 | TRUE |
| Historical | Thakmarpha | Gumbel | 20 | 16.43 | 2000, 2001 | 159.11 | TRUE |
| Historical | Thakmarpha | Gumbel | 25 | 16.87 | None | 159.11 | TRUE |
| Historical | Thakmarpha | Gumbel | 50 | 18.24 | None | 159.11 | TRUE |
| Historical | Thakmarpha | Gumbel | 100 | 19.60 | None | 159.11 | TRUE |

*Table C: SSP245 Flood frequency analysis*

| Scenario | Station | Model | Return Period | Threshold | Flood Years | Fit_AICc | Preferred_ Model |
|---|---|---|---|---|---|---|---|
| SSP245 | Chhoser | GEV | 10 | 9.47 | 2042, 2048, 2064, 2069, 2071, 2077, 2089, 2096, 2099 | 340.22 | FALSE |
| SSP245 | Chhoser | GEV | 20 | 10.44 | 2064, 2089, 2096, 2099 | 340.22 | FALSE |
| SSP245 | Chhoser | GEV | 25 | 10.74 | 2064, 2096, 2099 | 340.22 | FALSE |
| SSP245 | Chhoser | GEV | 50 | 11.65 | 2096 | 340.22 | FALSE |
| SSP245 | Chhoser | GEV | 100 | 12.53 | None | 340.22 | FALSE |
| SSP245 | Chhoser | Gumbel | 10 | 9.52 | 2042, 2048, 2064, 2071, 2077, 2089, 2096, 2099 | 338.17 | TRUE |
| SSP245 | Chhoser | Gumbel | 20 | 10.56 | 2064, 2089, 2096, 2099 | 338.17 | TRUE |
| SSP245 | Chhoser | Gumbel | 25 | 10.89 | 2064, 2096, 2099 | 338.17 | TRUE |
| SSP245 | Chhoser | Gumbel | 50 | 11.90 | 2096 | 338.17 | TRUE |
| SSP245 | Chhoser | Gumbel | 100 | 12.90 | None | 338.17 | TRUE |
| SSP245 | Dhakarjhong | GEV | 10 | 15.24 | 2042, 2048, 2064, 2069, 2071, 2077, 2078, 2089, 2096, 2099 | 440.65 | FALSE |
| SSP245 | Dhakarjhong | GEV | 20 | 17.09 | 2064, 2089, 2096, 2099 | 440.65 | FALSE |
| SSP245 | Dhakarjhong | GEV | 25 | 17.68 | 2064, 2096, 2099 | 440.65 | FALSE |
| SSP245 | Dhakarjhong | GEV | 50 | 19.48 | 2064, 2096 | 440.65 | FALSE |
| SSP245 | Dhakarjhong | GEV | 100 | 21.28 | None | 440.65 | FALSE |
| SSP245 | Dhakarjhong | Gumbel | 10 | 15.24 | 2042, 2048, 2064, 2069, 2071, 2077, 2078, 2089, 2096, 2099 | 438.50 | TRUE |
| SSP245 | Dhakarjhong | Gumbel | 20 | 17.09 | 2064, 2089, 2096, 2099 | 438.50 | TRUE |
| SSP245 | Dhakarjhong | Gumbel | 25 | 17.67 | 2064, 2096, 2099 | 438.50 | TRUE |
| SSP245 | Dhakarjhong | Gumbel | 50 | 19.47 | 2064, 2096 | 438.50 | TRUE |

| Scenario | Station | Model | Return Period | Threshold | Flood Years | Fit_AICc | Preferred_ Model |
|---|---|---|---|---|---|---|---|
| SSP245 | Dhakarjhong | Gumbel | 100 | 21.26 | None | 438.50 | TRUE |
| SSP245 | Jomsom | GEV | 10 | 19.08 | 2032, 2064, 2068, 2071, 2077, 2083, 2093, 2094, 2096, 2097, 2099 | 489.46 | FALSE |
| SSP245 | Jomsom | GEV | 20 | 21.49 | 2071, 2077, 2097 | 489.46 | FALSE |
| SSP245 | Jomsom | GEV | 25 | 22.25 | 2071, 2077, 2097 | 489.46 | FALSE |
| SSP245 | Jomsom | GEV | 50 | 24.58 | 2071 | 489.46 | FALSE |
| SSP245 | Jomsom | GEV | 100 | 26.89 | None | 489.46 | FALSE |
| SSP245 | Jomsom | Gumbel | 10 | 19.11 | 2032, 2064, 2068, 2071, 2077, 2083, 2093, 2094, 2096, 2097, 2099 | 487.32 | TRUE |
| SSP245 | Jomsom | Gumbel | 20 | 21.57 | 2071, 2077, 2097 | 487.32 | TRUE |
| SSP245 | Jomsom | Gumbel | 25 | 22.34 | 2071, 2077, 2097 | 487.32 | TRUE |
| SSP245 | Jomsom | Gumbel | 50 | 24.74 | 2071 | 487.32 | TRUE |
| SSP245 | Jomsom | Gumbel | 100 | 27.12 | None | 487.32 | TRUE |
| SSP245 | Lete | GEV | 10 | 31.06 | 2000, 2001, 2004, 2013 | 199.87 | FALSE |
| SSP245 | Lete | GEV | 20 | 32.72 | 2000, 2001 | 199.87 | FALSE |
| SSP245 | Lete | GEV | 25 | 33.21 | 2000, 2001 | 199.87 | FALSE |
| SSP245 | Lete | GEV | 50 | 34.61 | None | 199.87 | FALSE |
| SSP245 | Lete | GEV | 100 | 35.84 | None | 199.87 | FALSE |
| SSP245 | Lete | Gumbel | 10 | 31.82 | 2000, 2001, 2004 | 198.98 | TRUE |
| SSP245 | Lete | Gumbel | 20 | 34.30 | 2000 | 198.98 | TRUE |
| SSP245 | Lete | Gumbel | 25 | 35.09 | None | 198.98 | TRUE |
| SSP245 | Lete | Gumbel | 50 | 37.51 | None | 198.98 | TRUE |
| SSP245 | Lete | Gumbel | 100 | 39.92 | None | 198.98 | TRUE |
| SSP245 | Ranipauwa | GEV | 10 | 23.17 | 2042, 2068, 2069, 2071, 2077, 2080, 2089, 2096, 2097, 2099 | 499.00 | FALSE |

| Scenario | Station | Model | Return Period | Threshold | Flood Years | Fit_AICc | Preferred_ Model |
|---|---|---|---|---|---|---|---|
| SSP245 | Ranipauwa | GEV | 20 | 26.72 | 2077, 2089, 2096 | 499.00 | FALSE |
| SSP245 | Ranipauwa | GEV | 25 | 27.93 | None | 499.00 | FALSE |
| SSP245 | Ranipauwa | GEV | 50 | 31.94 | None | 499.00 | FALSE |
| SSP245 | Ranipauwa | GEV | 100 | 36.37 | None | 499.00 | FALSE |
| SSP245 | Ranipauwa | Gumbel | 10 | 22.58 | 2042, 2068, 2069, 2071, 2077, 2080, 2089, 2096, 2097, 2099 | 498.11 | TRUE |
| SSP245 | Ranipauwa | Gumbel | 20 | 25.14 | 2077, 2089, 2096, 2099 | 498.11 | TRUE |
| SSP245 | Ranipauwa | Gumbel | 25 | 25.95 | 2077, 2089, 2096 | 498.11 | TRUE |
| SSP245 | Ranipauwa | Gumbel | 50 | 28.45 | None | 498.11 | TRUE |
| SSP245 | Ranipauwa | Gumbel | 100 | 30.94 | None | 498.11 | TRUE |
| SSP245 | Samar Gaun | GEV | 10 | 17.32 | 2042, 2052, 2077, 2080, 2084, 2089, 2096, 2097, 2099 | 440.03 | FALSE |
| SSP245 | Samar Gaun | GEV | 20 | 19.34 | 2042, 2089, 2096 | 440.03 | FALSE |
| SSP245 | Samar Gaun | GEV | 25 | 20.00 | 2089, 2096 | 440.03 | FALSE |
| SSP245 | Samar Gaun | GEV | 50 | 22.07 | 2096 | 440.03 | FALSE |
| SSP245 | Samar Gaun | GEV | 100 | 24.19 | None | 440.03 | FALSE |
| SSP245 | Samar Gaun | Gumbel | 10 | 17.18 | 2042, 2052, 2069, 2077, 2078, 2080, 2084, 2089, 2096, 2097, 2099 | 438.07 | TRUE |
| SSP245 | Samar Gaun | Gumbel | 20 | 19.01 | 2042, 2077, 2089, 2096, 2099 | 438.07 | TRUE |
| SSP245 | Samar Gaun | Gumbel | 25 | 19.59 | 2089, 2096 | 438.07 | TRUE |
| SSP245 | Samar Gaun | Gumbel | 50 | 21.37 | 2096 | 438.07 | TRUE |
| SSP245 | Samar Gaun | Gumbel | 100 | 23.14 | None | 438.07 | TRUE |
| SSP245 | Thakmarpha | GEV | 10 | 20.75 | 2068, 2069, 2071, 2077, 2083, 2084, 2089, 2094, 2096, 2097, 2098, 2099 | 473.43 | FALSE |
| SSP245 | Thakmarpha | GEV | 20 | 23.64 | 2077 | 473.43 | FALSE |
| SSP245 | Thakmarpha | GEV | 25 | 24.62 | 2077 | 473.43 | FALSE |

| Scenario | Station | Model | Return Period | Threshold | Flood Years | Fit_AICc | Preferred_ Model |
|---|---|---|---|---|---|---|---|
| SSP245 | Thakmarpha | GEV | 50 | 27.80 | None | 473.43 | FALSE |
| SSP245 | Thakmarpha | GEV | 100 | 31.25 | None | 473.43 | FALSE |
| SSP245 | Thakmarpha | Gumbel | 10 | 20.33 | 2032, 2068, 2069, 2071, 2077, 2083, 2084, 2089, 2094, 2096, 2097, 2098, 2099 | 472.48 | TRUE |
| SSP245 | Thakmarpha | Gumbel | 20 | 22.53 | 2068, 2071, 2077, 2099 | 472.48 | TRUE |
| SSP245 | Thakmarpha | Gumbel | 25 | 23.23 | 2077, 2099 | 472.48 | TRUE |
| SSP245 | Thakmarpha | Gumbel | 50 | 25.39 | 2077 | 472.48 | TRUE |
| SSP245 | Thakmarpha | Gumbel | 100 | 27.52 | None | 472.48 | TRUE |

*Table D: SSP585 Flood Frequency Analysis*

| Scenario | Station | Model | Return Period | Threshold | Flood Years | Fit_AICc | Preferred_Model |
|---|---|---|---|---|---|---|---|
| SSP585 | Chhoser | GEV | 10 | 11.84 | 2068, 2077, 2078, 2080, 2081, 2084, 2085, 2092, 2093, 2094, 2098, 2100 | 403.50 | FALSE |
| SSP585 | Chhoser | GEV | 20 | 13.54 | 2068, 2092, 2093, 2098 | 403.50 | FALSE |
| SSP585 | Chhoser | GEV | 25 | 14.10 | 2068, 2092, 2098 | 403.50 | FALSE |
| SSP585 | Chhoser | GEV | 50 | 15.86 | 2092 | 403.50 | FALSE |
| SSP585 | Chhoser | GEV | 100 | 17.70 | None | 403.50 | FALSE |
| SSP585 | Chhoser | Gumbel | 10 | 11.69 | 2068, 2077, 2078, 2080, 2081, 2084, 2085, 2092, 2093, 2094, 2098, 2100 | 401.74 | TRUE |
| SSP585 | Chhoser | Gumbel | 20 | 13.17 | 2068, 2077, 2085, 2092, 2093, 2098 | 401.74 | TRUE |
| SSP585 | Chhoser | Gumbel | 25 | 13.63 | 2068, 2092, 2093, 2098 | 401.74 | TRUE |
| SSP585 | Chhoser | Gumbel | 50 | 15.07 | 2092 | 401.74 | TRUE |
| SSP585 | Chhoser | Gumbel | 100 | 16.50 | None | 401.74 | TRUE |
| SSP585 | Dhakarjhong | GEV | 10 | 19.39 | 2068, 2077, 2078, 2080, 2081, 2084, 2085, 2092, 2093, 2094, 2098, 2100 | 504.74 | FALSE |
| SSP585 | Dhakarjhong | GEV | 20 | 22.41 | 2068, 2092, 2093, 2098 | 504.74 | FALSE |
| SSP585 | Dhakarjhong | GEV | 25 | 23.40 | 2068, 2092, 2098 | 504.74 | FALSE |
| SSP585 | Dhakarjhong | GEV | 50 | 26.52 | None | 504.74 | FALSE |
| SSP585 | Dhakarjhong | GEV | 100 | 29.74 | None | 504.74 | FALSE |
| SSP585 | Dhakarjhong | Gumbel | 10 | 19.15 | 2068, 2077, 2078, 2080, 2081, 2084, 2085, 2092, 2093, 2094, 2097, 2098, 2100 | 502.93 | TRUE |
| SSP585 | Dhakarjhong | Gumbel | 20 | 21.80 | 2068, 2077, 2092, 2093, 2098, 2100 | 502.93 | TRUE |
| SSP585 | Dhakarjhong | Gumbel | 25 | 22.65 | 2068, 2092, 2093, 2098 | 502.93 | TRUE |
| SSP585 | Dhakarjhong | Gumbel | 50 | 25.24 | 2092 | 502.93 | TRUE |
| SSP585 | Dhakarjhong | Gumbel | 100 | 27.82 | None | 502.93 | TRUE |

| Scenario | Station | Model | Return Period | Threshold | Flood Years | Fit_AICc | Preferred_Model |
|---|---|---|---|---|---|---|---|
| SSP585 | Jomsom | GEV | 10 | 23.97 | 2068, 2077, 2078, 2080, 2081, 2092, 2093, 2094, 2097, 2100 | 545.02 | FALSE |
| SSP585 | Jomsom | GEV | 20 | 27.65 | 2068, 2077, 2080, 2092, 2093, 2094 | 545.02 | FALSE |
| SSP585 | Jomsom | GEV | 25 | 28.84 | 2077, 2080, 2092, 2094 | 545.02 | FALSE |
| SSP585 | Jomsom | GEV | 50 | 32.57 | None | 545.02 | FALSE |
| SSP585 | Jomsom | GEV | 100 | 36.39 | None | 545.02 | FALSE |
| SSP585 | Jomsom | Gumbel | 10 | 23.75 | 2068, 2077, 2078, 2080, 2081, 2092, 2093, 2094, 2097, 2100 | 543.04 | TRUE |
| SSP585 | Jomsom | Gumbel | 20 | 27.12 | 2068, 2077, 2080, 2092, 2093, 2094 | 543.04 | TRUE |
| SSP585 | Jomsom | Gumbel | 25 | 28.18 | 2077, 2080, 2092, 2094 | 543.04 | TRUE |
| SSP585 | Jomsom | Gumbel | 50 | 31.47 | None | 543.04 | TRUE |
| SSP585 | Jomsom | Gumbel | 100 | 34.73 | None | 543.04 | TRUE |
| SSP585 | Lete | GEV | 10 | 50.25 | 2068, 2078, 2087, 2092, 2093, 2094, 2096, 2098, 2099 | 636.76 | FALSE |
| SSP585 | Lete | GEV | 20 | 56.43 | 2078, 2087, 2092, 2093, 2094, 2096 | 636.76 | FALSE |
| SSP585 | Lete | GEV | 25 | 58.42 | 2078, 2087, 2092, 2096 | 636.76 | FALSE |
| SSP585 | Lete | GEV | 50 | 64.65 | 2087, 2092 | 636.76 | FALSE |
| SSP585 | Lete | GEV | 100 | 70.98 | None | 636.76 | FALSE |
| SSP585 | Lete | Gumbel | 10 | 49.95 | 2068, 2078, 2087, 2092, 2093, 2094, 2096, 2098, 2099 | 634.74 | TRUE |
| SSP585 | Lete | Gumbel | 20 | 55.69 | 2078, 2087, 2092, 2093, 2094, 2096 | 634.74 | TRUE |
| SSP585 | Lete | Gumbel | 25 | 57.52 | 2078, 2087, 2092, 2096 | 634.74 | TRUE |
| SSP585 | Lete | Gumbel | 50 | 63.13 | 2087, 2092, 2096 | 634.74 | TRUE |
| SSP585 | Lete | Gumbel | 100 | 68.71 | None | 634.74 | TRUE |
| SSP585 | Ranipauwa | GEV | 10 | 28.50 | 2068, 2078, 2087, 2092, 2093, 2094, 2096, 2099 | 561.82 | FALSE |
| SSP585 | Ranipauwa | GEV | 20 | 32.51 | 2078, 2087, 2092, 2093, 2096 | 561.82 | FALSE |

| Scenario | Station | Model | Return Period | Threshold | Flood Years | Fit_AICc | Preferred_Model |
|---|---|---|---|---|---|---|---|
| SSP585 | Ranipauwa | GEV | 25 | 33.80 | 2078, 2087, 2092, 2096 | 561.82 | FALSE |
| SSP585 | Ranipauwa | GEV | 50 | 37.84 | 2087 | 561.82 | FALSE |
| SSP585 | Ranipauwa | GEV | 100 | 41.94 | None | 561.82 | FALSE |
| SSP585 | Ranipauwa | Gumbel | 10 | 28.31 | 2068, 2078, 2087, 2089, 2092, 2093, 2094, 2096, 2099 | 559.79 | TRUE |
| SSP585 | Ranipauwa | Gumbel | 20 | 32.02 | 2068, 2078, 2087, 2092, 2093, 2096 | 559.79 | TRUE |
| SSP585 | Ranipauwa | Gumbel | 25 | 33.20 | 2078, 2087, 2092, 2096 | 559.79 | TRUE |
| SSP585 | Ranipauwa | Gumbel | 50 | 36.83 | 2087 | 559.79 | TRUE |
| SSP585 | Ranipauwa | Gumbel | 100 | 40.44 | None | 559.79 | TRUE |
| SSP585 | Samar Gaun | GEV | 10 | 21.88 | 2068, 2078, 2081, 2087, 2092, 2093, 2094, 2096, 2098 | 509.89 | FALSE |
| SSP585 | Samar Gaun | GEV | 20 | 24.88 | 2078, 2087, 2092, 2093, 2096, 2098 | 509.89 | FALSE |
| SSP585 | Samar Gaun | GEV | 25 | 25.85 | 2087, 2092, 2093, 2096 | 509.89 | FALSE |
| SSP585 | Samar Gaun | GEV | 50 | 28.89 | 2092 | 509.89 | FALSE |
| SSP585 | Samar Gaun | GEV | 100 | 32.00 | None | 509.89 | FALSE |
| SSP585 | Samar Gaun | Gumbel | 10 | 21.70 | 2068, 2078, 2081, 2087, 2092, 2093, 2094, 2096, 2098 | 507.92 | TRUE |
| SSP585 | Samar Gaun | Gumbel | 20 | 24.44 | 2068, 2078, 2087, 2092, 2093, 2096, 2098 | 507.92 | TRUE |
| SSP585 | Samar Gaun | Gumbel | 25 | 25.31 | 2078, 2087, 2092, 2093, 2096, 2098 | 507.92 | TRUE |
| SSP585 | Samar Gaun | Gumbel | 50 | 27.99 | 2092 | 507.92 | TRUE |
| SSP585 | Samar Gaun | Gumbel | 100 | 30.66 | None | 507.92 | TRUE |
| SSP585 | Thakmarpha | GEV | 10 | 26.19 | 2068, 2078, 2087, 2092, 2093, 2094, 2096, 2098, 2099 | 547.07 | FALSE |
| SSP585 | Thakmarpha | GEV | 20 | 29.95 | 2078, 2087, 2092, 2093, 2094, 2096 | 547.07 | FALSE |
| SSP585 | Thakmarpha | GEV | 25 | 31.17 | 2087, 2092, 2096 | 547.07 | FALSE |
| SSP585 | Thakmarpha | GEV | 50 | 35.00 | None | 547.07 | FALSE |
| SSP585 | Thakmarpha | GEV | 100 | 38.92 | None | 547.07 | FALSE |

| Scenario | Station | Model | Return Period | Threshold | Flood Years | Fit_AICc | Preferred_Model |
|---|---|---|---|---|---|---|---|
| SSP585 | Thakmarpha | Gumbel | 10 | 25.96 | 2068, 2075, 2078, 2087, 2092, 2093, 2094, 2096, 2098, 2099 | 545.11 | TRUE |
| SSP585 | Thakmarpha | Gumbel | 20 | 29.36 | 2078, 2087, 2092, 2093, 2094, 2096 | 545.11 | TRUE |
| SSP585 | Thakmarpha | Gumbel | 25 | 30.44 | 2078, 2087, 2092, 2096 | 545.11 | TRUE |
| SSP585 | Thakmarpha | Gumbel | 50 | 33.77 | 2087, 2092, 2096 | 545.11 | TRUE |
| SSP585 | Thakmarpha | Gumbel | 100 | 37.08 | None | 545.11 | TRUE |

# IOE Graduate Conference

## Certificate of Participation

THIS CERTIFICATE IS AWARDED TO

*Apechhya Aryal*

in recognition of an invaluable contribution as

**POSTER PRESENTER**

**at the 16th IOE Graduate Conference**

Organized by Tribhuvan University, IOE, Thapathali Campus in association with IOE, Office of the Dean held from April 18-20, 2025 at Thapathali Campus, Kathmandu, Nepal.

**Dr. Raj Kumar Chaulagain**
Convener
16th IOE Graduate Conference

**Dr. Khem Gyanwali**
Campus Chief
Thapathali Campus

**Prof. Dr. Sushil Bahadur Bajracharya**
Dean
Institute of Engineering

त्रिभुवन विश्वविद्यालय
Tribhuvan University
इन्जिनियरिङ्ग अध्ययन संस्थान
Institute of Engineering
थापाथली क्याम्पस
THAPATHALI CAMPUS
Accredited By University Grants Commission (UGC) Nepal, 2024

GPO Box- 280, Thapathali, Kathmandu
Tel: 01-5339766
E-mail: info@tcioe.edu.np
Website: www.tcioe.edu.np
गोश्वारा पो. नं. २८०, थापाथली, काठमाडौं
फोन: ०१-५३३५७६६

Date: April 21, 2025

**To Whom It May Concern:**

This is to certify that the paper titled **"Projected Drought Conditions in Mustang, Nepal: A Quantitative Assessment of Historical and Future SPI Trends Using CMIP6 Models"** (Submission# **440**) submitted by **Apechhya aryal** as the first author, which had been accepted for presentation after the peer-review process, has successfully been presented at the 16th IOE Graduate Conference held during April 18 - 20, 2025. Kindly note that the final revision of the papers and publication process of the conference proceedings is still underway and hence inclusion of the accepted manuscript in the conference proceedings is contingent upon timely response to further edits during the publication process.

INSTITUTE OF ENGINEERING
16th IOE Graduate Conference, 2025
THAPATHALI CAMPUS

Dr. Raj Kumar Chaulagain,
Convener,
16th IOE Graduate Conference

# Projected Drought Conditions in Mustang, Nepal: A Quantitative Assessment of Historical and Future SPI Trends Using CMIP6 Models

Apechhya Aryal [a], Dhiraj Pradhananga [b],

[a] *Department of Applied Science and Chemical Engineering, Pulchowk Campus, Institute of Engineering, Tribhuvan University, Kathmandu, 44600, Nepal*
[b] *Department of Meteorology, Tri-Chandra Multiple Campus, Tribhuvan University, Kathmandu, Nepal*
[a]079msccd005.apechhya@pcampus.edu.np

**Abstract**
Climate change has significantly intensified extreme weather events worldwide, with drought emerging as one of the most severe threats to water security, agriculture, and livelihoods, particularly in arid and semi-arid regions. These regions experience prolonged dry spells due to limited precipitation and rising temperatures, exacerbating socio-economic vulnerabilities. Mustang, Nepal, situated in the trans-Himalayan rain-shadow region, is especially prone to prolonged droughts due to its unique geographical and climatic conditions. The region receives minimal annual precipitation, and increasing temperatures have further amplified the frequency and severity of drought events, posing significant challenges to local communities that rely on traditional farming and livestock rearing. This study evaluates historical and future drought conditions in Mustang using the Standardized Precipitation Index (SPI) and bias-corrected simulations from CMIP6 climate models. Historical drought patterns from 1980 to 2014 are analyzed using observed meteorological data to assess changes in drought frequency, duration, and intensity. These findings are then compared with future projections under the SSP2-4.5 and SSP5-8.5 climate scenarios to understand how drought characteristics may evolve over time. The analysis reveals a noticeable increase in severe and extreme drought events, particularly in the latter half of the 21st century, with a pronounced intensification after 2050. Under higher emission scenarios, drought durations are projected to lengthen, and the frequency of consecutive dry years is expected to rise, leading to greater water stress for agriculture, ecosystems, and human settlements. Additionally, policymakers should prioritize long-term climate adaptation planning, including early warning systems and community-based water governance frameworks, to ensure sustainable water availability in the face of increasing climate variability. By integrating scientific research with local adaptation efforts, it is possible to enhance the resilience of Mustang's communities and ecosystems to the growing threats posed by climate change-induced droughts.

**Keywords**
Drought assessment, CMIP6 projections, Standardized Precipitation Index (SPI),Himalayan climate variability

## 1. Introduction

Climate change is characterized by long-term trends in temperature, precipitation, atmospheric pressure, and humidity, along with other environmental factors that influence weather patterns over extended periods[1]. Climate change is driving an increase in extreme weather conditions worldwide, with drought emerging as one of the most severe and persistent threats to water security, ecosystems, and livelihoods[2]. The impacts of drought are particularly pronounced in arid and semi-arid regions, where shifts in precipitation patterns and rising temperatures exacerbate water scarcity. [3].In the Himalayas, climate variability has led to significant changes in temperature and precipitation, intensifying drought conditions in high-altitude regions such as Mustang [4]. Droughts, unlike sudden disasters such as floods or landslides, develop over time, making them difficult to predict and manage. They disrupt agriculture, reduce water availability, and threaten biodiversity, making them a critical concern for communities that depend on natural water sources [5]. Floods and droughts are among the major natural hazards in the Himalayan region. According to a report by the Intergovernmental Panel on Climate Change (IPCC), the increasing frequency and intensity of these events will further exacerbate rural poverty in parts of Asia[6]. The increasing frequency and severity of droughts highlight the urgent need for better monitoring and adaptation strategies to mitigate their long-term effects [7]. Despite contributing just 0.025 percent of global greenhouse gas (GHG) emissions, Nepal faces disproportionate climate change impacts, particularly in its mountainous and rain-shadow regions [8]. Extreme weather conditions and water resource scarcity affect arid and semi-arid regions[9]. Drought is generally viewed as a sustained and regionally extensive occurrence of appreciably below-average natural water availability, either in the form of precipitation, surface water runoff, or ground water[10]. The consequences of prolonged drought in Mustang are severe, leading to environmental degradation, reduced agricultural productivity, and increased water stress. The Dhye village people are recognized as Nepal's first climate refugees,historical records indicate that mass migration from Dhye has occurred three times, with the most recent displacement directly linked to climate change. Similarly, in Samdzong village, unreliable irrigation due to drought led to failed crops and dying livestock, forcing 17 households (86 residents) to relocate to a new settlement named "Namashung," meaning green meadow [11]. Erratic precipitation patterns further complicate drought conditions in Mustang. While the region experiences prolonged dry periods, occasional extreme rainfall events trigger flash floods due to the dry, compacted soil's inability to absorb sudden water inflows [12]. This phenomenon, known as the

drought-to-flood transition, poses additional challenges for water management and disaster preparedness. Despite the severity of these impacts, research on drought in Nepal's high-altitude regions remains limited, with most studies focusing on flood hazards [13]. Drought presents a prolonged and equally devastating threat to water security, agriculture, and human settlements.

## 2. Methods and Methodology

### 2.1 Study Area

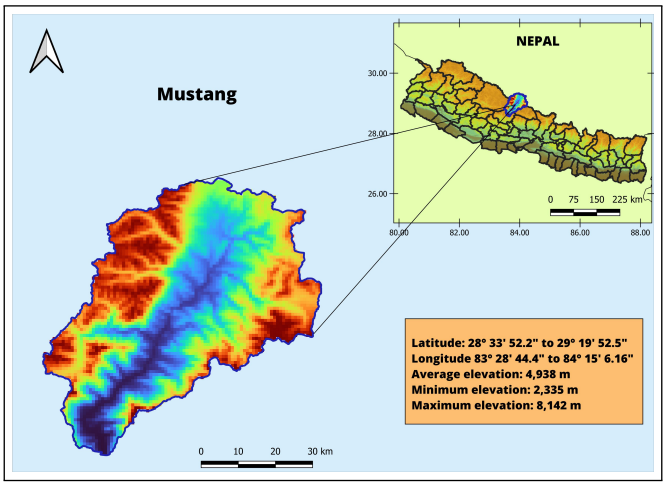


**Figure 1:** Location of Study Area

The climate and weather patterns of Mustang, Nepal, are heavily influenced by its position in the shadow of the Himalayan rains, creating a high-altitude desert environment. The region is known for its cold and dry climate, with annual precipitation often less than 300 mm, most of which occurs during the monsoon season [14]. Winters are severe, with temperatures frequently falling below freezing, while summers are milder but remain arid. The landscape, marked by rugged cliffs, deep canyons, and limited vegetation, reflects the extreme weather conditions. However, climate change is increasingly disrupting these patterns, leading to significant environmental and socio-economic challenges.In recent decades, Mustang has experienced irregular rainfall, extended droughts, and unpredictable snowfall, which has disturbed its fragile ecosystems. These changes have reduced water availability and affected agricultural practices, which are vital for local livelihoods [15]. The retreat of glaciers in the Himalayas has further intensified the scarcity of water, affecting both natural habitats and human communities. In addition, extreme weather events, such as unseasonal storms and flash floods, have become more frequent, increasing the risk of landslides and soil erosion. These events endanger infrastructure, homes and the rich cultural heritage of the region, including ancient caves and monasteries [16].

### 2.2 Research Problem and Objectives

Despite the growing evidence of drought-related impacts in high-altitude regions like Mustang, there is a lack of focused research addressing the drivers, patterns, and local responses to drought. The region's vulnerability is intensified by limited water infrastructure, fragile ecosystems, and high dependence on climate-sensitive livelihoods.

Research Objectives:

1.To analyze long-term trends and variability in precipitation and temperature in Mustang District.

2.To assess the severity, frequency, and spatial extent of droughts in the region.

**Figure 2:** New settlement that was built on Namasungh for the relocation from Samdzong.
Source:https://thehimalayantimes.com/nepal/prolonged-drought-hits-mustang-locals-hard

### 2.3 Methodology

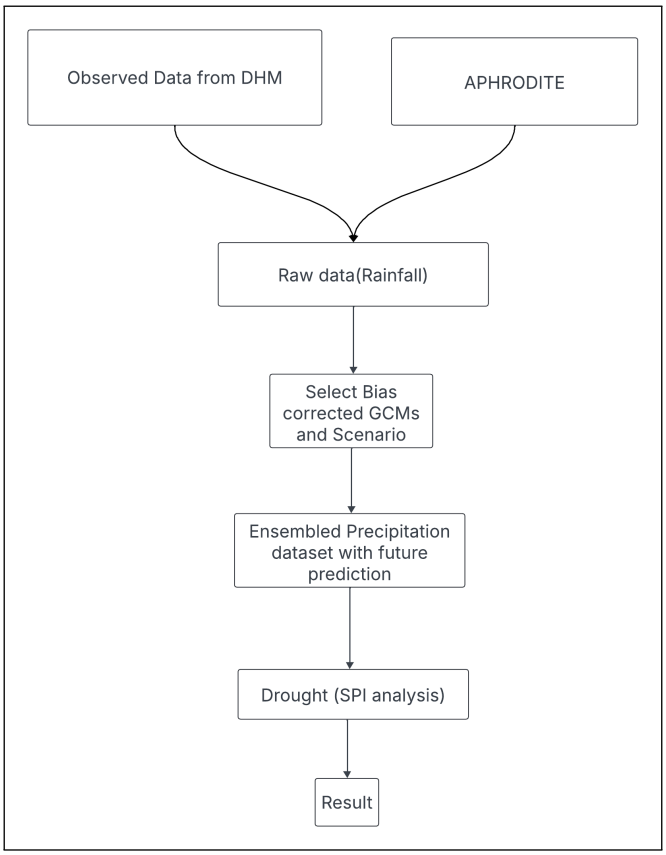


**Figure 3:** Methodology

## 2.4 Data

### 2.4.1 Observed Data

This study investigates historical climate trends in Mustang, Nepal, using data from eight observation stations carefully chosen for their extensive records, completeness, and wide geographic distribution. These stations offer a well-rounded representation of the region's diverse climatic conditions. Monthly precipitation records from 1980 to 2014 were obtained from the Department of Hydrology and Meteorology (DHM), Government of Nepal. To ensure data reliability, a homogeneity test was performed to detect inconsistencies or missing values. Any data gaps were addressed using APHRODITE, improving consistency and precision. The selected stations provide a representative sample that contributes to a comprehensive understanding of climate patterns in Mustang.

### 2.4.2 Model Simulations

This study uses six bias-corrected climate models CMIP6 specifically designed for Nepal, with a uniform spatial resolution of 0.25° × 0.25°. The bias correction approach, developed by[17], integrates observational data from various sources, including meteorological station measurements across South Asia. For regions outside India, additional reference data from[18] were incorporated.

A detailed description of the selected models is provided in Table 1, with additional data set information accessible through the reference source.The selected six models are based on shared socioeconomic pathways (SSPs) and consider two climate scenarios: SSP245 (moderate emissions) and SSP585 (high emissions) [19]. SSP2-4.5 reflects a "middle-of-the-road" scenario with moderate population growth, economic development, and emissions peaking around 2040 before declining. It leads to about 2.5–3°C warming by 2100. In contrast, SSP5-8.5 assumes continued fossil fuel use and limited climate policies, with emissions rising throughout the century, potentially causing over 4°C warming. The dataset includes historical climate data from 1980 to 2014 and projections from 2025 to 2100. Although these models initially varied in spatial resolution, bias correction has standardized all datasets to a 0.25° resolution, ensuring consistent coverage across six South Asian countries—Bangladesh, Bhutan, India, Nepal, Pakistan, and Sri Lanka. In addition, an ensemble mean dataset derived from these six CMIP6 models has been used to assess precipitation patterns and calculate the drought index (Table 1). Historical and projected CMIP6 climate simulations were obtained from $https://zenodo.org/records/3873998.YKOjiqgzY2w$.

| Model Name | Native Spatial Resolution (°) | Spatial Resolution After Bias Correction (°) | Historical Period | Projection Period |
|---|---|---|---|---|
| ACCESS-ESM1-5 | 1.25 × 1.875 | 0.25 × 0.25 | 1980-2014 | 2025-2100 |
| EC-Earth3 | 0.701 × 0.703 | 0.25 × 0.25 | 1980–2014 | 2025–2100 |
| EC-Earth3-Veg | 0.701 × 0.703 | 0.25 × 0.25 | 1980–2014 | 2025–2100 |
| MPI-ESM1-2-HR | 0.935 × 0.937 | 0.25 × 0.25 | 1980–2014 | 2025–2100 |
| MPI-ESM1-2-LR | 1.865 × 1.875 | 0.25 × 0.25 | 1980–2014 | 2025–2100 |
| MRI-ESM2-0 | 1.1215 × 1.125 | 0.25 × 0.25 | 1980–2014 | 2025–2100 |

**Table 1:** Selected GCM

### 2.4.3 Calculation of SPI

Many drought indices have been developed for the calculation of drought using different climatic parameters such as precipitation, temperature, and evaporation[20].In this study, we use the Standardized Precipitation Index (SPI) to assess drought conditions based on precipitation data. The standardized precipitation index (SPI) is one of the most widely used indexes [21]. The popularity of the SPI is founded on the simplicity of the calculation procedure and the perceived spatial comparability of index values[22] SPI uses precipitation records accumulated on different time scales, usually 1 to 48 months, to develop a probabilistic assessment of extreme conditions relative to climatology [23]. The SPI calculation follows the methodology described by [24], which standardizes precipitation values over a given time scale by fitting them to a probability distribution. For SPI computation, we fit the monthly precipitation series($P_i$)to a gamma distribution and then transform it into a standard normal distribution. This approach ensures that SPI values follow a normal distribution with a mean of zero and a standard deviation of one. SPI values can be both positive and negative, with positive values (SPI 1) indicating wetter-than-normal conditions and negative values (SPI 1) representing drier-than-normal conditions. A threshold of 1 is used to identify drought conditions are categorized into three levels:

- Moderate drought: 1.5 < SPI 1
- Severe drought: 2.0 < SPI 1.5
- Extreme drought: SPI Greater than 2.0

# 3. Result

## 3.1 Observed and Historical Drought Condition

The temporal variation of SPI-1 over Nepal at different timescales (1–12 months) for both observed and historical datasets during 1980–2014 is shown in Figures 4 and 5. The seasonal drought cycle captured in the heat maps reveals alternating wet and dry periods, with significant drought events occurring in the late 1980s, early 1990s, and post-2005 periods. Both observed and historical datasets show recurring drought conditions, particularly between 1990–1993 and after 2005. However, the historical dataset (Figure 5) displays more pronounced drought events, with extreme negative SPI values occurring in 1980–1985, 1990–1993, and post-2005. The observed dataset (Figure 4) also captures these dry spells but with slightly lower intensity, suggesting a potential underestimation of extreme drought severity in the historical dataset. The scatter plot (Figure 6) compares SPI values from observations and CMIP6 historical data, showing a moderate positive correlation($R^2 = 0.46$, $p < 0.01$). This indicates that while the CMIP6 historical dataset captures overall drought trends, it exhibits significant deviations, particularly underestimating mild-to-moderate droughts while

exaggerating some extreme events. The spread of points around the 1:1 line highlights these discrepancies, suggesting biases in CMIP6 drought simulations. The SPI-1 variations indicate that Nepal experienced wet conditions between 1998–2004 and dry conditions between 1990–1993 and after 2005. The frequency and severity of droughts have increased, with major events recorded in 1992, 1994, 2005, 2006, 2009, and 2012. Compared to observations, the historical dataset underestimated drought duration and severity, but overestimated drought frequency, suggesting a bias towards capturing shorter but more frequent dry spells.

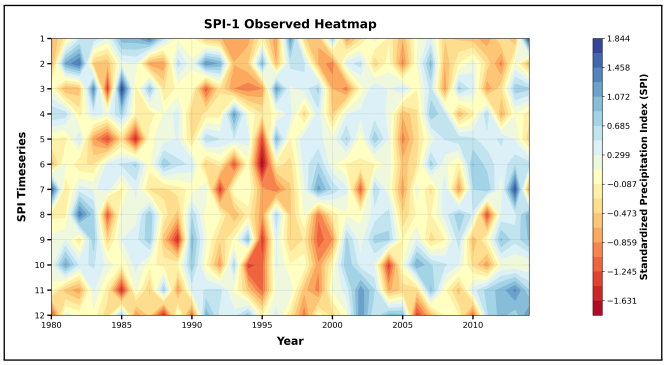


**Figure 4:** Observed SPI

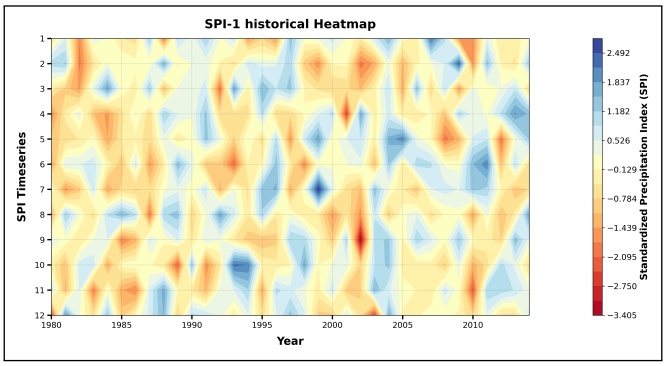


**Figure 5:** Historical SPI

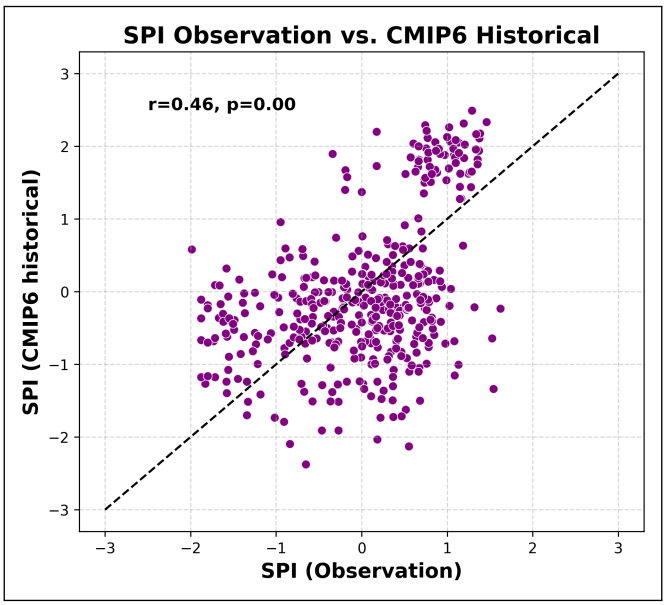


**Figure 6:** Correlation Calculation

### 3.1.1 Projected Drought Condition

Future climate projections under SSP2-4.5 and SSP5-8.5 scenarios indicate an increasing trend in drought frequency, severity, and duration across Nepal. The SPI-1 heatmaps for the 21st century (Figures 7 and 8) shows a clear shift towards drier conditions, with more frequent extreme droughts projected under the high-emission scenario (SSP5-8.5). The results suggest that the early 21st century (2025–2060) will experience more severe and prolonged droughts than the late 21st century (2061–2100). Under SSP2-4.5 (Figure 7), drought events remain persistent, though slightly less intense compared to SSP5-8.5 (Figure 8). The projected extreme drought frequency is 3.7However, SSP5-8.5 (Figure 8) projects more intense and prolonged droughts, with extreme SPI anomalies reaching -4.43 by the late 21st century. The frequency of drought events is expected to peak around 2040–2055, coinciding with a projected decline in precipitation and rising temperatures. The cumulative SPI frequency distributions confirm that moderate to extreme drought conditions will become more common, particularly in the premonsoon and winter seasons, when water availability is already limited.

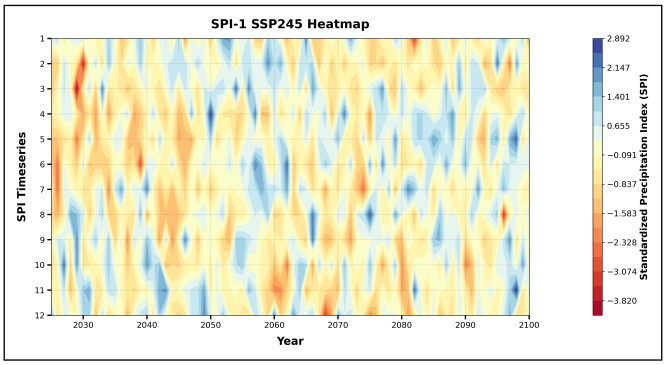


**Figure 7:** SSP245 SPI

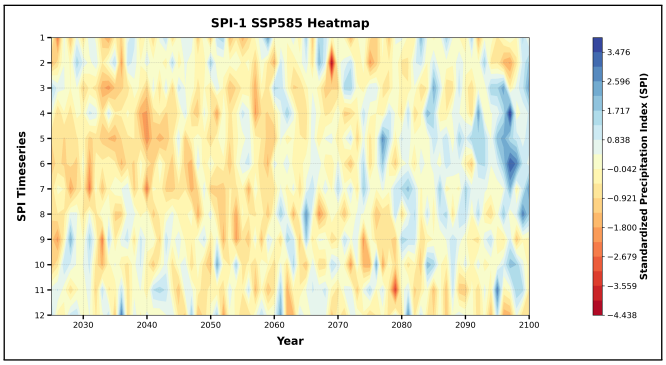


**Figure 8:** SSP585 SPI

## 4. Discussion

The results of this study underscore the growing vulnerability of Mustang, Nepal, to worsening drought conditions, both in terms of historical trends and future projections. Historical SPI trends indicate that Mustang has experienced multiple severe drought episodes, particularly during the late 1980s, early 1990s, and post-2005 periods. Although both observed and modeled data show similar patterns, the CMIP6 models

tend to overestimate extreme droughts while underestimating milder dry periods. This discrepancy suggests that while the models effectively capture broader drought trends, certain biases remain, especially in representing the full range of drought intensity. The social and environmental impacts of these historical droughts have been profound. Communities in Mustang, such as Dhye and Samdzong, have already faced forced migration due to prolonged drought conditions, making them some of Nepal's first climate refugees. Additionally, erratic precipitation patterns, including unexpected heavy rainfall, have led to rapid drought-to-flood transitions, complicating water resource management in the region.Looking ahead, climate projections for Mustang indicate an even more challenging scenario. Under both SSP2-4.5 and SSP5-8.5 emission pathways, the frequency and intensity of droughts are expected to increase significantly. The increasing severity of droughts will further strain Mustang's limited water resources, posing a serious threat to agriculture, biodiversity, and local communities. Reduced precipitation, coupled with rising temperatures, will exacerbate soil moisture deficits, making traditional farming methods unsustainable. The growing unpredictability of precipitation patterns will also make it harder for communities to plan agricultural cycles and manage water resources efficiently. Beyond climate change, several natural and human-induced factors also contribute to Mustang's drought vulnerability. Located in the rain shadow of the Himalayas, Mustang receives minimal annual rainfall due to the obstruction of monsoon clouds by mountain ranges. The region's natural aridity is compounded by limited water infrastructure and inefficient traditional irrigation systems, which further exacerbate water scarcity. Additionally, overgrazing and land degradation reduce soil moisture retention, while drying springs and unsustainable agricultural practices strain water availability. The expansion of tourism and infrastructure development has also led to increased water demand, adding pressure to the region's fragile water system.

Implications for Adaptation and Mitigation Strategies Given the anticipated increase in drought conditions, there is an urgent need for proactive adaptation measures to protect the water security of Mustang and agricultural sustainability. Potential strategies include:

- Enhancing Water Conservation and Storage Systems: Rainwater harvesting, improved reservoir capacity, and efficient irrigation technologies can help mitigate water shortages.
- Promoting Climate-Resilient Agriculture: Shifting towards drought-resistant crop varieties and sustainable farming techniques will be crucial in adapting to prolonged dry spells.
- Strengthening Community-Based Adaptation Initiatives: Local knowledge and traditional water management practices should be integrated into climate resilience policies.
- Advancing Climate Policy and Regional Cooperation: Addressing long-term drought risks requires national and international collaboration on climate adaptation and mitigation strategies.

## 5. Conclusion

This study provides critical insights into the evolving drought conditions in Mustang, Nepal, by analyzing historical and future SPI trends using CMIP6 models. The results indicate that Mustang has already experienced significant drought events, with an increasing trend projected for the coming decades. Under both moderate and high emissions scenarios, drought frequency, severity, and duration are expected to worsen, posing a serious threat to water availability, agriculture, and local livelihoods. Given the increasing risks associated with climate-induced aridity, immediate action is required to develop sustainable water management practices and climate adaptation strategies. The findings emphasize the necessity of integrating scientific research, policy interventions, and community-based resilience-building measures to mitigate the long-term impacts of drought in Mustang and similar high-altitude regions. Future research should focus on improving the accuracy of climate models, assessing socio-economic vulnerabilities, and developing integrated solutions for sustainable water resource management in Nepal's trans-Himalayan region.

## Acknowledgments

The authors sincerely appreciate the support and guidance provided by the Institute of Engineering (IOE), Pulchowk Campus, the Department of Applied Science and Chemical Engineering, without which this study would not have been complete.

## References

[1] K. Abbass, M.Z. Qasim, H. Song, M. Murshed, H. Mahmood, and I. Younis. A review of the global climate change impacts, adaptation, and sustainable mitigation measures. *Environmental Science and Pollution Research*, 29(28):42539–42559, 2022.

[2] P. M. Forster, C. J. Smith, T. Walsh, W. F. Lamb, R. Lamboll, M. Hauser, A. Ribes, D. Rosen, N. Gillett, M. D. Palmer, J. Rogelj, K. von Schuckmann, S. I. Seneviratne, B. Trewin, X. Zhang, M. Allen, R. Andrew, A. Birt, A. Borger, T. Boyer, J. A. Broersma, L. Cheng, F. Dentener, P. Friedlingstein, J. M. Gutiérrez, J. Gütschow, B. Hall, M. Ishii, S. Jenkins, X. Lan, J.-Y. Lee, C. Morice, C. Kadow, J. Kennedy, R. Killick, J. C. Minx, V. Naik, G. P. Peters, A. Pirani, J. Pongratz, C.-F. Schleussner, S. Szopa, P. Thorne, R. Rohde, M. Rojas Corradi, D. Schumacher, R. Vose, K. Zickfeld, V. Masson-Delmotte, and P. Zhai. Indicators of global climate change 2022: annual update of large-scale indicators of the state of the climate system and human influence. *Earth System Science Data*, 15(6):2295–2327, 2023.

[3] Huaijun Wang, Yaning Chen, Yingping Pan, Zhongsheng Chen, and Zhiguo Ren. Assessment of candidate distributions for spi/spei and sensitivity of drought to climatic variables in china. *International Journal of Climatology*, 39(11):4392–4412, 2019.

[4] Suman Aryal, Tek Narayan Maraseni, and Geoff Cockfield. Changes in transhumance systems in nepal: Analysing socio-ecological impacts using driver-pressure-state-impact-response framework. In *Agriculture, Natural*

*Resources and Food Security: Lessons from Nepal*, pages 297–314. Springer International Publishing, Cham, 2022.

[5] Neeta Nandgude, T. P. Singh, Sachin Nandgude, and Mukesh Tiwari. Drought prediction: A comprehensive review of different drought prediction models and adopted technologies. *Sustainability*, 15(15), 2023.

[6] Y. Hijioka, E. Lin, J. J. Pereira, R. T. Corlett, X. Cui, G. E. Insarov, R. D. Lasco, E. Lindgren, and A. Surjan. Asia. In V. R. Barros, C. B. Field, D. J. Dokken, M. D. Mastrandrea, K. J. Mach, T. E. Bilir, M. Chatterjee, K. L. Ebi, Y. O. Estrada, R. C. Genova, B. Girma, E. S. Kissel, A. N. Levy, S. MacCracken, and P. R. Mastrandrea, editors, *Climate Change 2014: Impacts, Adaptation, and Vulnerability, Part B: Regional Aspects*, pages 1327–1370. Cambridge University Press, Cambridge, UK and New York, NY, USA, 2014.

[7] Intergovernmental Panel on Climate Change (IPCC). *Climate Change 2023: Synthesis Report*. IPCC, Geneva, Switzerland, 2023.

[8] Hari Krishna Shrestha and Suresh Prasain. Climate change impact and adaptation measures needed in upper mustang to prevent more climate refugees. *Research Briefs*, 125:1–6, 2016.

[9] H.F. Abd-Elhamid, M. Zeleňáková, T. Soľáková, O.K. Saleh, and A.M. El-Dakak. Monitoring flood and drought risks in arid and semi-arid regions using remote sensing data and standardized precipitation index: A case study of syria. *Journal of Flood Risk Management*, 17(1):e12961, 2024.

[10] Ayman Balla Mustafa and Asim Faraz. Camel systems and pastoralists' lifestyle in semi-deserts and mountains: Constraints and challenges. *PASTURES & PASTORALISM www. grassrootsjournals. org/pp ISSN 2817-3457| 01 (2023)*, page 93, 2023.

[11] Emily Amburgey. *Migration and translocal livelihoods: transformation amidst climate change in Mustang, Nepal*. PhD thesis, University of British Columbia, 2024.

[12] Marie Delalay, Alan D Ziegler, Mandira Singh Shrestha, Robert James Wasson, Karen Sudmeier-Rieux, Brian G McAdoo, and Ishaan Kochhar. Towards improved flood disaster governance in nepal: A case study in sindhupalchok district. *International journal of disaster risk reduction*, 31:354–366, 2018.

[13] Gaurav Parajuli, Shankar Neupane, Sandeep Kunwar, Ramesh Adhikari, and Tri Dev Acharya. A gis-based evacuation route planning in flood-susceptible area of siraha municipality, nepal. *ISPRS International Journal of Geo-Information*, 12(7):286, 2023.

[14] Pradeep M Tulachan. Mountain agriculture in the hindu kush–himalaya. *Mountain Research and Development*, 21(3):260–267, 2001.

[15] Uttam Babu Shrestha, Shiva Gautam, and Kamaljit S Bawa. Widespread climate change in the himalayas and associated changes in local ecosystems. *PloS one*, 7(5):e36741, 2012.

[16] International Centre for Integrated Mountain Development (ICIMOD). *Annual Report 2020*. ICIMOD, Kathmandu, Nepal, 2020.

[17] Vimal Mishra, Udit Bhatia, and Amar Deep Tiwari. Bias-corrected climate projections for south asia from coupled model intercomparison project-6. *Scientific data*, 7(1):338, 2020.

[18] Justin Sheffield, Gopi Goteti, and Eric F. Wood. Development of a 50-year high-resolution global dataset of meteorological forcings for land surface modeling. *Journal of Climate*, 19(13):3088–3111, 2006.

[19] Su-Yuan Li, Li-Juan Miao, Zhi-Hong Jiang, Guo-Jie Wang, Kaushal Raj Gnyawali, Jing Zhang, Hui Zhang, Ke Fang, Yu He, and Chun Li. Projected drought conditions in northwest china with cmip6 models under combined ssps and rcps for 2015–2099. *Advances in Climate Change Research*, 11(3):210–217, 2020.

[20] S. Sharma, K. Hamal, N. Khadka, M. Ali, M. Subedi, G. Hussain, M.A. Ehsan, S. Saeed, and B. Dawadi. Projected drought conditions over southern slope of the central himalaya using cmip6 models. *Earth Systems and Environment*, 5:849–859, 2021.

[21] M. N. Lorenzo, H. Pereira, I. Alvarez, and J. M. Dias. Standardized precipitation index (spi) evolution over the iberian peninsula during the 21st century. *Atmospheric Research*, 297:107132, 2024.

[22] Sorin Cheval. The standardized precipitation index–an overview. *Romanian Journal of Meteorology*, 12(1-2):17–64, 2015.

[23] Carmelo Cammalleri, Jonathan Spinoni, Paulo Barbosa, Andrea Toreti, and Jürgen V. Vogt. The effects of non-stationarity on spi for operational drought monitoring in europe. *International Journal of Climatology*, 42(6):3418–3430, 2022.

[24] T.B. McKee, N.J. Doesken, and J. Kleist. The relationship of drought frequency and duration to time scales. In *Proceedings of the 8th Conference on Applied Climatology*, volume 17, pages 179–183, 1993.

# 6% Overall Similarity

The combined total of all matches, including overlapping sources, for each database.

## Filtered from the Report

- Bibliography
- Quoted Text
- Small Matches (less than 10 words)

## Match Groups

**40** Not Cited or Quoted 5%
Matches with neither in-text citation nor quotation marks

**12** Missing Quotations 1%
Matches that are still very similar to source material

**0** Missing Citation 0%
Matches that have quotation marks, but no in-text citation

**0** Cited and Quoted 0%
Matches with in-text citation present, but no quotation marks

## Top Sources

5% Internet sources
4% Publications
0% Submitted works (Student Papers)

## Integrity Flags

**0 Integrity Flags for Review**

No suspicious text manipulations found.

Our system's algorithms look deeply at a document for any inconsistencies that would set it apart from a normal submission. If we notice something strange, we flag it for you to review.

A Flag is not necessarily an indicator of a problem. However, we'd recommend you focus your attention there for further review.

## Match Groups

- **40** Not Cited or Quoted 5%
  Matches with neither in-text citation nor quotation marks
- **12** Missing Quotations 1%
  Matches that are still very similar to source material
- **0** Missing Citation 0%
  Matches that have quotation marks, but no in-text citation
- **0** Cited and Quoted 0%
  Matches with in-text citation present, but no quotation marks

## Top Sources

5% Internet sources
4% Publications
0% Submitted works (Student Papers)

## Top Sources

The sources with the highest number of matches within the submission. Overlapping sources will not be displayed.

| | | |
|---|---|---|
| 1 | Internet | link.springer.com <1% |
| 2 | Internet | elibrary.tucl.edu.np <1% |
| 3 | Internet | www.e3s-conferences.org <1% |
| 4 | Internet | www.frontiersin.org <1% |
| 5 | Internet | philstat.org <1% |
| 6 | Internet | assets.researchsquare.com <1% |
| 7 | Internet | saarc-sdmc.gujarat.gov.in <1% |
| 8 | Internet | www.ltrc.lsu.edu <1% |
| 9 | Internet | www.mdpi.com <1% |
| 10 | Internet | www.nature.com <1% |

11 Internet
sciencedocbox.com <1%

12 Internet
assets-eu.researchsquare.com <1%

13 Internet
kth.diva-portal.org <1%

14 Publication
Jan-Philip M. Witte, Gé A. P. H. van den Eertwegh, Paul J. J. F. Torfs. "Absolute Met... <1%

15 Internet
www.icimod.org <1%

16 Internet
authors.library.caltech.edu <1%

17 Internet
1library.co <1%

18 Publication
Yingqiang Xu, Abeer Albalawneh, Maysoon Al-Zoubi, Hiba Baroud. "Variance-base... <1%

19 Publication
Lau, Ka Lun. "Projecting Future Air Temperature of Hong Kong for the 21st Centu... <1%

20 Publication
Ramchandra Karki, Shabeh ul Hasson, Udo Schickhoff, Thomas Scholten, Jürgen B... <1%

21 Publication
Aminjon Gulakhmadov, Xi Chen, Nekruz Gulahmadov, Muhammmad Rizwan et al.... <1%

22 Internet
tinread.upit.ro <1%

23 Publication
Amrit Prasad Sharma, Xudong Fu, Giri R. Kattel. "Is there a progressive flood risk ... <1%

24 Publication
Md. Rejaur Rahman, Habibah Lateh. "Spatio-temporal analysis of warming in Ban... <1%

25 Publication

Tirivarombo, S.. "Regional droughts and food security relationships in the Zambe... <1%

26 Internet

grips.repo.nii.ac.jp <1%

27 Internet

oceanrep.geomar.de <1%

28 Internet

www2.mdpi.com <1%

29 Publication

Jess Melbourne-Thomas, Alberto C. Naveira Garabato, Marilyn Raphael. "Antarcti... <1%

30 Publication

S.T. Pavan Kumar, Biswajit Lahiri, M.M. Nageswararao, Rafael Alvarado, Silkame ... <1%

31 Internet

bmcpulmmed.biomedcentral.com <1%

32 Internet

ks.dku.kz <1%

33 Internet

medcraveonline.com <1%

34 Internet

utpedia.utp.edu.my <1%

35 Internet

www.guntherkonnen.com <1%

36 Publication

"Climate Change, Extreme Events and Disaster Risk Reduction", Springer Science ... <1%

37 Publication

Dolores Rey, Ian P. Holman, Jerry W. Knox. "Developing drought resilience in irrig... <1%

38 Publication

I Putu Gustave Suryantara Pariartha, Rishikesh Sharma, Srinivas Rallapalli, Ajit Pr... <1%

39 Publication

Sonali P., Subir Paul. "Spatio-temporal dependency of vegetation dynamics on cli... <1%

40 Internet

cdr.lib.unc.edu <1%

41 Internet

climate.pusan.ac.kr <1%

42 Internet

etd.aau.edu.et <1%

43 Internet

livemcqs.com <1%

44 Internet

www.hindawi.com <1%